AN ABSTRACT OF THE DISSERTATION OF

Zlatko Dimcovic for the degree of Doctor of Philosophy in Physics presented on June 14, 2012.

Title: Discrete-time Quantum Walks via Interchange Framework and Memory in Quantum Evolution

Abstract approved: _____

Yevgeniy Kovchegov

One of the newer and rapidly developing approaches in quantum computing is based on "quantum walks," which are quantum processes on discrete space that evolve in either discrete or continuous time and are characterized by mixing of components at each step. The idea emerged in analogy with the classical random walks and stochastic techniques, but these unitary processes are very different even as they have intriguing similarities. This thesis is concerned with study of discrete-time quantum walks.

The original motivation from classical Markov chains required for discrete-time quantum walks that one adds an auxiliary Hilbert space, unrelated to the one in which the system evolves, in order to be able to mix components in that space and then take the evolution steps accordingly (based on the state in that space). This additional, "coin," space is very often an internal degree of freedom like spin.

We have introduced a general framework for construction of discrete-time quantum walks in a close analogy with the classical random walks *with memory* that is rather different from the standard "coin" approach. In this method there is no need to bring in a different degree of freedom, while the full state of the system is still described in the direct product of spaces (of states). The state can be thought of as an arrow pointing from the previous to the current site in the evolution, representing the one-step memory. The next step is then controlled by a single local operator assigned to each site in the

space, acting quite like a scattering operator.

This allows us to probe and solve some problems of interest that have not had successful approaches with "coined" walks. We construct and solve a walk on the binary tree, a structure of great interest but until our result without an explicit discrete time quantum walk, due to difficulties in managing coin spaces necessary in the standard approach. Beyond algorithmic interests, the model based on memory allows one to explore effects of history on the quantum evolution and the subtle emergence of classical features as "memory" is explicitly kept for additional steps. We construct and solve a walk with an additional correlation step, finding interesting new features.

On the other hand, the fact that the evolution is driven entirely by a local operator, not involving additional spaces, enables us to choose the Fourier transform as an operator completely controlling the evolution. This in turn allows us to combine the quantum walk approach with Fourier transform based techniques, something decidedly not possible in classical computational physics. We are developing a formalism for building networks manageable by walks constructed with this framework, based on the surprising efficiency of our framework in discovering internals of a simple network that we so far solved.

Finally, in line with our expectation that the field of quantum walks can take cues from the rich history of development of the classical stochastic techniques, we establish starting points for the work on non-Abelian quantum walks, with a particular quantum-walk analog of the classical "card shuffling," the walk on the permutation group.

In summary, this thesis presents a new framework for construction of discrete time quantum walks, employing and exploring memoried nature of unitary evolution. It is applied to fully solving the problems of: A walk on the binary tree and exploration of the quantum–to–classical transition with increased correlation length (history). It is then used for simple network discovery, and to lay the groundwork for analysis of complex networks, based on combined power of efficient exploration of the Hilbert space (as a walk mixing components) and Fourier transformation (since we can choose this for the evolution operator). We hope to establish this as a general technique as its power would be unmatched by any approaches available in the classical computing. We also looked at the promising and challenging prospect of walks on non-Abelian structures by setting up the problem of "quantum card shuffling," a quantum walk on the permutation group.

Relation to other work is thoroughly discussed throughout, along with examination of the context of our work and overviews of our current and future work.

Discrete-time Quantum Walks via Interchange Framework and Memory in Quantum Evolution

by

Zlatko Dimcovic

A DISSERTATION

submitted to

Oregon State University

in partial fulfillment of
the requirements for the
degree of

Doctor of Philosophy

Presented June 14, 2012
Commencement June 2012

Doctor of Philosophy dissertation of Zlatko Dimcovic presented on June 14, 2012.

APPROVED:

Major Professor, representing Physics

Chair of the Department of Physics

Dean of the Graduate School

I understand that my dissertation will become part of the permanent collection of Oregon State University libraries. My signature below authorizes release of my dissertation to any reader upon request.

Zlatko Dimcovic, Author

ACKNOWLEDGEMENTS

It is my pleasure to thank my advisor, who directly brought me into a field of research completely new for me, for his astute guidance and constant stimulating discussions. This literally would have not happened without him. I very much value our friendship that developed. I am looking forward to our continued work and interaction.

I thank my committee, who dealt with a field of research unrelated to their daily work and still managed to provide support that was important and that mattered.

This is a great opportunity for me to thank my wife for her thoughtful, uncompromising, and simply wonderful support. I thank greatly my mom, who has been there for me all along. I am very grateful for the presence of the loved and loving ones in my life.

TABLE OF CONTENTS

Page

TABLE OF CONTENTS (Continued)

Page

LIST OF FIGURES

Figure Page

LIST OF FIGURES (Continued)

Figure Page

LIST OF TABLES

Table Page

LIST OF APPENDIX FIGURES

Chapter 1: Introduction

1.1 Quantum computation

Quantum computing is an exciting and broad field of research, involving and combining many areas of physics, mostly very diverse [1–3]. It is also an interdisciplinary field. Its original premise is the quest for a computing device that directly utilizes quantum mechanical properties of physical systems that implement it, with expectations of vast improvements in speed of calculations. This firstly means that one must have good enough control over the medium used, so that explicit quantum mechanical behaviour is maintained; there is no gain in speed of a "quantum computer" if classical behaviour takes over. Note that this does not necessarily mean that we have to control single constituents: We need to have control over specific *properties*, which may involve particular phenomena in a bulk or in very complex systems. A few examples of such implementations are based on NMR, quantum dots and other solid state approaches, ion trapping, superconductivity, or semi-conductor nanowires.

The biggest question has always been of how to reach the actual computer; one has to use very large number of systems in order to perform realistic calculations, and keeping that under tight control is challenging. As the field has developed, the focus is indeed more and more on enlarging the physical systems used to 'compute' while avoiding interaction with environment that disturbs the particular properties used ("decoherence"). This direction spurred very interesting ideas and novel physics, for example related to topological considerations or quantum mechanical phase transitions (to name some), but solutions are not yet in sight. The number of computing elements ("qubits") used in experiments is still counted in tens. While for simulations of quantum systems useful results may be expected with as little as around a hundred qubits, it is clear that for more general purposes we need scarily more qubits. The search for physical systems that will support large scale implementations, and for ways to suppress or deal with decoherence and error correction [4], can be labeled as the main quest in the field of quantum computing at present [5]. Thus quantum "computing" today is a developed and intense

research effort toward detailed understanding of a broadest variety of physical systems.

In order to use quantum propagation over all paths, superposition, and entanglement[1] for efficient calculation we need suitable algorithms—precise ways to manipulate quantum systems in order to solve computational problems—since the algorithms from classical computer science cannot utilize such properties. This is one of the aspects where mathematics and computer science get involved in earnest.

It was precisely the discovery of particular algorithms that started a broad interest in quantum computing. In particular, the famous Shor's factoring algorithm [6] of 1994 was perceived as a "bolt out of the blue," as an unexpected practical capability of quantum systems. Since those early days a large body of algorithms has been established [7], but the ones that carry "exponential speedup" are far and few in between, much harder to come by, and not feasible for all types of problems of interest for computing. Work on quantum algorithms is itself a diverse field of research, often requiring breakthroughs in understanding of, and deep insight into, properties of various systems.

Far beyond a search for a powerful computing platform, this field has proven itself to be an extremely fruitful framework for novel ideas and approaches, breakthroughs, and new directions in physics. It is a broad and varied research playground, pushing all involved sciences. In many papers it is difficult to draw a line between focus on quantum computation and on fundamental research in physics, and they often blend smoothly. This has spawned advances, both theoretical and experimental, in fields ranging from foundations of quantum mechanics to transport phenomena to quantum phase transitions to superconductivity, to name a few. In terms of scale, the research ranges from manipulation of single photons to topological aspects of condensed matter systems.

Quite apart from development of particular fields of physics, work in this field has initiated articulate and systematic study of *information* as a physical concept. This direction involves foundations of quantum theories and makes connections with topics ranging from quantum gravity pursuits to condensed matter physics (holographic principle and area law [8, 9], for example). It has directly interacted with classical information theory, bridging gaps between diverse scientific disciplines. The field of quantum computing is also a laboratory for all manner of explorations on entanglement [10, 11].

In the opinion of this author, work in quantum information and computation has already contributed to development of physics, with yet better future prospects.

[1] While entanglement is considered the critical resource, this is debated and researched.

1.2 Quantum walks

Introduction of stochastic techniques in classical computing had a great impact and changed the field. Nowadays randomized algorithms form a whole direction in classical computing, presenting distinct and effective approaches. They are ubiquitous in physics. The effectiveness of randomized approaches is based on the surprisingly fast convergence of such processes, enabling effective arrival to answers, as established and studied in theory of probability and stochastic processes. Random walks follow simple rules for local evolution to explore global properties, which results (among other benefits) in algorithmically efficient exploration of huge spaces of states. This is very well suited for computation. Equally important is the fact that the stochastic nature of such processes affords us an approach completely different from deterministic algorithms.

The main motivation for quantum walks was to utilize such ideas with quantum mechanical evolution. Quantum walk is a processes on a discrete space of states, where at each step a decision is made where to propagate, or more precisely, in what exact superposition. The state space is generally encoded by a graph, where nodes represent states and the transitions are generally allowed between nearest neighbors (represented by connections between nodes of the graph). The steps can be taken at discrete time intervals or continuously in time, splitting the field into discrete– and continuous-time quantum walks. A very big difference is the fact that this "decision" has to be controlled by a unitary operator, rather than by a stochastic matrix[2] as it is in classical random walks. In general, a mixing of components in the superposition of the state is performed at each step, and based on the composition of the obtained state the process takes the next step, evolving to the next set of discrete states. The states need not relate to position but can be any property of the system that can 'walk.' Since this concerns quantum systems, the propagation proceeds along all available paths, in a superposition evolved by unitary operators, resulting in the interference between paths—properties absent in classical random walks. Because of this, quantum processes 'see' larger structures than the classical ones can [12, IV], and quantum walks should be even better at the game of learning about global properties via local evolution, championed by classical Markov chains and stochastic algorithms.

Thus quantum walks can be described as general quantum mechanical processes on

[2] Containing the probabilities, with rows and columns each summing to 1.

a discrete space of states, with imposed particular mixing of components at every step. Possible physical implementations then include any system that can controllably (for practical purposes) move through discrete transitions so they range across many fields of physics. A quantum walk is then a model for a process, representing propagation of a property of a system (not necessarily a particle).

Given the original motivation, it had been expected that quantum walks might directly repeat successes of classical stochastic approaches. However, this has not quite happened, at least not as dramatically. One of the most sought after algorithmic accomplishments is the "exponential speedup:" Run time of a program grows with the size of the problem exponentially slower that it does for the best classical algorithms for the same problem. For example: If the best classical algorithm has a run time which is polynomial with the size of a particular problem, and we find a quantum algorithm with the run time logarithmic with size, we have an exponential speedup.[3]

Only a few such algorithms have been found, and none for problems of acute interest in computing. On the other hand, speed is not everything and solving problems that are unwieldy for other approaches is probably more important. There have been a handful or two of such algorithms using quantum walks. Lastly, by now there are useful algorithmic solutions using quantum walks for many problems of interest. An overview is given in Sec. 1.2.3. In short, quantum walks have been fully established as a well-rounded algorithmic tool, while the field could make use of some successful algorithms.

An improvement of a different kind would be to extend uses of quantum walks to more complex problems, much like the classical stochastic techniques had evolved. Our initial study of quantum walks on the permutation group S_n, described in Ch. 6, is an example of one such direction, of using quantum walks on non-Abelian structures. Such problems are challenging, but with a very promising outcome. For example, Shor's algorithm uses cyclic groups and can be related to problems on an Abelian group. Any progress on non-Abelian structures, for example on the problem of finding hidden subgroups, would likely lead to uses unmatched even by Shor's algorithm.

Quantum walks are at present still mostly an algorithmic tool. However, given that they are generic quantum processes on a discrete space that should be efficient in ex-

[3] Problems with exponential complexity are considered to not have an "efficient" solution, since as the problem grows in size the run time very quickly becomes unfeasible. Then having an "exponential speedup" is not only about speed, but about having an efficient (usable) solution in the first place.

ploring the Hilbert space, they are also a promising tool for modeling and exploration of physical systems in general. There is a growing trend of using quantum walks for studies unrelated to algorithmic aspects or quantum computing, and as an approach to fundamental questions, in a wide range of fields. A listing of some results is given in Sec. 1.2.3. This identifies another direction for a further development of the field.

In order to introduce quantum walks we next present the construction of the standard coin-based one dimensional discrete-time quantum walk (DTQW), and then of the continuous-time quantum walk (CTQW).

1.2.1 Discrete-time quantum walks (DTQW)

In the following descriptions we use a graph to enumerate states in the space in which the process propagates. Connections between nodes indicate which transitions (steps) are allowed. In the first example we construct the walk in a space of one dimension, so our graph is going to be a line of nodes, with each node connected to its two nearest neighbors. A generalization to higher dimensions is straightforward and presented a little later in this section. Recall that the 'walk on states' does not in any way presume a configuration space; these are transitions between discrete states of some property (momentum, polarization, spin, ...)

A discrete-time quantum walk propagates over its space (graph) by repeatedly taking (discrete-time) steps to the neighboring nodes of the graph. A quantum walk will at each step make transitions to all connected nodes. While in classical random walks the direction of each step is randomly chosen, here it is the amplitudes (of the state components evolved to that site) that are determined anew for each step. However, for a walk that takes steps discrete in time the only possibility is an uninteresting propagation in one direction; other ways to 'walk' are not unitary [13]. (This is different for walks that can take steps at any time, the continuous-time ones. They are reviewed below.) Thus an additional, auxiliary, space is introduced and the mixing of components with the subsequent decision on amplitudes is done in this space. It is called the "coin space" and is an analog of the coin-toss implicit in the classical random walks.[4] The

[4] In classical walks one does not explicitly toss a coin at every step, except for the simplest walks. The evolution is rather given by the action of an operator constructed with probabilities. This does implement random choices, which is what the "coin tossing" terminology refers to.

need for an additional space carries consequences. DTQW are generally harder to work with mathematically. On the other hand, the extra space is an additional degree of freedom in implementations, thus allowing more control over the walk. However, it is also particularly sensitive to decoherence.

To construct such a process, then, we need a product of spaces. The space in which the state ($|v\rangle$) evolves is the n–dimensional Hilbert space $\mathcal{H}_V$, and we label the basis in this space as $\{|1\rangle, \ldots, |n\rangle\}$. The auxiliary "coin space" $\mathcal{H}_C$ with vectors $|c\rangle$ needs only two dimensions for the walk in one dimension. Let us call the basis in that space $\{|\uparrow\rangle, |\downarrow\rangle\}$, with the spin in mind, which is often used as the 'coin' degree of freedom in implementations (experiments). So our state is

$$|\psi(t)\rangle = |c\rangle \otimes |v\rangle = \Big(c_u|\uparrow\rangle + c_d|\downarrow\rangle\Big) \otimes \sum_{i=1}^{n} c_i|i\rangle = \begin{pmatrix} c_u \\ c_d \end{pmatrix} \otimes \sum_{i=1}^{n} c_i|i\rangle,$$

and it is evolved by an operator which is a direct product of an operator acting in the coin space, and an operator acting in the state space. The operator that mixes components in the coin space can be any unitary transformation; here we use the classic and most common Hadamard transformation,

$$C = H = \frac{1}{\sqrt{2}} \begin{pmatrix} 1 & 1 \\ 1 & -1 \end{pmatrix}, \quad \text{acting in the space spawned by } \{|\uparrow\rangle, |\downarrow\rangle\}.$$

After the action of this operator, the step in the state space is taken according to any rule that one choses in order to distinguish between components in the coin space. Here we use the standard prescription: The components with $|\uparrow\rangle$ take the step to the right, and components with $|\downarrow\rangle$ take the step to the left. This is mathematically implemented by projectors in the "shift" operator,

$$S \;=\; |\uparrow\rangle\langle\uparrow| \otimes \sum_j |j+1\rangle\langle j| \;+\; |\downarrow\rangle\langle\downarrow| \otimes \sum_j |j-1\rangle\langle j|.$$

Now we can write down the evolution, as a sequence of repeated steps,

$$U\Big(|c\rangle \otimes |v\rangle\Big) \;=\; S\,(C \otimes I)\,\Big(|c\rangle \otimes |v\rangle\Big) \;=\; S\,\Big(C|c\rangle \otimes |v\rangle\Big), \tag{1.1}$$

with S as shown just above. For example, trace through a few steps, starting in a sharp

state $|j\rangle$ with spin up, $|\psi_0\rangle = |\uparrow\rangle \otimes |j\rangle$. First the coin operator (Hadamard) mixes spins,

$$\Big(C\,|\uparrow\rangle\Big) \otimes |j\rangle = \frac{1}{\sqrt{2}} \begin{pmatrix} 1 & 1 \\ 1 & -1 \end{pmatrix} \begin{pmatrix} 1 \\ 0 \end{pmatrix} = \frac{1}{\sqrt{2}}\Big(|\uparrow\rangle + |\downarrow\rangle\Big),$$

and then the conditional shift is performed, so that $U|v\rangle = S(C|a\rangle \otimes |v\rangle)$ gives

$$\begin{aligned} |\psi_1\rangle &= \Big(|\uparrow\rangle\langle\uparrow| \otimes \sum_j |j+1\rangle\langle j| + |\downarrow\rangle\langle\downarrow| \otimes \sum_j |j-1\rangle\langle j|\Big)\ \frac{1}{\sqrt{2}}\Big(|\uparrow\rangle + |\downarrow\rangle\Big) \otimes |j\rangle \\ &= \frac{1}{\sqrt{2}}\Big(|\uparrow\rangle \otimes |j+1\rangle + |\downarrow\rangle \otimes |j-1\rangle\Big). \end{aligned}$$

So our state gets pushed both left and right, and in the next step things get more interesting since superpositions of amplitude start forming. For the second step we have $|\psi_2\rangle = U\,|\psi_1\rangle = S\,(C \otimes I)|\psi_1\rangle$, where

$$(C \otimes I)|\psi_1\rangle = \frac{1}{2}\Big(|\uparrow\rangle + |\downarrow\rangle\Big) \otimes |j+1\rangle + \frac{1}{2}\Big(|\uparrow\rangle - |\downarrow\rangle\Big) \otimes |j-1\rangle,$$

and now the shift produces a state that is spread out over more sites,

$$S\Big((C \otimes I)|\psi_1\rangle\Big) = \frac{1}{2}\Big(|\uparrow\rangle \otimes |j+2\rangle + 2\,|\downarrow\rangle \otimes |j\rangle - |\downarrow\rangle \otimes |j-2\rangle\Big).$$

The next step results in a state that already shows the main characteristics of a quantum walk. The action of the coin operator,

$$(C \otimes I)|\psi_2\rangle = \frac{1}{2\sqrt{2}}\Big(|\uparrow\rangle + |\downarrow\rangle\Big) \otimes |j+2\rangle + \frac{2}{2\sqrt{2}}\Big(|\uparrow\rangle - |\downarrow\rangle\Big) \otimes |j\rangle - \frac{1}{2\sqrt{2}}\Big(|\uparrow\rangle - |\downarrow\rangle\Big) \otimes |j-2\rangle,$$

followed by the conditional shift, produces

$$\begin{aligned} |\psi_3\rangle &= S\Big((C \otimes I)|\psi_2\rangle\Big) \\ &= \frac{1}{2\sqrt{2}}\Big(|\uparrow\rangle \otimes |j+3\rangle + |\downarrow\rangle \otimes |j+1\rangle + |\uparrow\rangle \otimes |j+1\rangle \\ &\qquad + |\downarrow\rangle \otimes |j-1\rangle - |\uparrow\rangle \otimes |j-1\rangle + |\downarrow\rangle \otimes |j-3\rangle\Big) \\ &= \frac{1}{2\sqrt{2}}\Big[|\uparrow\rangle \otimes |j+3\rangle + \Big(|\uparrow\rangle + |\downarrow\rangle\Big) \otimes |j+1\rangle - \Big(|\uparrow\rangle - |\downarrow\rangle\Big) \otimes |j-1\rangle + |\downarrow\rangle \otimes |j-3\rangle\Big]. \end{aligned}$$

We first see that the 'fronts' escape to both left and right, and that this will continue: Our process propagates linearly with the number of steps. Also, we can already see what happens in the middle. To spare the reader from repeated calculation, look at how the second and third term, with states $|j+1\rangle$ and $|j-1\rangle$ respectively, behave under the coin operator:

$$\begin{aligned}
&\text{for coin-states with } |j+1\rangle, \qquad C\colon (|\uparrow\rangle + |\downarrow\rangle) \;\to\; \Big(|\uparrow\rangle + |\downarrow\rangle + |\uparrow\rangle - |\downarrow\rangle\Big) \;\to\; 2\,|\uparrow\rangle \\
&\text{for coin-states with } |j-1\rangle, \qquad C\colon (|\uparrow\rangle - |\downarrow\rangle) \;\to\; \Big(|\uparrow\rangle + |\downarrow\rangle - |\uparrow\rangle + |\downarrow\rangle\Big) \;\to\; 2\,|\downarrow\rangle,
\end{aligned}$$

where normalization factors have been omitted for simplicity. The only states that could take us back to the starting state at $|j\rangle$ with the next shift have just lost that ability: $|j+1\rangle$ with the $|\uparrow\rangle$ will now be shifted only to $|j+2\rangle$, while $|j-1\rangle$ shifts to $|j-2\rangle$ since it has only the $|\downarrow\rangle$ component. In other words, cancellations happen that lead to the absence of an appreciable amplitude at the origin, while the amplitude further away builds.

This is of course only a hint at this point, shown here for illustration, but it is indeed how the walk behaves. A numerical simulation of such a walk is shown on Fig. 1.1, where the probability is shown as a function of position for a walk that started at $j = 0$, after 100 steps for one initial condition and after 125 for a different one (for clarity). The unevenness of left and right peaks is due to that particular initial state in the coin space ($|\uparrow\rangle$), combined with the use of Hadamard for the coin operator. Balanced propagation is easily obtained by choosing a different initial internal (coin) state, $\psi_0 = \frac{1}{\sqrt{2}}\big(|\uparrow\rangle + \boldsymbol{i}|\downarrow\rangle\big)\otimes|i\rangle$ (as shown in the figure), and/or a different coin operator.

The cancellations discussed above are the consequence of the unitary mixing of the coin states, and it is obvious here how Hadamard induces this. However, walks with many different coin operators have been studied, and this behaviour is in fact generic to such processes. This is probably best seen with a generalized Hadamard,

$$C = \begin{pmatrix} \sqrt{p} & \sqrt{1-p} \\ \sqrt{1-p} & -\sqrt{p} \end{pmatrix},$$

which in general leads to walks with similiar properties. Note that the choice of $p = 1/2$ restores the Hadamard transform. On another note, unrelated as of yet, we should

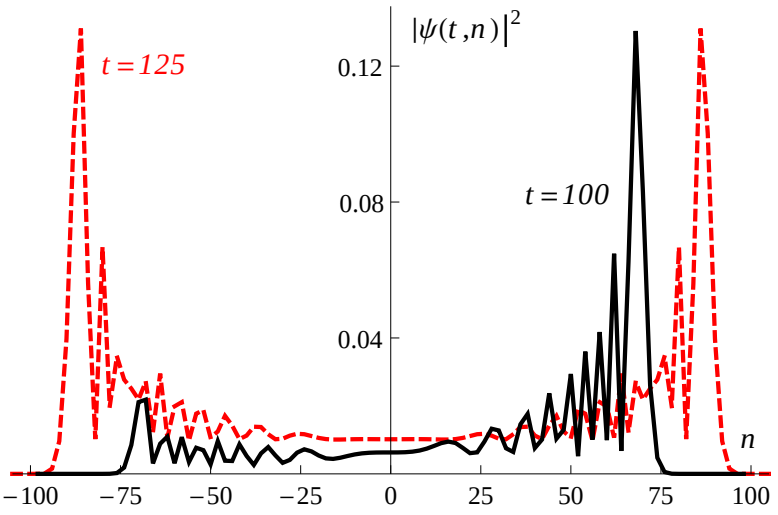

Figure 1.1: Probability distribution of a standard coin-based one-dimensional discrete-time quantum walk, over sites on the graph (n). This walk started at $n = 0$. The solid black curve is the walk with the initial coin state $|\uparrow\rangle$, shown at $t = 100$; the dashed red is for the initial coin state $\big(|\uparrow\rangle + \boldsymbol{i}|\downarrow\rangle\big)/\sqrt{2}$, shown at $t = 125$. Different times are for clarity; at the same time the right-hand peaks overlap nearly entirely. At every odd site probabilities are zero; this is omitted for clarity. Distributions integrate to 1.

mention here that the above relaxation of the Hadamard brings up other very interesting observations, discussed in the beginning of Chapter 2.

Now we sketch a fuller mathematical treatment of a walk on a regular graph[5] defined as a repeated application of a conditional shift operator that follows the action of a components-mixing ("coin") operator, seen in Eq. (1.1). The full state of the system is given in the product space $\mathcal{H}_V \otimes \mathcal{H}_C$, where $|v\rangle \in \mathcal{H}_V$ is the state that evolves while $|c\rangle = \sum_{a=1}^{d} c_a|a\rangle \in \mathcal{H}_C$ is the auxiliary state in the "coin space," like the $\{|\uparrow\rangle, |\downarrow\rangle\}$ used above, but now of an arbitrary dimension d. Thus our system at every step can make a transition to d states, implemented by a conditional shift operator, while the amplitudes

[5] "Graph" is an abstract representation of a set of objects by "vertices" (nodes), with "edges" between them indicating their relation. It is often shown by a diagram with dots, some of which are connected. Example: for a Hilbert space of states we can assign a vertex (on a graph which enumerates $\mathcal{H}$) for each state and connect those between which transitions are allowed. Formally, a graph is an ordered pair $G = (V, E)$ where V is a set of vertices and E set of edges connecting pairs of vertices. Graphs are studied in mathematics and computer science, and used in many fields. "Constant order" means that the number of connections is the same for all nodes. Some examples of graphs: Figs. (3.2) and (5.1).

are 'decided' by the mixing of the d-components of the coin-state. Note that it is implied that states in our $\mathcal{H}_V$ are enumerated on a graph. The evolution is then given by

$$U|c,v\rangle = S\Big(C\otimes I\Big)|c\rangle\otimes|v\rangle = S\Big(C\,|c\rangle\otimes|v\rangle\Big) = S\left(\sum_{a=1}^{d} c_a|a\rangle\otimes|v\rangle\right)$$
$$= \sum_{a=1}^{d}|a\rangle\langle a|\otimes S_a\left(\sum_{a=1}^{d} c_a|a\rangle\otimes|v\rangle\right) = \sum_{a=1}^{d} c_a|a\rangle\otimes S_a|v\rangle,$$

where the S_a operator is the shift along the $|a\rangle$ direction. In the previous example these were the operators $|j+1\rangle\langle j|$ and $|j-1\rangle\langle j|$.

At this point the most effective way to analytically approach this problem is via its eigenvalue problem, and we show that procedure for completeness. This was established in one of the first systematic examinations of properties of quantum walks, in 2001 [14]. In order to simplify the presentation the one-dimensional walk is analyzed, and on the cycle (the line with n nodes with identified ends), which does not, however, rob one of generality. The following analysis can be carried over to any graphs of constant order.

The shift performed after the coin-based choice (projection) of direction on the graph is the group action, that can be understood as shifting the graph, $S_a|v\rangle = \chi(g_a^{-1})|v\rangle$, where $\chi(g_a^{-1})$ is the character of the (inverse of the) corresponding group element g_a. Then the action of the evolution operator is

$$U|c,v\rangle = \Big(\sum_{a=1}^{d}\chi(g_a^{-1})\,c_a|a\rangle\Big)\otimes|v\rangle.$$

This means that we need eigenvectors for the operator $H_k = \mathrm{diag}\{\chi(g_a^{-1})\}\cdot C$, where k labels the representation. At this point we specify the cycle, for which the group action is the rotation by nodes, and with $w^k = e^{\frac{2\pi i}{n}k}$ the operator is

$$H_k = \begin{bmatrix} w^k & 0 \\ 0 & w^{-k}\end{bmatrix}\frac{1}{\sqrt{2}}\begin{bmatrix}1 & 1\\ 1 & -1\end{bmatrix} = \frac{1}{\sqrt{2}}\begin{bmatrix}\omega^k & \omega^k\\ \omega^k & -\omega^k\end{bmatrix}$$

Now the eigenvalue problem can be solved. (For some more detail see Appendix B.)

The sketched construction from [14] yields theorems about this walk, establishing natural analogs of mixing times and other quantities critical in uses of randomized algo-

rithms in classical computing. (However, note that the unitary quantum evolution does not reach a stationary state.) The limiting distribution is uniform over the nodes of the graph, and is independent of the initial state, while the exact behaviour of the walk does strongly depend on the initial state.

On the cycle or line quantum walks are nearly quadratically faster than the classical ones, and algorithmically (in terms of complexity) the speedup is quadratic: In n steps the peak(s) of the quantum process are located $\sim n$ away from the starting node, thus the quantum walk propagates linearly with time. This is called ballistic propagation. In classical random walks the site reached in n steps is $\sim \sqrt{n}$, which is diffusive propagation. An important finding is that for general graphs, quantum walks are at most polynomially faster. So to utilize them for significant speedups one needs applications in particular problems, not mere speed of propagation. The fact that they can propagate up to quadratically faster surely helps with this quest.

Next we briefly introduce continuous-time quantum walks, for completeness of an overall view of quantum walks. (This thesis is concerned exclusively with discrete-time quantum walks.) While they are a very different construct, they still are quantum mechanical processes on a discrete space with mixing of components and the general properties of quantum walks are the same as for the described discrete-time ones.

1.2.2 Continuous-time quantum walks (CTQW)

The continuous time quantum walks are again processes on a discrete space with mixing of components at every step. However, beyond this they differ markedly from the discrete-time ones: Everything happens in one space (no auxiliary "coin" spaces), transitions happen continuously in time, and these walks have a tight formal similarity to classical random walks. The CTQW formalism reflects the physical properties of the process more directly, and are simpler to use in comparison; on the other hand, the extra degree of freedom of the DTQW (the "coin" which is usually some internal degree of freedom like spin) does afford that approach with more flexibility in implementations, and possibly more power in algorithmic uses. We should mention here that the precise relation between continuous- and discrete-time quantum walks is not well understood, which is one of the long standing questions in this field. Mainly because of the 'extra' space used by DTQW, so far it has not been found how to directly reconcile these two

processes. This is very different from the classical case, where walks continuous and discrete time walks are very directly related. The clearest findings are certain relations in their limiting behaviour [15, 16], which loosely speaking relate a DTQW to two CTQW's. In the following description we again consider the Hilbert space of states as enumerated on a graph.

The CTQW on a graph is defined by a *direct* analogy with a continuous time classical random walk. In general, given a graph G with N vertices[6] one can define the *adjacency matrix*

$$A_{jk} = \begin{cases} 1 & (j,k) \in G \\ 0 & \text{otherwise} \end{cases}$$

which describes the connectivity of G, as the non-zero entries are associated with pairs of nodes that are connected. In terms of this matrix, for the purpose of convenience one can also define the *Laplacian* $L = A - D$, where D is the diagonal matrix with $D_{jj} = \deg(j)$, the degree of vertex j (number of nodes it is connected to). The continuous time random walk on G is a Markov process with a fixed probability per unit time γ of jumping to an adjacent vertex. In other words, the probability of jumping to any connected vertex in a time ϵ is $\gamma\epsilon$ (in the limit $\epsilon \to 0$). This walk can be described by the first-order, linear differential equation

$$\frac{dp_j(t)}{dt} = \gamma \sum_k L_{jk}\, p_k(t)\,, \tag{1.2}$$

where $p_j(t)$ is the probability of being at vertex j at time t. This is a stochastic matrix, with columns of L summing to zero, conserving probability.

A continuous time quantum walk encoded on a graph takes place in an N-dimensional Hilbert space spanned by states $|j\rangle$, where j is a vertex in G. Then one can write a general state $|\psi(t)\rangle = \sum q_j(t)|j\rangle$ in this basis, with amplitudes $q_j(t) = \langle j|\psi(t)\rangle$, as usual. The dynamics of the system is then given by the Schrödinger equation in this discrete space,

$$i\hbar \frac{dq_j(t)}{dt} = \sum_k H_{jk}\, q_k(t), \tag{1.3}$$

where H is the Hamiltonian. The similarity with the classical random walk (1.2) is striking. They are related simply by $H = -\gamma L$, with the remaining factor of $\boldsymbol{i}$. In other

[6] The graph is "undirected" (transitions are the same in either direction) and with no self-loops.

words, the CTQW can be understood as defined by letting $H = -\gamma L$ for a classical random walk and with added $\boldsymbol{i}$. Thus to build a CTQW for some problem we construct the Laplacian (or the adjoint matrix) for the graph on which this problem is represented, and this gives us the Hamiltonian as $H = -\gamma L$. Then the dynamics follows from the discrete Schrödinger equation (1.3); the physics here is transparent. The complex constant in the quantum walk makes a world of a difference between it and classical random walks, of course. Still, the formal similarity between them is useful, given the large body of knowledge about classical stochastic processes.

There are variations in how CTQW are defined. First, the choice of the sign is such that the Hamiltonian is positive semidefinite. In that sense, $L = A - D$ was defined so that L on a lattice is a discrete approximation to (continuous) ∇^2. A free particle in the continuum has the positive semidefinite Hamiltonian $H = -\nabla^2$ (in appropriate units).

Another comment regards the use of the Laplacian for CTQW definition. The Laplacian is not the only possible Hamiltonian for a quantum walk. While the classical walk (1.2) requires $\sum_j L_{jk} = 0$ to be a valid Markov process (conserving probability), for the process (1.3) it is required that $H = H^\dagger$, so that it is a valid (unitary) quantum process. Then one could also choose, for example, $H = -\gamma A$, and this is done often as well. For non-regular graphs the two choices result in different walks.

1.2.3 Overview of the development of the field and literature

To conclude this introduction here we briefly summarize the development of the field of quantum walks, with a basic overview of the literature. An explicit model for a quantum walk was introduced in 1993 for DTQW [17], and as an approach to using quantum mechanics for decision problems in 1998 for CTQW [12]. (Note that an interesting, while not often credited, work [18] from 1992 treated tunneling diffusion with "quantum random walk model.") Around the turn of the decade the idea of quantum walks was thoroughly examined and many properties analogous to classical random walks were introduced [14, 19, 20]; the basics of the field were established. A standard and most quoted review by Kempe [21] at this point must be considered dated, but it is an excellent introduction to the field. A somewhat newer overview with focus on algorithms is [22].

Over the following decade some important algorithms were found, along with ones useful to many standard problems. Highlights of successful algorithms include exam-

ples of an exponential speedup over classical computation [23, 24], and algorithms with polynomial speedup: Spatial search [25–29], optimal algorithm for element distinctness [30] which was generalized [31] (and used for triangle finding, checking matrix multiplication and testing group commutativity), evaluation of balanced binary tree games [32] and Boolean formulas [33–35]. A recent thorough survey is given in the introduction of [15]. A gentle overview of uses is [36]. The general focus on decoherence in quantum computing has not missed quantum walks, for a review see [37].

In a more general sense, quantum walks have been recognized as a "universal computational primitive" with CTQW [38], and then in a similar manner with DTQW [39]. This makes them a complete model for computation. Recently, a thorough work constructed and analyzed such a model using many particles, finding serious improvements and possibility of efficient implementation [40].

As mentioned earlier, quantum walks are also used for fundamental investigations and modeling of physical systems in general, unrelated to quantum computing. Some problems for which quantum walks are used include: quantum lattice gases [13], arrow of time [41], generalized quantum theory [42], exciton trapping [43, 44], topological phases [45], quantum phase transitions [46], novel topological constructs (non-Abelian anyons) [47]. Examples of general physical modeling include phenomena such as electrical breakdown [48, 49], photosyntesis [50, 51], topological transitions with application to spin pumping and vortex transport [52], use of continuous time quantum walks in transport phenomena [53], Anderson localization [54], molecule formation [55], and with an early precursor of quantum walks, quantum diffusion [18].

Implementations have been carried out in various systems over years. Current interest in quantum computing toward realistic (scalable) solutions translates into similar trends in quantum walks as well. Since it is mostly difficult to estimate how scalable various systems will prove, the search for the most promising candidates is ongoing. The ideas that come up are sometimes new in the corresponding branches of physics.

Some of the most prominent current approaches are now briefly mentioned, as an illustration rather than a comprehensive review. Developments with NMR (for example [56]) are now seemingly considered unlikely for large scale implementations, but are still being pursued. Trapped ions are used, for example for constructing a walk in phase space [57] and in position space [58], with two ions [59] reporting a walk with 23 steps, and with a generalized Hadamard coin [60]. (A newer overview of methods with trapped

ions is [61]). Much work has been done with optical approaches, for example: A five-step walk with passive optical elements using coherent states [62], single-photon walks with tunable decoherence [63], with correlated photons [64], study of decoherence and disorder in a 28-step walk of photons on a periodic lattice [65], with waveguides in large systems with negligible decoherence [66], while a new work on a walk with two entangled particles, executed with parallel waveguides written in glass [67], allowed examination of both fermionic and bosonic behavior. This is possibly a new venue in exploration of quantum systems in general. Similar recent study [68] reported continuous transition between statistics. A recent (2012) review of photonic quantum *simulations*[7] is [69]. A demonstration of the entanglement between formal and experimental work is seen in an interesting recent study of entanglement generation by quantum walks [70]. Please note that all this is a sampling of the more prominent works, neither complete nor comprehensive, and that some very interesting (newer) ideas are not mentioned.

1.3 About this dissertation

The work described in this thesis is focused on uses of discrete-time quantum walks along a few research directions. We mostly use the framework that we introduced (Ch. 2), which gives us a tool rather different (sec. 2.1.3) from the standard coined formalism described earlier in this Introduction and thus provides a different approach to various problems. In this section the higher-level ideas and motivation behind this work are described, followed by a brief listing of specific problems and Chapters.

Judged by the lessons from the history of the classical random walks and stochastic processes, the field of quantum walks at this stage can break new ground and expand its reach into new types of problems (or so we believe). Following some of the well-known trends in the development of these classical fields, and having taken cues from some of their techniques and approaches, we identified specific research objectives that also pursue our broader goals, as outlined here. We find these directions to be strongly suggested by the evolution of uses of stochastic processes in classical physics and computing.

While quantum walks originated in physical considerations, early on they were estab-

[7] The original motivation for quantum computing—to use quantum systems in order to simulate behaviour of quantum systems, with efficiency far beyond classical computers. "Quantum simulations" is one field where useful results can be expected with as little as 50 qubits (according to some authors).

lished entirely as an algorithmic tool. Further, almost all effort in DTQW has been put behind one approach, where additional internal spaces are used to mix components, mimicking classical coins. This has brought successes, but not as much as hoped for, while there are other approaches and yet other possibilities. Also, a very different approach that is employed by CTQW, where walks happen in one space, has proven considerably more successful. It is also intriguing that yet many other analogs in the classical probability and stochastic techniques have decidedly not been explored. On the other hand, along with their algorithmic purpose, quantum walks are legitimate (and very interesting) quantum processes in their own right, but only recently have diverse groups started using them as a tool for various explorations of physics.

We offer an approach that we believe brings together these two aspects, the constrained algorithmic use of DTQW and its undeveloped general use in physics. Being motivated by classical walks with memory (sec. 2.1.1), a field with a lot of experience from classical sciences, we think that it should be a good algorithmic tool, while it is in our opinion also suitable for utilizing the unitary (memoried) nature of quantum walks. Additionally, it removes the need for auxiliary ("coin") spaces, which are of a completely different nature and technically hard to handle in problems with any complexity. This is the first and main thrust of the work presented here: Uses of an approach that seems suitable for quantum processes with their unitarity, that is very different, and technically seems better suited for more complex problems given the absence of coin spaces.

The memory-based framework (sec. 2.1.2) should be promising for algorithmic uses also considering the well-known advantages of biased and memoried approaches in computer science. This is (in principle) demonstrated by solving a problem of a DTQW on the binary tree (Ch. 3), a desirable construct (sec. 3.1) that had not been available previously. On the other hand, the framework should also be a promising tool for fundamental investigations in physics, since by its design it explicitly hints at the unitarity of quantum evolution.[8] This is reflected in our construction and solution of a walk that carries deeper memory (Ch. 4), thus exploring the quantum nature of the walk and some subtle (and some not so subtle!) appearance of anomalies, or of classical

[8] Here is a brief digression offered as support. The accepted resolution of the two-decade lasting information-loss paradox in black hole physics came about by insistence on the critical role of the unitarity of quantum evolution (of the scattering matrix in QFT) [71]. It resulted in the formulation of the holographic principle—which in turn connects to some fundamental ideas in quantum computing.

features. Various physics exploration and modeling has been done with CTQW by now (sec. 1.2.3). Removing coin spaces and implementing memory in the construction, as in our framework for example, should help a step in that direction for DTQW as well.

Quite separately, but still due to properties of the introduced framework, another surprising possibility came up; this is our second driving idea. It is known that quantum computing in principle allows one to use the Fourier transformation *alongside with* the quantum analog of randomized approaches, that is, of quantum walks.[9] This is strictly off limits in the classical sciences; Fourier transforms *or* randomized algorithms—these are the two main tools. In our framework these ideas come together very directly (sec. 5.1), what is otherwise possible *in principle*—but has not been done. It is very clear that a tool combining the primary approaches would wield unmatched power. We apply this idea to a toy but interesting problem (sec. 5.2), followed by a detailed and involved roadmap for making this into a well-rounded research direction (sec. 5.2.1).

There are other ideas, but the described ones are in a sense an overriding motivation behind this work: Use of a different framework, and a relaxed and flexible use of walks with Fourier transformation. In short, to introduce fresh approaches, and thus to pose and solve problems of interest that have been inaccessible or unnoticed so far.

Much of work in this thesis is centered around the framework [72] and its exploration and applications, commented above. The exception is Chapter 6, on walks on non-Abelian groups (precisely, on the permutation group S_n). The material in Chapters 2 and 3 is published [72], the work described in Chapter 4 is mostly completed and is being prepared for publication. The results in the Chapter 5 are very distinct findings, but for which we still want to find a specific application and communicate them in that fashion. The Chapter 6 on a walk on S_n contains some partial and preliminary research results on a well-known direction which is unexplored, difficult, and promising. While the results are distinct and on the level of known published work, we consider this a work in progress.

Appendices contain some of the "usual" appendix-style material (side calculations and such), but also a lot of material that is integral for the presented work, which has been relegated to appendix in order to enhance the readability of the main text.

[9] Classical stochastic techniques are based on the very efficient exploration of the phase space, examining global properties through local evolution. Quantum walks have the mixing of components instead of stochasticity, while they also have superposition of states and entanglement that makes them see larger structures. In spite of the differences, they may well be a true—and better—analog.

Chapter 2: A framework for discrete-time quantum walks

Much of the development of quantum walks has been motivated by classical random walks and stochastic processes. In that, ideas were drawn almost exclusively from *memoryless* classical walks. These are processes where the 'walker' only knows its current position in the state space: As the coin of is flipped (the stochastic evolution operator applied) and the next step is taken, no "memory" remains of the previous position: There is nothing in the state that would keep any information about the previous state. The classical Markov process very quickly reaches a state where its distribution reveals no information about how the process got into that state. This is an important property of the classical Markov chains.

However, quantum walks are unitary processes—they are reversible and thus in principle should be thought of as carrying memory of the previous evolution. One can turn time and track the evolution backwards, which is directly opposite to the basic property of memoryless evolution of classical random walks. The relation between unitarity and memory in quantum evolution in general has been noted [13, 42] but not studied explicitly, at least not in this context.

On the other hand, in the theory of probability there is a large body of work on walks with "internal states," which provide important models in a range of sciences. In short, these are processes where the state has more information than merely its position on the graph (in the state space). An important special case are "walks with memory" where the internal state is some particular information about the previous evolution.[1] A common example is the "persistent walk" ("walk with inertia" or "correlated walk"), where the state is described by its position on the graph and by the direction of the step just taken (in getting to that state). The state of such a walk can be given by two indices, of the previous and current sites on the graph, for example. Then the assignment of probabilities for evolution (for the next step) is based on this information: The probability to continue (p) is different from the probability to reverse ($1 - p$), and

[1] The "internal state" in principle can mean more general kind of information. For example, it may not necessarily change at every step.

one rather thinks of an arrow describing the motion in the state space. This walk can be treated as a memoryless one as well (see 2.1.1 for a comment and A.2 for full analysis) but it is clearly a considerably different process. An explicit example is used below.

Altogether, if one is to use classical stochastic processes as any guide, it appears reasonable to ask whether an approach to quantum walks based on classical random walks *with memory* can be beneficial, and possibly superior. Following this, we introduced a framework for construction of discrete-time quantum walks [72] that is directly based on classical walks with memory. It utilizes a particular representation of that classical process, that we also introduce, that is very convenient for building quantum walks.[2] The framework is proving itself to be a fruitful source of new approaches to some problems of interest in quantum computing, and some of these ideas are described in this document.

In order to motivate the memoried approach to quantum walks explicitly, and to set an example for later use, we next present a simple example. First, the property of a one-dimensional "persistent walk" mentioned above is stated precisely: If the walk is at site i (on the graph, representing a state in its $\mathcal{H}$) and it came to it from the site $i-1$, then it has the probability p to go in the next step to site $i+1$ (to continue) and probability $1-p$ to go to site $i-1$ (to reverse direction). If it has arrived to i from te other direction $(i+1)$, then the probability to step to $i-1$ (to continue) is p and the probability to go back to $i+1$ (to reverse) is $1-p$.

Hadamard walk as a persistent walk Consider a standard coined quantum walk in 1 dimension, on the line, as analyzed in the introduction. But now let us relax the probabilities in the Hadamard matrix and use for the coin operator the generalized Hadamard instead, and evolve the state for one step starting from sharp up ($|\uparrow\rangle$) and down ($|\downarrow\rangle$) states. Recall that the action of the 'coin' operator,

$$C \;=\; \begin{pmatrix} \sqrt{p} & \sqrt{1-p} \\ \sqrt{1-p} & -\sqrt{p} \end{pmatrix}, \quad \text{here on the 'coin state'} \quad |\uparrow\rangle \;=\; \begin{pmatrix} 1 \\ 0 \end{pmatrix},$$

is followed by the conditional shift,

$$S \;=\; |\uparrow\rangle\langle\uparrow| \otimes \sum_j |j+1\rangle\langle j| \;+\; |\downarrow\rangle\langle\downarrow| \otimes \sum_j |j-1\rangle\langle j|.$$

[2] The classical representation has been tailor-made for this purpose.

Thus we have, starting from the 'up' state,

$$S \cdot (C \otimes I) \left|\uparrow\right\rangle \otimes \left|i\right\rangle = S \cdot \left(\sqrt{p} \left|\uparrow\right\rangle \otimes \left|i\right\rangle + \sqrt{1-p} \left|\downarrow\right\rangle \otimes \left|i\right\rangle\right)$$
$$= \sqrt{p} \left|\uparrow\right\rangle \otimes \left|i+1\right\rangle + \sqrt{1-p} \left|\downarrow\right\rangle \otimes \left|i-1\right\rangle. \tag{2.1}$$

For the 'down' ($\left|\downarrow\right\rangle$) initial coin state,

$$S \cdot (C \otimes I) \left|\downarrow\right\rangle \otimes \left|i\right\rangle = \sqrt{1-p} \left|\uparrow\right\rangle \otimes \left|i+1\right\rangle - \sqrt{p} \left|\downarrow\right\rangle \otimes \left|i-1\right\rangle. \tag{2.2}$$

This is precisely a persistent walk, as described classically: It continues moving in the same direction with the probability p (obtained by squaring the amplitude), while it changes the direction with the probability $1-p$. In the states with superposition of coin-states the action is the same, on each component. The superposition of states in Hilbert space provides for the enlargement of the space dimension discussed in our classical persistent walk example (which accommodated for modes moving in different directions). On a cycle (a line with N sites and identified ends) with its periodicity we have $\left|i+1\right\rangle = \omega^{-k}\left|i\right\rangle$, where $\omega = e^{2\pi \boldsymbol{i}/N}$, and the evolution can be represented as

$$U\left|c,v\right\rangle = S \cdot (C \otimes I) \left|c\right\rangle \otimes \left|v\right\rangle \;=\; \frac{1}{\sqrt{N}} \begin{bmatrix} w^{-k}\sqrt{p} & w^{-k}\sqrt{1-p} \\ w^{k}\sqrt{1-p} & -w^{k}\sqrt{p} \end{bmatrix} \left|c\right\rangle \otimes \left|v\right\rangle$$

We have the same eigenvalue problem as in the unbiased example of [14], but yielding a clear and natural interpretation of a persistent walk.

General coin has been studied (for example, [46, 60, 73, 74]), as well as persistent ("correlated") walks and their relation to DTQW [16, 75, 76]. With this example we point out the direct correspondence between them. Note that the directionality of the walk shows up as soon as the coin transformation is allowed to have $p \neq 0.5$. In other words, the standard Hadamard transform generally implements a persistent walk (rather than a memoryless one), only with equal probabilities.

2.1 Interchange framework for discrete-time quantum walks

In this section the framework for DTQW is constructed, that forms the core of much of the work described in this document. We first construct a representation for classical

walks with memory, in particular for walks with memory $k = 2$, that is, with one-step memory. Then this is used as an analog to define a quantum walk. The main charactertics of walks defined this way are: They do not need auxiliary coin spaces, while they propagate on the product of (state) spaces; the evolution is completely controlled by a local operator, assigned to every vertex of the graph, acting both as a coin and as a scattering operator; this operator acts only in one space of the product, and it can be chosen without any constraints other than unitarity. This framework unifies all other major approaches to discrete-time quantum walks: It implements memory in the walk (more directly and generally than the Szegedy walk [77]), the core component of the evolution operator mixes components like the standard coin operator does, and it acts like a scattering operator in the "scattering walk" [78–80]. Also, these approaches are directly reproduced from it. Its relation to the standard coined walk, to the Szegedy walk, and to the scattering walk are discussed in the last section. Note that the following classical representation is not needed for the construction of the quantum walk framework, but is presented for insight.

2.1.1 A representation for classical memory–2 walks

Walks with memory 2 are such Markov processes where the next step depends on two states: the current one, and the previous one. Walks with memory are generally studied by using a suitably enlarged state space. In particular, a memory–2 Markov chain can be represented as a memoryless one over the space with n^2 states. The transition matrix is then large ($n^2 \times n^2$) and sparse.

Instead, here we represent a Markov chain with memory k by a probability distribution $\mu(t)$ of dimension k, while the Markov tensor $\mathcal{M}$ is then of dimension $k+1$. For a memory–2 walk over n sites, the space has dimension n, and each state is labeled by two indices (the site the walker came from, and the current site). So the probability distribution is 2–dimensional,

$$\mu(t) = \begin{bmatrix} \mu_{0,0}(t) & \cdots & \mu_{0,n-1}(t) \\ \vdots & & \vdots \\ \mu_{n-1,0}(t) & \cdots & \mu_{n-1,n-1}(t) \end{bmatrix}.$$

The matrix μ_{ij} can also be given by a column of rows r_i, or by a row of columns c_i, what we will use shortly. The following representation for the third-rank tensor $\mathcal{M}$ and its action is convenient.

Let $p_{ij|k}$ be the conditional probability for the transition $j \to k$, given that the walk came to j from i. All transition probabilities $\{p_{ij|k}\}$ define the evolution operator $\mathcal{M} = [P_0 P_1 \dots P_{n-1}]$, as n layers of $n \times n$ transition matrices P_j, $j = 0, 1, \dots, n-1$, one for each site:

$$P_j = \begin{bmatrix} p_{0,j|0} & p_{0,j|1} & \cdots & p_{0,j|n-1} \\ \vdots & & & \vdots \\ p_{n-1,j|0} & p_{n-1,j|1} & \cdots & p_{n-1,j|n-1} \end{bmatrix}.$$

P_j are by construction transition probability matrices, and this is the only requirement imposed on them.

The evolution of the state, $\mu_{t+1} = \mu_t \, \mathcal{M}$, with $\mathcal{M}$ acting to the left, is defined as

$$\mu(t) \mapsto \mu(t+1) \; : \; r_j(t+1) = c_j^{\mathsf{T}}(t) P_j,$$

for each $j = 0, 1, \dots, n-1$, where r_j and c_j^{T} are the j-th row and transposed column, respectively, of the matrix μ. In words: *at each site j, the P_j associated with that site acts on the transposed j–th column of $\mu(t)$, giving the j–th row of the evolved $\mu(t+1)$.*

Instead of an $n^2 \times n^2$ probability matrix, we use a set of n different $n \times n$ probability matrices P_j. They implement the evolution: the j–th column of $\mu(t)$ has probabilities to arrive to j from any site, and after the action of P_j the j–th row of $\mu(t+1)$ has probabilities to go from j to any site. Thus action of all transition matrices on all columns evolves the probability distribution over all paths. The stochastic nature of the process is carried by the assignment of $\{p_{ij|k}\}$ transition probabilities in P_j matrices [3].

The P_j transition matrices are simple in most cases of interest. Consider the cycle, a space $\{0, 1, \dots, n\}$ with identified ends (0 and n), with only nearest-neighbor transitions, $(j \pm 1, j) \to (j, j \pm 1)$. Take the persistent walk, with probability p to continue, and $1-p$ to reverse,

$$\begin{aligned} &(j-1, j) \to (j, j+1), \quad \text{with probability } p \\ &(j-1, j) \to (j, j-1), \quad \text{with probability } 1-p. \end{aligned}$$

[3] This representation is not explored in the literature.

To obtain this walk, the P_j matrices have the following block centered at (j,j) (mod n),

$$P_j \quad : \quad \begin{array}{|ccc|} \hline 1-p & 0 & p \\ 0 & 1 & 0 \\ p & 0 & 1-p \\ \hline \end{array} \qquad \begin{array}{l} \text{This block is centered at } (j,j) \text{ (mod } n), \\ \text{with 1s on the rest of the diagonal, and} \\ \text{0s elsewhere (except for B.C.).} \end{array} \tag{2.3}$$

The rest of the diagonal of P_j has 1s, other elements are 0, except for the transitions between sites $0 \equiv n$, and $n-1$ or 1 (boundary conditions), which are $p_{0,n-1|0} = 1-p$ (reverse), $p_{0,n-1|1} = p$ (continue), etc. Action of these P_j by the above prescription carries the walk.

2.1.2 Quantum walks: The interchange framework

The above classical procedure for memory–2 walks is directly elevated to define quantum processes. Consider a basis in an N–dimensional Hilbert space, with vectors labeled as $\{|i\rangle, i = 1, 2, \ldots N\}$. They represent states that the walk is performed on, enumerated on a general graph. The full state of the walk is in the product of such spaces ($\mathbb{C}^N \times \mathbb{C}^N$), spanned by these bases, and it is given by states at the previous ($|i\rangle$) and current ($|j\rangle$) step,

$$|\psi(t)\rangle = \sum_{ij} c_{ij}(t)\, |i\rangle \otimes |j\rangle. \tag{2.4}$$

The evolution is specified by

$$|\psi(t+1)\rangle = \widehat{U}\widehat{X}\, |\psi(t)\rangle, \quad |\psi(t)\rangle = (\,\widehat{U}\widehat{X})^t\, |\psi(0)\rangle, \tag{2.5}$$

where $\widehat{X}$ is the interchange operator, and $\widehat{U}$ is defined via unitary operators U_j in $\mathbb{C}^N$, assigned for each site,

$$\begin{aligned} &\widehat{X}\colon\ |i\rangle \otimes |j\rangle \mapsto |j\rangle \otimes |i\rangle \\ &\widehat{U} = \sum_{j=0}^{N-1} \Pi_j \otimes U_j, \quad \text{where} \quad \Pi_j = |j\rangle\langle j|. \end{aligned} \tag{2.6}$$

Π_j selects the first state in the product, and U_j acts on the second. Note that while the construction utilizes the product of states, the key component of the evolution operator

(U_j) acts on single states. Before explicit examples, we make a few general comments.

Consider a state of the walk $|i\rangle \otimes |j\rangle$, as represented by an arrow pointing from the previous (i) to the current (j) site. The interchange initiates the walk forward by 'reversing the arrow.' Then the U_j operator distributes the 'tip of the arrow,' now at the originating site i, to all sites the process can access. They are generally in the subspace of adjacent nodes. Thus the evolved superposition is obtained. This is best seen in the forthcoming example of the binary tree (Fig. 3.2). The definition (2.5) can be given in terms of one $(N^2 \times N^2)$ matrix. However, the explicit separation of the reversal $(\widehat{X})$ is crucial, providing the following: Then U_j completely control the evolution over the site j, by acting on the originating state $|i\rangle$, and sending the process over all paths to a new state.[4] The framework does not place any conditions on these operators, except for unitarity of quantum evolution. We are free to choose (or construct) them as needed to implement quantum walks. They can be adjusted for each site as well (by construction), and/or with time. We will see examples for all these properties.

Note that this construction needs no mention of classical processes. The representation of classical memoried walks in Sec. 2.1.1 is given for motivation and insight, and we now comment on this relation. The discussed interplay between interchange and (local) U_j, critical for this formulation, has a clear analog in the classical representation—recall the transposition before (local) P_j evolve the distribution. Also, the freedom to craft any (unitary) U_j to implement quantum walks corresponds to a classical property, as P_j may be any (probabilistic) matrices. Finally, the classical representation has no explicit coin toss, and there is no need in the quantum case to mimic randomization via a coin degree of freedom; here U_j drive the walk and mix components.

In this section we presented the formal definition of the framework, along with a few comments. Its utility is seen in its use, and some examples follow immediately, with much more in the later Chapters. In the context of the discussion of the relation of this formalism to other approaches, the next section begins with an example of the construction of a DTQW in the most familiar setting, for a walk on a line. In that case it is most clearly seen how to reproduce coined walks, and how this framework relates to them.

More representative constructions come in the next two Chapters, showing first a

[4] For a superposition $\sum a_k |i_k\rangle \otimes |j\rangle$, where k indexes all adjacent nodes, after $\widehat{X}$'s action on all componentes the operator acts on each one in turn, $\left(|j\rangle\langle j| \otimes U_j\right) \sum_k |j\rangle \otimes |i_k\rangle = \sum_k |j\rangle \otimes U_j |i_k\rangle$.

walk on the binary tree, and then a walk with an increased level of tracked correlation (with a two-step memory). Such walks display substantially different features. The two-step-memory walk in Chapter 4 also allows a much deeper view of the relation of this model with the coined formalism. Finally, the walk over connected graphs in Chapter 5 uses the framework for a very different problem, which is not clear at all how to approach with coined walks.

2.1.3 Relation to other approaches

For a comparison with a memoryless (coined) approach, consider a walk on the line, over the state space $S = \{|j\rangle, j = 0, 1, \ldots\}$. The quantum walk (2.1)–(2.2) is obtained with

$$U_j(p) = \begin{bmatrix} \ddots & & & & & & \\ & 1 & & & & & \\ & & \sqrt{1-p} & 0 & \sqrt{p} & & \\ & & 0 & 1 & 0 & & \\ & & -\sqrt{p} & 0 & \sqrt{1-p} & & \\ & & & & & 1 & \\ & & & & & & \ddots \end{bmatrix}, \quad \text{centered at } (j, j).$$

The rest of the diagonal has 1s, other elements are 0. (On a cycle there are elements needed for boundary conditions, like in the classical case.) The square roots provide for probability being the square of the amplitude, the $-\sqrt{p}$ sign is needed for unitarity. In this simple case, the choice of U_j follows from the classical memoried walk (2.3), but in general a classical analog is not needed.

To see the equivalence with the coined walk, look at one evolution step from sharp states. Starting from $|i-1\rangle \otimes |i\rangle$ (the system is in the state $|i\rangle$, having been in $|i-1\rangle$ at the previous step),

$$\begin{aligned} \widehat{U}\widehat{X}\,|i-1\rangle \otimes |i\rangle &= \widehat{U}\,|i\rangle \otimes |i-1\rangle \\ &= \Big(\sum_{j\in S} |j\rangle\langle j| \otimes U_j\Big)\,|i\rangle \otimes |i-1\rangle \\ &= \sqrt{1-p}\,|i\rangle \otimes |i-1\rangle + \sqrt{p}\,|i\rangle \otimes |i+1\rangle. \end{aligned}$$

Similarly, for the initial $|i+1\rangle \otimes |i\rangle$ state,

$$\widehat{U}\widehat{X}\,|i+1\rangle \otimes |i\rangle = -\sqrt{p}\,|i\rangle \otimes |i-1\rangle + \sqrt{1-p}\,|i\rangle \otimes |i+1\rangle.$$

This is an isomorphism of the memoryless–based walk (2.1)–(2.2), via identification

$$|i-1\rangle \otimes |i\rangle \Leftrightarrow |\uparrow\rangle \otimes |i\rangle \quad \text{and} \quad |i+1\rangle \otimes |i\rangle \Leftrightarrow |\downarrow\rangle \otimes |i\rangle.$$

This analysis applies to arbitrary superposition of such states, as each component is evolved separately. The choice of $p = 1/2$ restores Hadamard walk. Thus the interchange framework reproduces coined quantum walks on the line directly, with the above choice for U_j. Similarly, any coined walk can be encoded in U_j. We will see an involved example in Chapter 4, along with a detailed comparison of that construction to a particular related coined walk in Sec. 4.3.

Memory in quantum walks is mentioned in literature. For example, it was noted in study of the classical limit via decoherence and multiple coins [81, 82]. Incidentally, a direct relation between coined walks and classical memoried walks was observed [83], but not discussed. Recently a particular "quantum walk with memory" [84, 85] was studied. The way "memory" is used in that work has a very different meaning from the one assumed and established here. We draw on the notion of the explicit memory in classical walks, what in quantum processes best relates to history (or explicit correlation over previous evolution). This is pursued in detail in the walk discussed in Chapter 4.

An important approach directly resorting to ideas of memoried walks is the Szegedy walk [77]. This is the most prominent tool in DTQW not using a coin degree of freedom, chosen for that reason to examine the relation between DTQW and CTQW in [15], for example. Its construction starts from a classical Markov chain, and the resulting evolution operator explicitly carries classical transition probabilities. The Szegedy walk is contained in the interchange framework, via the specific choice

$$(U_j)_{km} = 2\sqrt{p(j,i_k)p(j,i_m)} - \delta_{km},$$

where $p(i,j)$ need be classical transition probabilities. The approach discussed here does not require a specific form of the evolution operator. It is fully defined by (2.4)–(2.6) alone, without reference to classical walks, and quantum processes with desired

properties are set by choosing U_j without constraints. Some benefits of this are seen in the next section, where we construct a symmetric DTQW on a semi-infinite binary tree. A Szegedy walk on a binary tree cannot be obtained with equal probabilities for each branch, as there is no (real) solution for probabilities $p(i, j)$ which yield 1/3 probability for the quantum walk.[5]

Szegedy walk is also a translation of a memoryless walk into a walk with memory. The interchange framework is a direct analog of an explicit representation for memory–2 Markov chains. This is reflected in some of its properties, discussed above. The Szegedy walk has also been generalized [86], but in the particular context of search algorithms and in a way very different from what is presented here.

The interferometry–motivated [78] scattering walk [79] has states defined on graph edges, scattering off of vertices (or subgraphs). Its main motivation was related to implementations, for *"a quantum optical network built from passive, linear optical elements such as beam splitters and phase shifters"* [87], proposed in [88] as a follow-up of the model [78, 79] by one of the authors. The initial form had particular constraints on how the walks are constructed. The later, more general formulation [80] can be formally reconciled with the present framework. Scattering walk has recently been used, still in the particular form reflecting the main scattering approach, for certain search problems [80, 89, 90]. These papers hint at the benefits of coinless algorithms. The designs and interpretations of the two frameworks are different, and complementary: The scattering approach is indeed deeply rooted in scattering theory and does not seem directed toward general algorithm construction, nor to ideas related to stochastic processes, both of which underlie the motivation, construction, and expected uses of the present framework.

Two newer approaches relate to the framework described here. A "quantum snake walk" introduced in [91] works with the paths taken by the walk, what in principle relates to one of the directions we pursue (see Ch. 4). However, their construction is aimed at a very particular idea, is strictly one-dimensional, and it is for CTQW.

A more established paper [92] introduces "inhomogeneous quantum walks," in which the probability amplitude for transitions depends on the position. Their coin may be different at different states, which clearly introduces many possibilities. As this work indicates, the position dependent coin has been seen in the past (see references in this

[5] In the Szegedy walk the above equation is solved for $p \in \mathbb{R}$ (since p draw from a classical walk), such that to obtain U_j for the desired quantum walk. This is by construction and cannot be bypassed.

paper). This is certainly similar to one capability of the interchange framework, to assign different evolution operators to different sites, or generally allow position dependence. It is a built-in property of the framework discussed here, used as needed in a few circumstances, in the next Chapter and more significantly in Chapter 5. The variable coin is a very different property from what we study, but this work is related and it may be interesting to examine how. Note that the formalism of our framework also has a built-in capability to have a time dependent evolution operator as well, $U_j(t)$.

2.2 Discussion

In this Chapter we have constructed a very general framework for DTQW, arising naturally from Markov chains with memory. It is unifying of other approaches: The U_j operator implements (one-step) memory by acting on the originating site, can be interpreted as a scattering operator on j, while mixing components like coined walks do. The formalism is used for a few different problems presented in the coming Chapters. Here we summarize the basic properties of the framework and its intended uses and expected capabilities.

One of the main directions we intend to pursue with this formalism is general algorithm building. We expect very specific advantages over the coined approaches, based on the expectation that quantum processes can explore the state space efficiently (like classical random walks do): The 'arrowed' walk provided by the construction should be helpful for that. Another major benefit is that such walks are formally much less cumbersome and troubling than the coined ones, since the state space (still a product of spaces) does not involve degrees of freedom of a completely different nature. This is directly seen with the construction of the walk on the binary tree (Chapter 3), which we have not yet seen accomplished with coined walks. Both of these factors should also make the approach suitable for general modeling and investigations, and we point out some ideas in the next Chapter.

Another major motivation is the relation between memoried approaches and the unitarity of the quantum mechanical evolution, potentially leading to questions related to foundations of quantum mechanics. We certainly believe that this must make the framework a very interesting candidate for examination of the quantum processes. In this sense, Szegedy's approach is more directly related to our work than any of the others

are, but that walk has a serious restriction on the evolution operator and is complicated to use in practice.

This framework also has a place in the context of our broader research goals. Quantum computing in principle allows for Fourier transformation and stochastic approaches, the two major and distinct computational techniques, to be used together. The formalism that we presented can facilitate this, as seen to some extent with construction of networks in Chapter 5. These ideas are introduced in the context of the work presented there, and will be further discussed in the Conclusion.

Before moving to a full example we remark on the versatility of this approach. It reproduces coined walks on the line, the Szegedy's and scattering walks, and handles a walk on a binary tree (next Chapter)—each by a simple choice for U_j. This demonstrates flexibility, and it seems that the framework can help with problems that have so far been prohibitively difficult.

Chapter 3: DTQW on a semi-infinite binary tree

3.1 Significance of the problem and introduction

The binary tree is a common model in physics, a basic data structure in classical computing, and a structure of interest in quantum computing. We offer here a tiny sampling of work that illustrates the breadth of its use.

A computationally important problem is solved in [32], where a quantum algorithm for the binary NAND (not-AND logic gate) tree is constructed, with a distinct improvement over the optimal classical algorithm.[1] An efficient *classical* simulation of quantum many-body systems is accomplished in [93], by computing (classically) certain "tree tensor networks" and starting a new approach in that dynamic field. The paper also shows how to classically simulate any "one-way" quantum computation. Quantum transport efficiency at the nanoscale is found to be improved by interactions with environment in [94]. To round up this briefest listing of uses of the binary tree we mention the study of ground states of quantum critical Hamiltonians in many-body systems [95].

Perhaps more to the point, one of the initiating works in the field of quantum walks [12] used it as a model for decision trees, one of the most successful present algorithms [23] solves a particular problem on connected binary trees and, along with the mentioned NAND tree problem—they all use CTQW.

We have not seen any such progress in using DTQW on the binary tree. This seems to be due mostly to trouble in handling coin spaces that are necessary for (coined) DTQW. In this section we use the established framework to set and calculate a symmetric DTQW on the semi-infinite binary tree. We orient our tree with the root (single starting node) at the left, with the tree spanning to the right, Fig. 3.1.

We focus on the following basic question. The walk is started from a single component state at a site in the tree at a level n, and we wish to find its amplitude at the root as a function of time (step) and the initial distance n. This can be considered an algorithm

[1] The quantum walk's complexity is $O(N^{0.5})$, compared with the best classical $O(N^{0.753})$. This work uses CTQW. It has been applied to the Boolean formula evaluation [33–35].

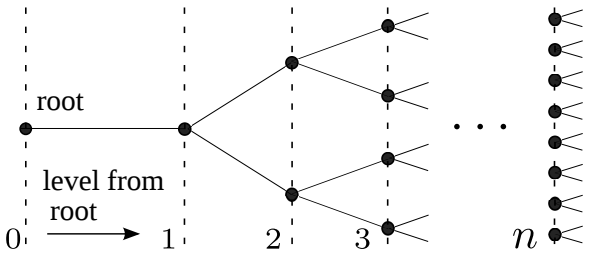

Figure 3.1: Conventions used for our binary tree.

for finding the root of the tree, which may have interesting applications discussed at the close of this Chapter. Note that it is not clear what to expect, in particular in how this will compare with the classical walk on the same structure (Appendix I).

3.2 Interchange framework for a DTQW on the binary tree

The desired symmetric walk has equal probability to step to either of the connecting nodes, having come from either direction. (The analysis remains unchanged for different choices of local U_j.) The state of the walk is given in the direct product of spaces, each spanned by states defined at nodes, $S = \{|i\rangle\}$. Label a node in the tree as j, and the nodes connected to it as i_1 (to its left, toward the root), i_2, and i_3 (to its right, away from the root), as in Fig. 3.2. Consider an evolution step for a single-component state at j, for example $|\psi_0\rangle = |i_2\rangle \otimes |j\rangle$. The action of the interchange $\widehat{X}$ reverses the state. Next we want to write down the U_j matrix, acting on $|i_2\rangle$, such that the evolved state has equal probabilities for either branch. Formally U_j operate in the space of all nodes, but they are reduced to the subspace of nodes to which transitions are allowed; here the adjacent ones. Thus U_j can be written in a block-diagonal form, with the non-trivial transition matrix U_j^{red} in $\{|i_1\rangle, |i_2\rangle, |i_3\rangle\}$, and an identity matrix over the remaining dimensions. The matrix elements need to satisfy the unitarity of U_j and equal squared amplitudes of components of the state evolved by it. The obtained evolution operator, with (reduced) transition matrix U_j^{red} in the basis $\{|i_1\rangle, |i_2\rangle, |i_3\rangle\}$, is

$$U_j = \begin{bmatrix} U_j^{\text{red}} & 0 \\ 0 & \mathbb{I} \end{bmatrix}, \quad \text{with} \quad U_j^{\text{red}} = \frac{1}{\sqrt{3}} \begin{bmatrix} 1 & a & a \\ a & 1 & a \\ a & a & 1 \end{bmatrix}, \tag{3.1}$$

where $a = e^{2\pi \boldsymbol{i}/3}$. This representation holds for graphs of any degree, where dimensions of U_j^{red} and $\mathbb{I}$ change accordingly. At the root the walk can only get reflected, what is performed by interchange $\widehat{X}$; then U_0 is the identity matrix. This will be accounted for. For all other states, we now follow the prescription (2.5)–(2.6). With $\widehat{U} = \sum_{i\in S} \Pi_i \otimes U_i$, the step is

$$\begin{aligned} |\psi_1\rangle = \widehat{U}\widehat{X}\,|\psi_0\rangle &= \left(\sum_{i\in S} |i\rangle\langle i| \otimes U_i\right) \widehat{X}\,|i_2\rangle \otimes |j\rangle \\ &= |j\rangle \otimes U_j|i_2\rangle = \ |j\rangle \otimes \frac{1}{\sqrt{3}}\,(\,a\,,1\,,a\,,0\,,\ldots)^{\mathsf{T}}. \end{aligned}$$

Thus the state is evolved by $\widehat{U}\widehat{X}$ to the superposition

$$|i_2\rangle \otimes |j\rangle \to |j\rangle \otimes \left(\frac{a}{\sqrt{3}}\,|i_1\rangle + \frac{1}{\sqrt{3}}\,|i_2\rangle + \frac{a}{\sqrt{3}}\,|i_3\rangle\right). \tag{3.2}$$

Each component of the superposition (3.2) takes the next step from its node in the same way, and the process spreads over the tree. For a superposition at j, the operator U_j acts on each originating state,

$$\widehat{U}\widehat{X}\,|\psi\rangle^{(j)} = \widehat{U}\widehat{X}\sum_{i\in S} c_{ij}\,|i\rangle\otimes|j\rangle = \sum_{i\in S} c_{ij}\,|j\rangle \otimes U_j|i\rangle,$$

fully specifying propagation over site j. We only need the evolution step of a sharp state for this calculation.

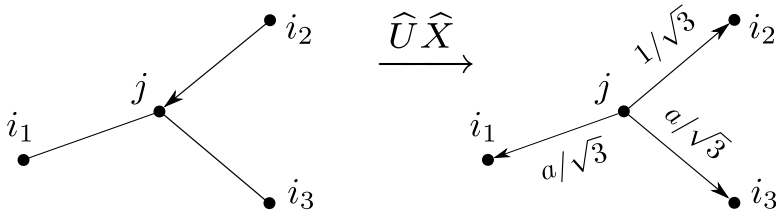

Figure 3.2: A step taken from a state $|i_2\rangle \otimes |j\rangle$, Eqs. (3.1)–(3.2). The state $|j\rangle$ is sent by $\widehat{U}\widehat{X}$ over all available paths. Probabilities for either branch are chosen to be equal, regardless of how the walk approaches the site j (the walk is symmetric). Each component of a general (superposition) state is evolved this way.

In comparison with Markov processes, a quantum walk can be considered as the

evolution of the amplitude distribution. Also, the causality typical of the local dynamics of the classical Markov evolution, seen in Sec. 2.1.1, is reflected in the quantum walk. Note how the concerted action of $\widehat{X}$ and U_j implements the 'arrowed' (memoried) nature of the evolution, mentioned in Sec. 2.1.2.

For organizing the calculation, it is useful to note the connection between directionality and weights of the components of the evolved state. The component that reverses the direction of the previous step has the coefficient $1/\sqrt{3}$, while the other two have $a/\sqrt{3}$, see Fig. 3.2. This is always the case for this walk (not only for $|i_2\rangle \otimes |j\rangle$), since it is symmetric, as explicit in Eqs. (3.1)–(3.2).

Outline of the calculation. The amplitude at the root at time t is computed as a sum of the contributions (amplitudes) of all possible (classical) paths that are at the root at that time. This is practically a discrete form of the path integral for a process with only nearest-neighbor transitions allowed, and is a standard technique [13, 20]. So we count all such classical paths on this structure, weighted appropriately.

The presence of a reflective boundary (the root) complicates the classification and counting, and we use regeneration structures, which are then handled via the z–transform. The obtained explicit expression for the transform is complicated, and analytically the asymptotic of its inverse is found, using the method of steepest descent. The full amplitude is calculated numerically.

For brevity in involved descriptions, we sometimes use "paths $h(t)$" to refer to "those paths that contribute to the part of the amplitude (that is named) $h(t)$."

3.2.1 Path counting and regeneration sums

Enumeration of paths, weighted with appropriate coefficients (amplitude), is a combinatorial problem. Given the symmetry between up and down directions, the tree can be projected to a line bisecting it. The paths on the tree can be classified, and this results in rules for an equivalent walk on that line.

A component of the state at a site is directed either toward or away from the root; and it can either continue in the same direction or reverse it in the next step. For example, the component directed toward the root (to the left) can continue toward the root (taking the branch to the left), with the amplitude $a/\sqrt{3}$, or it can turn and step away

from the root, other branch leading away, with the total amplitude of $(1+a)/\sqrt{3}$. See Fig. 3.2 or Eq. (3.2). Summarized by the direction of the previous step, the walk on the line can take the next step as follows:

When directed away from the root (to the right), it can:

— turn back, with the coefficient $1/\sqrt{3}$ ("*left–turn*");

— continue, with $(a+a)/\sqrt{3}$ ("*right–step*").

When directed toward the root (to the left), it can:

— turn away, with $(1+a)/\sqrt{3}$ ("*right–turn*");

— continue, with $a/\sqrt{3}$ ("*left–step*").

There is a special case, not following the above classification, which complicates the counting of paths considerably. We need to count weighted paths that are at the root at time t. Paths generally reach the root in fewer than t steps, then going back and forth in the tree, possibly touching the root again in the process, before finally finding themselves at the root at time t. Whenever they touch the root their next step can only be a turn back, with the coefficient 1, and this does not fall into the above classification. To account for it the paths need be enumerated particularly carefully.

All paths that are at the root at time t have the following structure. They touch the root for the first time at one point (step s), and we call the amplitude for this part of the path $h_n(s)$. Then they go out in the tree, eventually coming back to the root at step t, possibly touching it multiple times in the process; we call the amplitude of this part of the path $G(t-s)$. This is encoded by the convolution over the first contact with the root, and the amplitude, represented by weighted paths that are at the root at step t, starting from level n, is

$$H_n(t) = \sum_{s\geq n}^{t} h_n(s)G(t-s). \tag{3.3}$$

After the root is touched for the first time, the remainder of the walk is a root–to–root path, considered independently as $G(t)$ (accounting for $n=0$ case, $G(t)=H_0(t)$). It consists of: a "simple loop" $g(s)$, that goes from the root into the tree and back to it (reaching it again for the first time), followed by the rest of the path $G(t-s)$, which may

touch the root multiple times, so again comprised of simple root–to–root loops (Fig. 3.3).

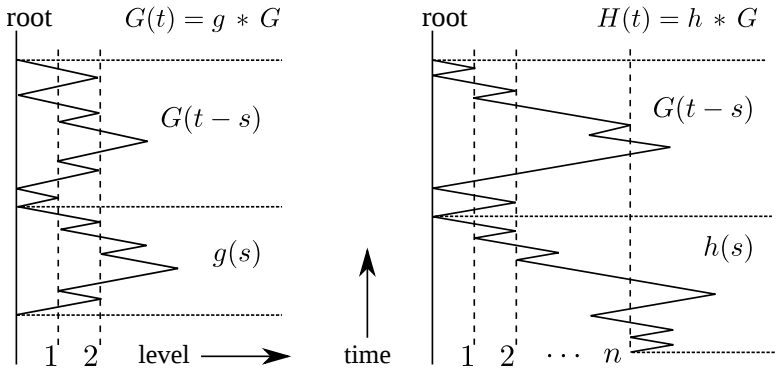

Figure 3.3: The number of paths is a convolution w.r.t. the first contact with root, with the regeneration structure (3.3)–(3.4).

This too is a convolution, with one adjustment. To correctly account for $t = 0$, it must be that $g(0) = 0$, as well as $G(0) = 1$ (since $t = 0 \Rightarrow s = t$). Thus $\delta_0(t)$ need be added. The amplitude of such root–to–root multi–loops $G(t)$ is

$$G(t) = \sum_{s=0}^{t} g(s)G(t-s) + \delta_0(t). \tag{3.4}$$

The regeneration sums (3.3)–(3.4) organize path counting. We work with them using the z–transform,

$$\widehat{f}(z) = \sum_{t=0}^{\infty} f(t)z^t, \quad |z| < 1.$$

Applying this transformation to Eqs. (3.3) and (3.4),

$$\begin{aligned} &\widehat{H}_n(z) = \widehat{h}_n(z)\,\widehat{G}(z), \text{ and } \widehat{G}(z) = \widehat{g}(z)\,\widehat{G}(z) + 1, \\ \Rightarrow \quad &\widehat{H}_n(z) = \widehat{h}_n(z)\,\frac{1}{1-\widehat{g}(z)}. \end{aligned} \tag{3.5}$$

We need transforms of amplitudes of paths reaching the root for the first time, $\widehat{h}_n(z)$, and of simple loops, $\widehat{g}(z)$.

At this point we note a known combinatorial result. The number of paths on a lattice

in two dimensions, going from $(0,0)$ to $(2n,0)$, taking only NE or SE steps, with k peaks, is given by Narayana numbers [96],

$$N(n,k) = \frac{1}{n}\binom{n}{k}\binom{n}{k-1}. \tag{3.6}$$

This expression applies to the number of paths comprising the simple loops g, where peaks are positions furthest from the root. We first need to identify and enumerate "*steps*" and "*turns*" in such paths, so that we can assign weights to them accordingly.

A simple loop must take an even number of steps. The first step is a reversal: it starts at the root, having arrived to it from the first node, and it can only step back onto the first node, so the coefficient for this step is 1. It is straightforward to establish that paths with k peaks take k *left–turns* and $k-1$ *right–turns*. Also, loops of t steps must take $\frac{t-2}{2} - (k-1)$ both *right–* and *left–steps*. Loops with $t = 2$ are different: they can only step away from the root and return to it in the next step (*left–turn*); their coefficient is $1 \times 1/\sqrt{3}$. Thus a simple loop with k peaks, for $t \geq 4$ steps, bears the coefficient:

$$\begin{aligned}
&\left(\frac{1}{\sqrt{3}}\right)^{k}\left(\frac{1+a}{\sqrt{3}}\right)^{k-1}\left(\frac{a}{\sqrt{3}}\right)^{t/2-k}\left(\frac{2a}{\sqrt{3}}\right)^{t/2-k} \\
&= \frac{1}{(\sqrt{3})^{t-1}}\left(\frac{1+a}{2a^2}\right)^{k-1}\left(2a^2\right)^{t/2-1} \\
&= \frac{1}{(\sqrt{3})^{t-1}}\left(\frac{-1}{2}\right)^{k-1}\left(2a^2\right)^{t/2-1} \quad (\text{as } a = e^{2\pi i/3}).
\end{aligned}$$

For $a = e^{2\pi \boldsymbol{i}/3}$ we have $1 + a + a^2 = 0$, used above. Summed over all possible numbers of peaks k, and with $t = 2$ case added, the amplitude of a simple loop is

$$g(t) = \frac{1}{\sqrt{3}}\,\delta_0(t-2) + \sum_{k=1}^{\frac{t-2}{2}} \frac{\left(2a^2\right)^{t/2-1}}{(\sqrt{3})^{t-1}}\left(\frac{-1}{2}\right)^{k-1} N\left(\frac{t-2}{2}, k\right).$$

Using the Narayana numbers (3.6), with $t = 2m+2$,

$$g(m) = \frac{1}{\sqrt{3}}\,\delta_0(m) \;+\; \frac{1}{m\sqrt{3}}\left(\frac{2a^2}{3}\right)^{m} \times \sum_{k=0}^{m-1}\left(\frac{-1}{2}\right)^{k}\binom{m}{k+1}\binom{m}{k}.$$

Since we will need the transform of $g(t)$, it is helpful to write the above sum as an

integral, using the identity (Appendix C)

$$\sum_{k=0}^{m-1}(\alpha\beta)^k\binom{m}{k+1}\binom{m}{k} \;=\; \frac{1}{2\pi}\int_0^{2\pi}\left(1+\alpha e^{ix}\right)^m\left(1+\beta e^{-ix}\right)^m\frac{e^{-ix}}{\alpha}dx.$$

Employing this, under the constraint $\alpha\beta=-1/2$,

$$g(m) = \frac{1}{\sqrt{3}}\,\delta_0(m) + \frac{1}{2\pi}\frac{1}{m\sqrt{3}}\left(\frac{2a^2}{3}\right)^m \times\int_0^{2\pi}\left(\frac{1}{2}+\alpha e^{ix}+\beta e^{-ix}\right)^m\frac{e^{-ix}}{\alpha}dx. \tag{3.7}$$

It is calculationally convenient to take the z–transform of $g(t)$ at this point. Since loops take even number of steps, and $\widehat{g}(z)_{t=0}=g(0)=0$, with $t=2m+2$,

$$\begin{aligned}\widehat{g}(z) &= \sum_{t=0}^{\infty}g(t)z^t = g(0)+g(2)z^2+\sum_{t=4,6,\ldots}g(t)z^t\\ &= \widehat{g}(z)_{m=0}+\sum_{m=1}^{\infty}g(m)z^{2m+2}.\end{aligned}$$

The transform of δ is 1, and Eq. (3.7) becomes

$$\widehat{g}(z) = \frac{1}{\sqrt{3}}z^2 + \frac{1}{2\pi\sqrt{3}}\,z^2\int_0^{2\pi}dx\,\frac{e^{-ix}}{\alpha} \times\left[\sum_{m=1}^{\infty}\frac{1}{m}\left(\frac{2a^2}{3}\right)^m\left(\frac{1}{2}+\alpha e^{ix}+\beta e^{-ix}\right)^m z^{2m}\right].$$

Now we make use of $\sum_{n=1}^{\infty}x^n/n=-\ln(1-x)$, $|x|<1$, and at this point pick $\alpha=-\beta=1/\sqrt{2}$, arriving at

$$\widehat{g}(z)=\frac{z^2}{\sqrt{3}} \;+\; \frac{z^2}{2\pi}\sqrt{\frac{2}{3}}\int_0^{2\pi}dx\;e^{-ix}\left\{-\ln\left[1-z^2\frac{2a^2}{3}\left(\frac{1}{2}+\frac{e^{ix}-e^{-ix}}{\sqrt{2}}\right)\right]\right\}.$$

Using $\omega = e^{-ix}$ and integrating by parts,

$$\widehat{g}(z) = \frac{1}{\sqrt{3}} z^2 \; - \; z^4 \, \frac{1}{2\pi i} \, \frac{2a^2}{3} \oint\limits_{|\omega|=1} \frac{\left(\frac{1}{\omega} + \omega\right) d\omega}{1 - \frac{2a^2 z^2}{3} \left(\frac{1}{2} + \frac{1}{\sqrt{2}} \left(\frac{1}{\omega} - \omega\right)\right)}.$$

Here the Residue Theorem is used. The singularity at $\omega = 0$ is removable, while one of the two zeros of the denominator is inside the integration contour. Finally,

$$\widehat{g}(z) = \frac{\sqrt{3}}{2a^2} \left[1 + \frac{1}{3}(az)^2 - \sqrt{1 - \frac{2}{3}(az)^2 + (az)^4} \right]. \tag{3.8}$$

This closed-form expression analytically extends $\widehat{g}(z)$ beyond the disk $|z| < 1$ on which it was defined. We now need to deal with $\widehat{h}_n(z)$.

Paths from the n-th level that reach the root for the first time in s steps, with amplitude $h_n(s)$, first reach the level $n-1$, generally going out into the tree in the meanwhile, then the level $n-2$, and so forth until the root is hit. This is organized into paths dropping by one level closer to the root (with amplitude h_1), convoluted with the rest of the walk, which itself is comprised of paths getting closer to the root by one level, $h_n = h_1 * h_{n-1} = \ldots = h_1 * \ldots * h_1$ (n times). Then the transform is

$$\widehat{h}_n(z) = \left[\widehat{h}_1(z)\right]^n. \tag{3.9}$$

Paths h_1, that for the first time reach one level closer to the root, are combinatorially equivalent to the paths that start at level 1 and touch the root for the first time.

Consider such a path, starting at level 1 and finding its way to the root for the first time, in more than one step (Fig. 3.4). It must have come to level 1 from level 2, and it first steps back to level 2. For comparison, now recall a root–to–root simple loop $g(s)$. It differs from h_1 by: the first step of g (with coefficient 1) is not taken by h_1 (which is already at level 1); and, the next step of g (for paths with $t > 2$) is a *right–step*, while the h_1 path takes a *right–turn*.

So we divide the expression for $g(s)$ by the coefficient associated with the second step of g that h_1 does not take, $2a/\sqrt{3}$, and multiply it by the coefficient of the step that h_1 takes instead, $(1+a)/\sqrt{3}$. We also divide by the coefficient of the first step of g, not taken at all by h_1, which is 1. In the special case $s = 1$ a single step is taken to the root

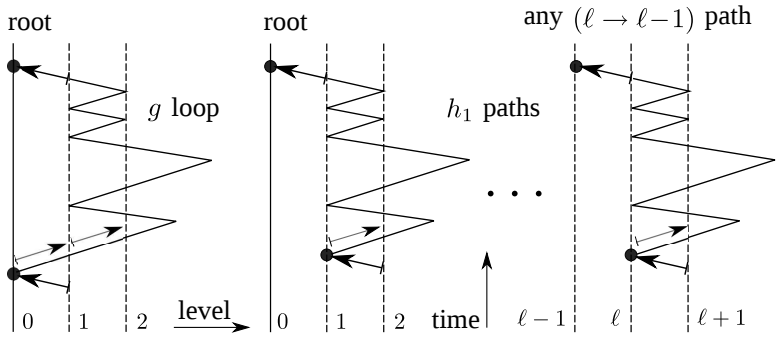

Figure 3.4: Combinatorial comparison of root–to–root loops (g) and paths getting closer to root by one level (h_1), see text.

from the first level, with $a/\sqrt{3}$. Finally, this path takes one step more as compared to $g(s)$, so we use the expression for $g(s+1)$, starting from $s=3$ since $g(2)$ corresponds to the special case $h_1(1)$. This gives us the expression for the amplitude h_1,

$$h_1(s) = \frac{a}{\sqrt{3}}\delta_0(s-1) + \frac{\frac{1+a}{\sqrt{3}}}{1\times\frac{2a}{\sqrt{3}}}\, g(s+1)\times \mathbb{1}_{s\in\{3,5,\ldots\}}.$$

Its transform is, using $1+a+a^2=0$ (as $a=e^{2\pi \boldsymbol{i}/3}$),

$$\begin{aligned}\widehat{h}_1(z) &= \frac{a}{\sqrt{3}}\,z + \frac{1+a}{2a}\left[\frac{1}{z}\sum_{t=3,5,\ldots} z^{t+1} g(t+1)\right] \\ &= \frac{a\,z}{\sqrt{3}} - \frac{a}{2\,z}\left(\widehat{g}(z) - \frac{z^2}{\sqrt{3}}\right) = \frac{a\sqrt{3}}{2}\,z - \frac{a}{2}\,\frac{\widehat{g}(z)}{z}.\end{aligned} \tag{3.10}$$

The sum above is just the transform of $g(t\geq 4)\,\big[\widehat{g}_{t\geq 4}\big]$, which is then written as $\widehat{g}-\widehat{g}_{t=2}$. With Eqs. (3.5), (3.9), and (3.10), the generating function for the amplitude of the process at the root is

$$\widehat{H}_n(z) = \Big[-\frac{a}{2}\Big]^n \left[\frac{\widehat{g}(z)-\sqrt{3}\,z^2}{z}\right]^n \frac{1}{1-\widehat{g}(z)},$$

with $\widehat{g}(z)$ given in Eq. (3.8). Now we need to invert this.

3.2.2 Inverse transform: $H_n(t)$ asymptotic

We take the inverse z–transform via an integral, using Laurent expansion and Residue Theorem (Appendix C.2),

$$\begin{aligned} H_n(t) &= \frac{1}{2\pi i}\oint_{|z|=r<1} \frac{\widehat{H}_n(z)}{z^{t+1}}dz \\ &= \frac{1}{2\pi i}\left[-\frac{a}{2}\right]^n \oint \frac{1}{z^{t+1}}\left[\frac{\widehat{g}(z)-\sqrt{3}\,z^2}{z}\right]^n \frac{dz}{1-\widehat{g}(z)}. \end{aligned}$$

This integral is too complicated to yield a closed-form solution. We look for its asymptotic behavior in the form

$$H_n(t) \;=\; \frac{(-a)^n}{2\pi i}\,\frac{1}{2^n}\oint\limits_{|z|=r} \frac{\left[\widehat{g}(z)-\sqrt{3}\,z^2\right]^n}{1-\widehat{g}(z)}\,\frac{dz}{z^{t+n+1}}, \tag{3.11}$$

using the steepest descent method. The calculation is discussed in Appendix F. The asymptotic of the amplitude of the process at the root, starting from a level n in the tree, with $\tau \equiv t-n$, is

$$\begin{aligned} H_n(t) \;\sim\; &\frac{(-a)^n}{2\pi i}\frac{1}{2^n} \;\times\; (\sqrt{2})^n(-1)^n \\ &\times \left[c_{1n}\,e^{-\boldsymbol{i}\gamma n}\,\frac{e^{-\boldsymbol{i}\,\lambda_1\frac{\tau}{2}}}{\tau^{3/2}} \;-\; c_{2n}\,e^{\boldsymbol{i}\gamma n}\,\frac{e^{-\boldsymbol{i}\,\lambda_2\frac{\tau}{2}}}{\tau^{3/2}}\right]. \end{aligned} \tag{3.12}$$

Constants c_{1n} and c_{2n} are linear in n, while γ and λ's are real constants (Appendix F). The probability is

$$|H_n(t)|^2 \;\sim\; \frac{C^2 - 2\,\mathrm{Re}\left\{c_1 c_2^*\,e^{-\boldsymbol{i}\left[2\gamma n+(\lambda_1-\lambda_2)\frac{\tau}{2}\right]}\right\}}{4\pi^2\,2^n\,\tau^3}, \tag{3.13}$$

where $C^2 = |c_1|^2+|c_2|^2 \sim n^2$. The oscillations of the exponential term are rapid at large times (and/or n), and this function behaves as $\sim \tau^{-3}$. The n dependence is $\sim n^2/2^n$ at large times. Also, we see that the walk is transient, in the sense introduced in [97–99], since $\sum_t^\infty |H_n(t)|^2$ is finite.

The observed power law decay differs sharply from the exponential tail of the classical

walk (Appendix I). On finite graphs built with binary trees, when the extent of the tree is limited by a matching tree or particular boundary conditions (sinks, reflective), this exponentially slower decay may lead to algorithms with significant speedups. The treatment in this section is meant to lay the groundwork for such investigations.

This behavior should also have general implications for physics of systems modeled with a binary tree.

3.2.3 Inverse transform: $H_n(t)$ computed

The transform is defined as $\widehat{H}_n(z) = \sum_{t \geq n} H_n(t) z^t$, and using its Taylor expansion and equating coefficients,

$$H_n(t) = \frac{\widehat{H}_n^{(t)}(z)|_{z=0}}{t!}. \tag{3.14}$$

This can be evaluated efficiently, for a range of values of t for a fixed n, providing the full amplitude. Symbolic calculation of derivatives (with MATHEMATICA) allows for values of n in the thousands. We note that the amplitude shows an interference pattern, with the main peak followed by (much) smaller, rapidly diminishing, secondary peaks. Probability at the root with time is shown in Fig. 3.5, for $n = 50$. The shape does not depend on n. At long times this exact result can be compared with asymptotics (3.13), see inset in Fig. 3.5. The tail exhibits t^{-3} dependence, in agreement with Eq. (3.13).

3.2.4 Comparison and algorithmic aspects

We considered an algorithm of finding the root starting at the n–th generation in the tree. Here we compare the quantum and classical walks, and their estimated run times, using data calculated via Eqs. (3.14) and (I.1). Probability peaks and times at which they are reached, for quantum and classical walks, are shown in Table 3.1 for a few initial levels n. Probability at the root for the classical walk is shown in Fig. 3.6. The best run time for a given n is estimated as follows. The inverse of the probability is the average number of times needed to run in order to hit the root; multiplying it by its time gives the total running time to hit the root. We need its minimum over all time steps, $\min\left\{t/|H_n(t)|^2\right\}$, usually the values for the peak. We use data up to $n = 5000$ in steps of 100 for the quantum walk, and up to $n = 2000$ in steps of 50 for the classical

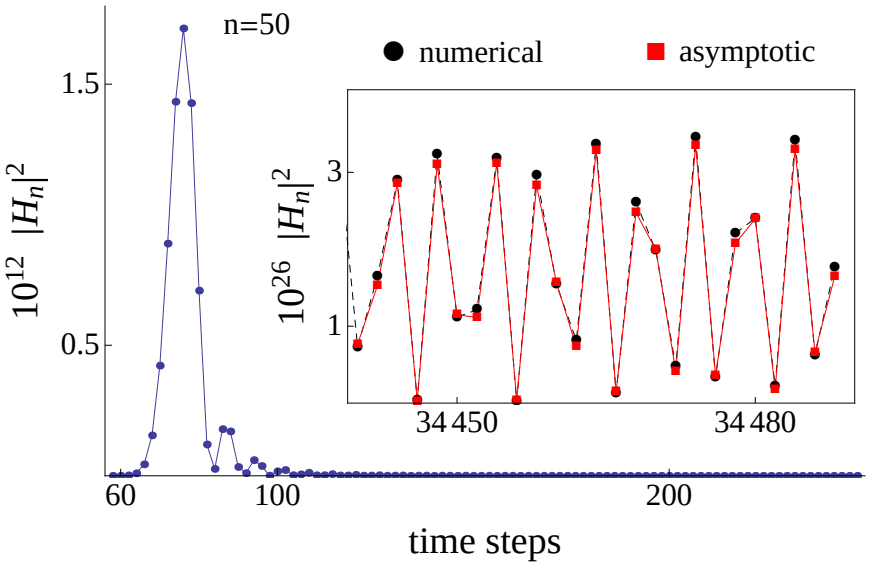

Figure 3.5: Probability at the root with time ($n = 50$), computed via Eq. (3.14). Inset compares this (points) with the steepest descent asymptotic (3.13) at same time steps (red squares).

initial level n	max $\lvert H_n\rvert^2$	(at t)	max $p_t(n)$	(at t)
10	6.8×10^{-4}	(16)	1.2×10^{-4}	(22)
20	3.9×10^{-6}	(30)	7.2×10^{-8}	(52)
50	1.7×10^{-12}	(76)	4.2×10^{-17}	(142)
100	5.3×10^{-23}	(150)	2.6×10^{-32}	(292)
200	7.6×10^{-44}	(298)	1.4×10^{-62}	(592)
500	5.1×10^{-106}	(738)	4.5×10^{-153}	(1492)

Table 3.1: Probability peaks at the root of the binary tree, with their times, for the quantum $\left[|H_n(t)|^2\right]$ and classical $\left[p_t(n,0)\right]$ walks, with the initial level in the tree n.

walk (numerical integration is more demanding). Using smaller increments in n does not affect the results. $\log_e$ of run times is fit with a polynomial and linear (Fig. 3.7). The polynomial fit establishes a linear trend (reached at $n \sim$ a few hundred), so the run

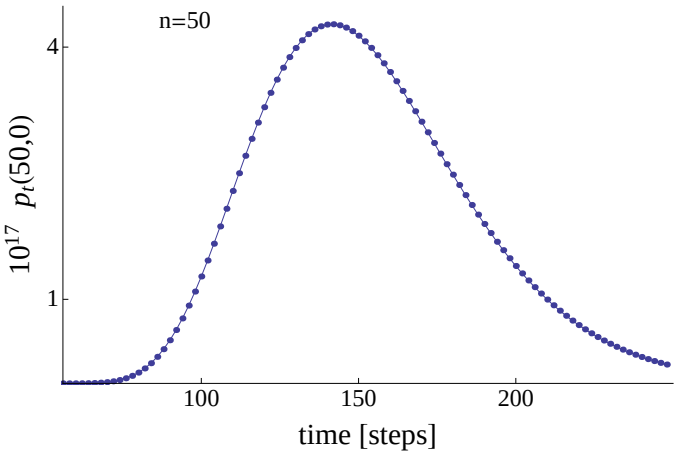

Figure 3.6: Classical walk, probability at the root. Appendix I.

time of the quantum walk is exponential in the initial distance from the root, $\sim e^{bn}$. The same holds for the classical walk, and then the ratio of slopes of their linear fits compares their run times.

This ratio does not change much over the whole range of data, being within a few percent of 2/3. Still, since an exponential complexity is fully felt at large n, the later portions of data are more relevant for algorithmic comparison. For the last quarter of data ranges, indicated in Fig. 3.7 by lines fit through data, the ratio of quantum to classical slopes is ≈ 0.685, within 3% of 2/3. Thus it appears reasonable to conjecture the algorithmic speedup of the order of 2/3. (For a run time T for the classical walk, one expects the run time on the order of $T^{2/3}$ for the quantum walk.)

We note the behavior of peaks' times with n. For the classical walk, $t^{cl}_{\max}(n) = 3n - 8$ (exact), while for the quantum walk $t^{qw}_{\max}(n) \approx 1.46n$ (where data allows for a fit $\sim 1.5n$, and for a $\sim \ln n$ correction).

3.3 Comments and summary

Quantum walks are quantum processes with a specific mixing of states; particular unitary processes. In this vein, we propose to approach and study them using ideas from classical random walks with memory, as formalized in the framework presented in Chapter 2. Here we used this approach to explicitly construct and calculate a DTQW on a binary tree,

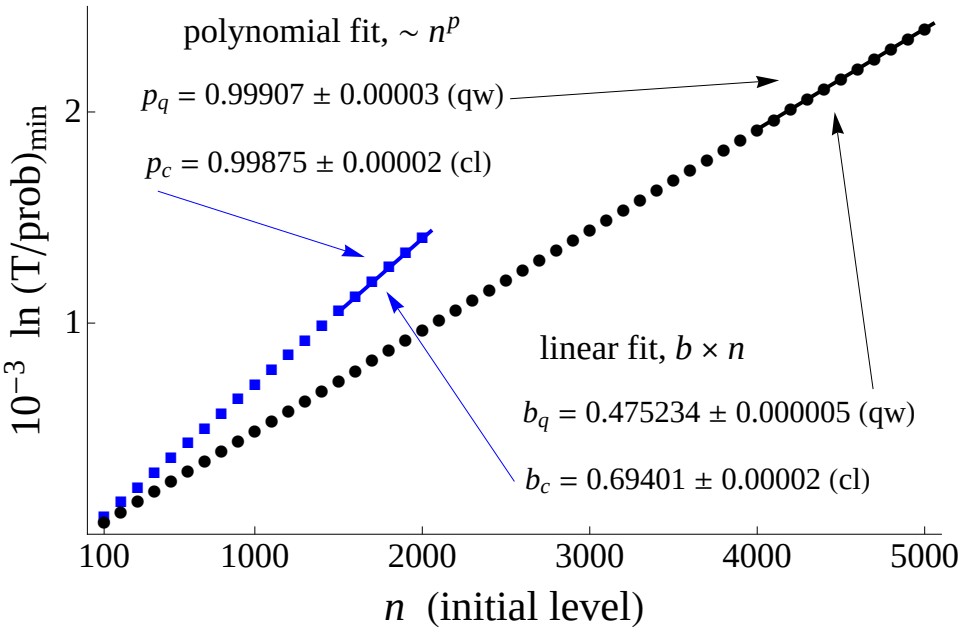

Figure 3.7: $\log_e$ of run time with initial level in the tree, for quantum (points) and classical (blue squares) walks. For plot clarity not all points are shown. Parameter values for polynomial ($\sim n^p$) and linear (bn) fits are shown, with lines through data used for fits, see text. The run time is $\sim e^{bn}$, and $b_q/b_c \to 2/3$ estimates the quantum over classical walk speedup.

which has not been available so far. We now summarize properties of the framework, and discuss some others that have been demonstrated by this problem.

Relation to memory in the walk is explicit in the construction, with the state given as a direct product of states at the previous and current sites. (This property can in principle be directly useful in algorithms, since memoried and biased approaches are known to be algorithmically beneficial in computer science.)

Walks are implemented by an operator with no restrictions other than unitarity, which is local on sites and acts on states in a single space.

The framework needs no "coin" degrees of freedom, is flexible, and applicable to general graphs. This approach may make it easier to obtain walks on structures for which significant speedups are expected, since some such constructs are too complex for extra coined spaces that are needed in the standard approach.

The evolution operator works separately on each component of the amplitude, reducing the state space, and effectively deconstructing the amplitude [as in in the binary tree example, Eqs. (3.1)–(3.2)]. This makes quantum-mechanical correlations and interference transparent in quantum walks, making their explicit study easier. It should also aid the use of quantum walks as a general tool for exploration and modeling of physical systems. We now summarize the particular findings of this Chapter.

We used the framework to build a symmetric discrete-time quantum walk on a semi-infinite binary tree. We start the walk at a level n in the tree, and find its amplitude at the root as a function of time and n. The construction of the walk is simple, but the calculation is dominated by the combinatorial complexity of a binary tree, in particular given the presence of a (reflective) boundary. The generating function of the amplitude is found explicitly, and its asymptotic is found via the steepest descent method. The full solution is computed numerically.

These solutions show interesting features. The asymptotic decays in time by the power law (as opposed to the exponential tail of the classical walk), representing long–range correlations. This hints at significant speedups on restricted structures. The amplitude exhibits a damped interference pattern, with a distinct and sharp peak. In comparison with the classical walk, the probability peak is reached quicker in time, and is orders of magnitude greater, already at small n. The run time for hitting the root on a semi-infinite binary tree is exponential with n for the quantum walk, as it is for the classical walk. This dependence is still clearly slower in n and, following suggestive data trends, we conjecture the polynomial algorithmic speedup of the order of $2/3$ over a classical walk. Also note that for a range of smaller n (appropriate in many practical applications) the dependence of probability on n is in fact yet much better, $\sim n^2/2^n$ as compared to the purely exponential suppression in the classical walk.

We also note the striking coincidence between our result on the decay time of the amplitude at the root ($\sim t^{-3}$ vs. classical exponential) and the exciton survival time results in the known work [43]. They use CTQW on the line[2] and also find the power-law time dependence (along with a few other matching features). They also specify a corresponding experimental technique, and this is from a well established group. Investigation of this agreement is planned in the very near future.

[2] Exciton trapping can be studied as a Grover-style quantum-walk search problem as well [44]. Survival time is there taken as a measure of the (trap) search efficiency.

3.4 Layout of how to calculate the speedup analytically

The above estimates of the speedup are obtained by fitting the results of evaluations of generating functions. While those are exact results, they are also limited to a specific range of values. Even though we pushed those parameters quite far, this is in principle troubling for reliability of estimates of what is inherently an asymptotic behaviour. Here we outline how we will compute the speedup analytically. This is work planned for immediate future.

Above we got for the run times $t^{cl}_{\max}(n) = 3n - 8$ (exact) and $t^{qw}_{\max}(n) \approx 1.46n$. Then, our algorithm is to run the QW from level n for αn steps, which is when the measurement is done. The algorithm for the calculation of the speedup is as follows.

Consider $|H_n(\alpha n)|^2$, using the fact that the observed propagation is clearly ballistic ($t \sim n$). Using the steepest descent calculate (asymptotics of) $H_n(\alpha n)$, and then

$$T_n^{(\mathrm{qw})}(\alpha) = \frac{\alpha n}{|H_n(\alpha n)|^2} \quad \text{is the run-time.}$$

This is an asymptotic quantity so this approach is sufficient. The integral provides an interesting steepest descent calculation. Then we will maximize the obtained expression with respect to α (and probably get $\alpha \approx 1.46$). This is the best run time $T_n^{(\mathrm{qw})}$.

Now consider $p_{\beta n}(n, 0)$ for the classical walk and do the same, with

$$T_n^{(\mathrm{cl})}(p) = \frac{\beta n}{p_{\beta n}(t)}, \quad \text{then optimized w.r.t. } \beta.$$

On the other hand, for the classical calculation it may be possible to use integral representations of Bessel's functions or some related polynomials. Finally, compare $\log T_n^{(\mathrm{qw})}$ and $\log T_n^{(\mathrm{cl})}$ and this gives the speedup.

A similar technique is used for asymptotic calculation of integrals, using the stationary phase method, in the following Chapter 4. Using $t = \alpha n$ has yet other benefits which are discussed along the calculation in Chapter 4. One should be aware of the possible silent issues with applying the steepest descent method to integrals with non-integer (αn) powers of complex functions, since roots with branches show up. However, our analysis shows that the calculation may be done. Also note that this trick was used in a very similar integral in one of the original works [14].

Chapter 4: DTQW with two-step correlation

In our observation quantum walks are most directly related to classical walks with one-step memory ("memory 2"). The presented framework (Ch. 2) provides an explicit realization of this, and as an example solves the problem of DTQW on the binary tree (Ch. 3). One question that readily asserts itself is about walks with increased correlation length, with yet more steps traced over. Since this directly relates to interference between the paths one expects to deal with some anomalies or with an outright appearance of classical features, at least to some extent.

The problem of quantum–to–classical transition is of broad importance, in fields ranging from quantum computing to many-body systems to foundations of quantum mechanics. While most works in quantum computing are concerned with appearance of classical behaviour as related to decoherence, there is a clear interest in general pursuits. On the other hand, having some controlled classical features in quantum walks would be very useful, for one thing for the purpose of using these processes for sampling.

Here we present a 1d DTQW with one additional level of memory (correlation), thus with two-step memory, which is based on the interchange framework introduced in Ch. 2. The solution of this walk indeed bears classical features while it retains ballistic propagation. Interestingly, it relates to a well known work on walks with multiple coins, that studies a different kind of a walk but finds similar results. The relation of our results to such and similar work is discussed at the close of this Chapter.

4.1 DTQW with two-step memory (correlation)

We look at a DTQW in 1 dimension which state carries memory of two previous steps. For example, when the walker is at the site i, it may have come to it from $i-1$, to which site it may have come from $i-2$ or from i. We will use the coin formalism for the analysis in this problem, to make comparison to other work easier. However, since the problem stems directly from the very basic ideas of the formalism presented so far, we first show how this walk would be treated with the interchange framework. It turns

out that it is easier to demonstrate this with a formal prescription for a general walk with n–step memory, on a general "regular graph" (with constant order). This is also an opportunity to present how the interchange framework, as defined by Eqs. (2.4) – (2.6), operates in a generalized form.

The state of the walk now depends on the previous n steps, so it will be in the direct product of n Hilbert spaces $\mathcal{H}^{\otimes n}$. Here we formally enumerate states in $\mathcal{H}$ on a graph by $\{|i_k\rangle, k \text{ integer}\}$.[1] The state can be written as

$$|\psi\rangle = \underbrace{|i_1\rangle \otimes |i_2\rangle}_{\substack{\text{furthest step} \\ \text{remembered}}} \otimes |i_3\rangle \otimes \cdots \otimes |i_{n-2}\rangle \otimes \underbrace{|i_{n-1}\rangle \otimes |i_n\rangle}_{\text{last step}}.$$

Note that the indices i_k, i_{k+1} (etc) do *not* imply consequtive sites on the graph, but rather trace the sites the walk went over (in general stepping back and forth). The last pair, $|i_{n-1}\rangle \otimes |i_n\rangle$, representing the last step taken as an arrow ending on the current site i_n, will in the next step become the previous step, etc. All arrows (pairs of states) except for the first one do not get mangled but only shifted along. The action of the interchange is such that the first arrow (the tail of the whole train) is made available for the evolution operator, so that its tip can get distributed to the available sites in the next step. (The operator works with all previous history.) The action of $\widehat{X}$ is

$$\widehat{X}|\psi\rangle = \widehat{X}\Big(|i_1\rangle \otimes |i_2\rangle \otimes |i_3\rangle \otimes \cdots \otimes |i_n\rangle\Big) = \underbrace{|i_2\rangle \otimes |i_3\rangle \otimes \cdots \otimes |i_n\rangle}_{n-1 \text{ step history}} \otimes |i_1\rangle \equiv |\psi^{(X)}\rangle,$$

where the last product $|i_n\rangle \otimes |i_1\rangle$ may not represent a valid connection on the graph; this is an intermediate part of the step. Now U can act on $|i_1\rangle$, sending it to all sites the walk can step onto and thus forming the tip of the last arrow of the evolved superposition,

$$\begin{aligned}\widehat{U}\Big(\widehat{X}|\psi\rangle\Big) &= \sum_{i_2,i_3,\ldots,i_n} \Big(|i_2\rangle\langle i_2| \otimes \cdots \otimes |i_n\rangle\langle i_n| \otimes U_{i_2,\ldots,i_n}\Big)\ |\psi^{(X)}\rangle \\ &= \sum_{i_2,i_3,\ldots,i_n} |i_2\rangle \otimes |i_3\rangle \otimes \cdots \otimes |i_n\rangle \otimes U_{i_2,\ldots,i_n}|i_1\rangle.\end{aligned}$$

[1] The formalism as stated applies to any regular graph, but it may be helpful to think of the walk on a line where the steps are between next neighbors. The full state can be thought of as made up of a string of arrows, where each arrow connects sites between which the transition happened at that step. This 'train' of arrows contains the history of all previous steps that we keep track of.

So in the step just taken we dropped the very last step carried previously ($|i_1\rangle \otimes |i_2\rangle$) while adding the newest one (just taken) to the front; the whole train with history moved by one step. Since we are now keeping track of more than the last step, the evolution operator involves all $\{i_2, \ldots, i_n\}$ sites. However, note that the matrix for it will have only two non-zero elements in each row and column and can be worked with. Now we apply this formalism to the two-step memory walk.

The prescription (2.5) and (2.6) applies as follows. All states in $\mathcal{H}$ are enumerated on a graph and labeled by vertex indices (integers). This construction is again for a regular graph of any order (not only a line), so for the purpose of this demonstration we label states by indices such as i, j, k. For the actual walk on the line, it is much more convenient to use $i, i \pm 1$ etc, as we do later.

Consider a walk to be in a state $|k\rangle$ (at a site k), having arrived to it from the state $|j\rangle$ (a nearest-neighbor to k) to which state it had arrived from $|i\rangle$ (j's nearest neighbor). The state is then $|\psi\rangle = |i\rangle \otimes |j\rangle \otimes |k\rangle$, and the evolution step is given by $\widehat{U}\widehat{X}|\psi\rangle$. We can think of this state as two continuing arrows, $i \to j$ (the "tail" of the walk) and then $j \to k$ (the front), so that the tip of the second arrow is on k, the current position of the walker. Then $\widehat{X}$ swaps them in a manner discussed above, so that the second arrow's bottom is now on k, since in the next step this arrow will have labeled the then-previous step, while the last site comes under action of the evolution operator. The action of the interchange operator is

$$\widehat{X}\colon |i\rangle \otimes |j\rangle \otimes |k\rangle \to |j\rangle \otimes |k\rangle \otimes |i\rangle,$$

and then the evolution operator for sites j, k is applied. For full states with superpositions of components such as the one above (with all states that can end on k),

$$\widehat{U}\big(\widehat{X}\psi\big) = \sum_{j,k}^{\text{all pairs}} \Big(|j\rangle\langle j| \otimes |k\rangle\langle k| \otimes U_{j,k}\Big)\Big(|j\rangle \otimes |k\rangle \otimes |i\rangle\Big) = \sum_{j,k}^{\text{all pairs}} |j\rangle \otimes |k\rangle \otimes U_{j,k}|i\rangle$$

In general, the unitary operator ($U_{j,k}$) is written, without any constraints, so to encode the desired walk. In this case (the two-step memory) it facilitates the steps possible in this particular process, as discussed below. At this point we conclude this brief presentation of the general formalism and of how the interchange framework would be used for this problem. For the purpose of a direct comparison with a well known, similar looking

result from the literature we switch to the coin formalism and proceed with the actual analysis of the problem. Then we will be able to directly point at crucial differences.

In this approach, the possible paths are captured by the coin states, while the state of the walk is given in a single $\mathcal{H}$, spanned by a basis $\{|1\rangle, |2\rangle, \ldots, |n\rangle\}$. We first organize possible paths for the last two steps and thus construct the coin space. Note that the coin approach works fine on the line, while it would be very difficult for general graphs.

For this quantum walk over $\mathbb{Z}_1$ the classification of steps can be done via types of "tails" as follows. The walk can come to site i from the left (from $i-1$), by either having continued from $i-2$, or by having reversed its previous direction, so where it had been on i. With the analogous consideration of the "left mover" (the state that has come to i from $i+1$), we have the following encoding of steps,

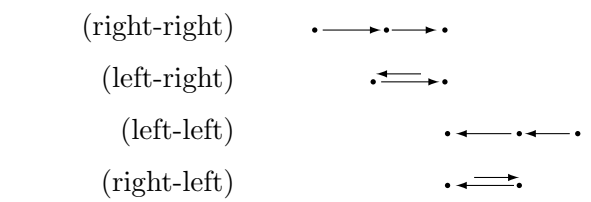

(right-right)	$(i-2) \to (i-1) \to i$	state $\|00\rangle$
(left-right)	$i \to (i-1) \to i$	state $\|01\rangle$
(left-left)	$(i+2) \to (i+1) \to i$	state $\|11\rangle$
(right-left)	$i \to (i+1) \to i$	state $\|10\rangle$.

The last column on the right is how we encode these states in the "coin" space, what is arbitrary (one could as well enumerate them as $\{1, 2, 3, 4\}$, for example). The full state is obtained by the tensor product of the space spanned by the above states with the state in the Hilbert space in which the process propagates, thus the full state is in $\mathbb{C}^4 \otimes \mathcal{H}$. We begin the walk in the state

$$|\psi_0\rangle = |00\rangle \otimes |0\rangle, \quad \text{with evolution specified by} \quad |\psi_{t+1}\rangle = \widehat{U}|\psi_t\rangle.$$

We use the evolution operator as given by the "coin" operator (Q) acting in the coin space designed above, and the conditional shift operator acting in the state space, in the way usual when using coined walks, $U = S(Q \otimes I)$. Our (unitary) coin operator Q is

$$Q = \begin{bmatrix} \sqrt{p} & \sqrt{1-p} & 0 & 0 \\ 0 & 0 & -\sqrt{q} & \sqrt{1-q} \\ \sqrt{1-p} & -\sqrt{p} & 0 & 0 \\ 0 & 0 & \sqrt{1-q} & \sqrt{q} \end{bmatrix}, \quad 0 \leq p, q \leq 1,$$

where p and q are parameters analogous to probabilities for left- and right-moving steps. This reflects ogranization of memoried classical walks into enlarged state spaces, with left- and right-moving modes. (For example, see Appendix A.2.)

Here their meaning is a little more involved. For the right-moving state, p is the probability to maintain its *trend*: If it had not changed direction in the previous step (right-right) then it has probability p to continue, thus to step to $i+1$, and if it had changed direction (left-right) then it does so again with the probability p, going back to $i-1$ (becoming right-left). The parameter q means the same for the states directed to the left at the time the step is to be taken.[2] Note that this performes full mixing in the coin space—the above matrix cannot be reduced (to two block-diagonal ones, for example), which will be a crucial point in comparison with other work.

Interesting observations can be made already at this stage. It is seen in the above matrix that the one-step-memory walk cannot be directly reproduced from this. (One would suspect that by manipulating the extreme values of p and q this walk may get reduced to a one-step memory case.) It is also seen that the Hadamard walk does not follow from it, either. This means that walks with explicit two-step memory represent processes with very different properties. This is not surprising (we expect differences, or classical features to show up) but it is nevertheless interesting to see it evident this early in the analysis. The conditional shift operator with this coin can be given as

$$S = \Pi_{00} \otimes \sum_i |i+1\rangle\langle i| + \Pi_{01} \otimes \sum_i |i-1\rangle\langle i| \\ + \Pi_{10} \otimes \sum_i |i+1\rangle\langle i| + \Pi_{11} \otimes \sum_i |i-1\rangle\langle i|,$$

where Π_{ij} are projectors on the corresponding coin states, for example $\Pi_{10} = |10\rangle\langle 10|$, etc. The projectors to coin states are matched with shift operators so to provide the mixing of the trends in the walk, as follows.

The steps to the right reaching the site $i+1$ happen for states with the coin component being directed to the right and maintaing the direction of the previous step (right-right), as well as for those being directed to the left and reversing the previous step (right-left).

[2] Then coin states could be labeled RR, LR, LL, RL. We do not use this since the correlations are meant to be generalized and the notation used nicely reflects the binary encoding; and, to avoid misleading identification with other, similar looking while very different, approaches seen elsewhere and discussed later.

The corresponding property holds for the other two projectors, Π_{01} and Π_{11}. In order to write down the local evolution equations, look at one step from the state

$$|\psi_t\rangle = \sum_{i\in\mathbb{Z}} \Big(a_t(i)|00\rangle + b_t(i)|01\rangle + c_t(i)|10\rangle + d_t(i)|11\rangle \Big) \otimes |i\rangle,$$

where $a_t(i)$ is the coefficient with the coin component $|00\rangle$ of the state $|i\rangle$ (at site i), at the time-step t, etc. Considering a step we get that the coefficients obey

$$\begin{aligned} a_{t+1}(i) &= \quad \sqrt{p}\; a_t(i-1) + \sqrt{1-p}\; b_t(i-1) \\ b_{t+1}(i) &= -\sqrt{q}\; c_t(i-1) + \sqrt{1-q}\; d_t(i-1) \\ c_{t+1}(i) &= \sqrt{1-p}\; a_t(i+1) - \quad \sqrt{p}\; b_t(i+1) \\ d_{t+1}(i) &= \sqrt{1-q}\; c_t(i+1) + \quad \sqrt{q}\; d_t(i+1). \end{aligned} \tag{4.1}$$

In order to solve this set of recursion relations, we will first take the Fourier transform, and then algebraically solve the obtained system for the transforms. Then we will need to invert the transform, ie. to find the original coefficients.

In these kinds of problems it is usual at that stage to be restricted to finding the asymptotic behavior, since the obtained expressions for the transforms are generally too complicated to be inverted exactly: The resulting amplitude is bound to be a complicated and oscillating function, and the integrals leading to it are likely not solvable. However, it is also usually possible to obtain full numerical results, as we do below as well. The numerical integration is feasible, specially given that useful results are obtained already for small number (~ 100) of steps. It should be noted here that we can recall no exact solutions in problems with discrete-time quantum walks on graphs.

On the other hand, the Fourier transforms are generating functions from which the amplitudes can also be computed exactly, if that is required. This has been done in the binary tree walk, as presented in the Chapter 3. In this problem we have no need for it since the numerical integration is satisfactory in every sense.

Here we change notation, so that the position on the lattice is n, while the index in the inverse space is k. We use the Fourier transform

$$\widehat{f}(k) = \sum_{n\in\mathbb{Z}} f(n) e^{\boldsymbol{i}\, k\, n},$$

where the normalization is omitted since we formally allow for an infinite line. This is accounted for when inverting the transform.

Applying this to the recursion equations (4.1) we obtain the set of linear equations for the transforms. To proceed with the following analysis we need them in the matrix form,

$$\begin{pmatrix} \widehat{a}_{t+1} \\ \widehat{b}_{t+1} \\ \widehat{c}_{t+1} \\ \widehat{d}_{t+1} \end{pmatrix} = M \begin{pmatrix} \widehat{a}_{t} \\ \widehat{b}_{t} \\ \widehat{c}_{t} \\ \widehat{d}_{t} \end{pmatrix} = M^{t+1} \begin{pmatrix} \widehat{a}_{0} \\ \widehat{b}_{0} \\ \widehat{c}_{0} \\ \widehat{d}_{0} \end{pmatrix},$$

where the succession of steps has been formalized by the repeated action of the evolution operator. We now have the operator driving the step-by-step evolution,

$$M = \begin{bmatrix} \sqrt{p}\, e^{\boldsymbol{i}\, k} & \sqrt{1-p}\, e^{\boldsymbol{i}\, k} & 0 & 0 \\ 0 & 0 & -\sqrt{q}\, e^{\boldsymbol{i}\, k} & \sqrt{1-q}\, e^{\boldsymbol{i}\, k} \\ \sqrt{1-p}\, e^{-\boldsymbol{i}\, k} & -\sqrt{p}\, e^{-\boldsymbol{i}\, k} & 0 & 0 \\ 0 & 0 & \sqrt{1-q}\, e^{-\boldsymbol{i}\, k} & \sqrt{q}\, e^{-\boldsymbol{i}\, k} \end{bmatrix}.$$

To find the explicit expressions for the transforms $(\widehat{a}, \ldots)$ we need to diagonalize the matrix M so that we can raise it to the power t. Thus we need to solve its eigenvalue problem. This involves the following 4–th order characteristic equation,

$$\lambda^4 - \left(\sqrt{p}\, e^{\boldsymbol{i}\, k} + \sqrt{q}\, e^{-\boldsymbol{i}\, k}\right) \lambda^3 + \left(\sqrt{p}\, e^{-\boldsymbol{i}\, k} + \sqrt{q}\, e^{\boldsymbol{i}\, k}\right) \lambda - 1 = 0,$$

with an extra condition $|\lambda| = 1$, since λ is an eigenvalue of a unitary operator M. One hopes that this can be made easier by the symmetries evident in our original equations. (Replacement of $p \leftrightarrow q$ and corresponding sign changes leave them unchanged, etc.)

However, as it turns out, the above equation still requires an involved algebraic analysis, as there is no factoring that would reduce the order of equations to solve. The expressions obtained in this analysis are rather unwieldy and not at all promising for the following large calculations, so we do not pursue this further at this time. The analysis leading to this conclusion is shown in Appendix D.

However, the special case $p = q$ clearly allows factoring directly, and even though it is less general, it is also physically more appropriate to study first. The rest of the analysis thus strictly applies to $p = q$, so to a walk where probabilities to change trend

of behaviour are the same for the left- and right-moving components.

The case $p = q$

Using $p = q$ the above characteristic equation factors yielding the eigenvalues

$$\lambda = \{\,\pm 1,\ \sqrt{p}\cos k \pm \boldsymbol{i}\sqrt{1 - p\cos^2 k}\,\}, \quad \text{or:} \quad \lambda = \{\,\pm 1,\ e^{\pm \boldsymbol{i}\omega_k}\,\},\ \omega_k = \cos^{-1}(\sqrt{p}\cos k).$$

The corresponding eigenvectors, $\{|v_i\rangle\}$, can be found using $(M - \lambda I)v = 0$,

$$\begin{pmatrix} \sqrt{p}e^{\boldsymbol{i}k} - \lambda & \sqrt{1-p}e^{\boldsymbol{i}k} & 0 & 0 \\ 0 & -\lambda & -\sqrt{p}e^{\boldsymbol{i}k} & \sqrt{1-p}e^{\boldsymbol{i}k} \\ \sqrt{1-p}e^{-\boldsymbol{i}k} & -\sqrt{p}e^{-\boldsymbol{i}k} & -\lambda & 0 \\ 0 & 0 & \sqrt{1-p}e^{-\boldsymbol{i}k} & \sqrt{p}e^{-\boldsymbol{i}k} - \lambda \end{pmatrix} \begin{pmatrix} 1 \\ \alpha \\ \beta \\ \gamma \end{pmatrix} = \begin{pmatrix} 0 \\ 0 \\ 0 \\ 0 \end{pmatrix},$$

and now in terms of λ the coefficients are

$$\alpha = \frac{\lambda e^{-\boldsymbol{i}k} - \sqrt{p}}{\sqrt{1-p}}, \quad \beta = \frac{\lambda^{-1}e^{-\boldsymbol{i}k} - \sqrt{p}e^{-2\boldsymbol{i}k}}{\sqrt{1-p}}, \quad \text{and} \quad \gamma = \frac{\sqrt{p}e^{-\boldsymbol{i}k} - \lambda^{-1}}{\sqrt{p}e^{-\boldsymbol{i}k} - \lambda}\, e^{-2\boldsymbol{i}k}.$$

Note that for $\lambda_{1/2}$ it is simply $\gamma = e^{-2\boldsymbol{i}k}$. By substituting λ_i we get explicit $|v_i\rangle$,

$$v_i = \begin{pmatrix} 1 \\ \alpha(\lambda) \\ \beta(\lambda) \\ \gamma(\lambda) \end{pmatrix} = \begin{pmatrix} 1 \\ \frac{\lambda e^{-ik} - \sqrt{p}}{\sqrt{1-p}} \\ \frac{\lambda^{-1}e^{-ik} - \sqrt{p}e^{-2ik}}{\sqrt{1-p}} \\ \frac{\sqrt{p}e^{-3ik} - \lambda^{-1}e^{-2ik}}{\sqrt{p}e^{-ik} - \lambda} \end{pmatrix}, \quad \text{with } \lambda = \{\,\pm 1,\ e^{\pm \boldsymbol{i}\omega_k}\,\},\ \omega_k = \cos^{-1}(\sqrt{p}\cos k).$$

To raise M to power t and stay in the same basis use the spectral decomposition of M,

$$M = \sum_{i=1}^{4} \lambda_i \frac{|v_i\rangle\langle v_i|}{\langle v_i|v_i\rangle}, \quad \text{and} \quad M^t = \sum_{i=1}^{4} (\lambda_i)^t \frac{|v_i\rangle\langle v_i|}{\langle v_i|v_i\rangle}.$$

Then we have

$$\begin{pmatrix} \widehat{a}_t \\ \vdots \end{pmatrix} = \left(\sum_{i=1}^{4} (\lambda_i)^t \, \frac{|v_i\rangle\langle v_i|}{\langle v_i|v_i\rangle} \right) \begin{pmatrix} \widehat{a}_0 \\ \vdots \end{pmatrix} = \sum_{i=1}^{4} \frac{(\lambda_i)^t}{\langle v_i|v_i\rangle} |v_i\rangle, \tag{4.2}$$

given our choice of the initial state ($|00\rangle$) and the fact that all $\{|v_i\rangle\}$ have 1 for the first coordinate (by design).

The presence of the $\lambda = 1$ eigenvalue indicates that there will be a stationary part of the limiting distribution, since the corresponding integrals will not go to zero as the integrand will not be raised to $t \to \infty$. (The integrals needed for the inverse are analyzed asymptotically, with the parameter $t \to \infty$.) This is decidedly not the case in general with QW's and it is very interesting. The $\lambda = -1$ hints at aperiodicity, with factors of ± 1 related to even vs. odd locations and number of steps. This will be seen to result in cancellations of amplitude at every odd site, what is typical in quantum walks.

4.1.1 Explicit expressions

The eigenvectors corresponding to the eigenvalues

$$\lambda_1 = 1, \quad \lambda_2 = -1, \quad \lambda_3 = e^{\boldsymbol{i}\omega_k}, \quad \lambda_4 = e^{-\boldsymbol{i}\omega_k}, \quad \text{where} \quad \omega_k = \cos^{-1}(\sqrt{p}\cos k),$$

will be much used, so here they are given explicitly,

$$v_1 = \begin{pmatrix} 1 \\ \dfrac{e^{-\boldsymbol{i}k} - \sqrt{p}}{\sqrt{1-p}} \\ \dfrac{e^{-\boldsymbol{i}k} - \sqrt{p}e^{-2\boldsymbol{i}k}}{\sqrt{1-p}} \\ e^{-2\boldsymbol{i}k} \end{pmatrix}, \; v_2 = \begin{pmatrix} 1 \\ \dfrac{-e^{-\boldsymbol{i}k} - \sqrt{p}}{\sqrt{1-p}} \\ \dfrac{-e^{-\boldsymbol{i}k} - \sqrt{p}e^{-2\boldsymbol{i}k}}{\sqrt{1-p}} \\ e^{-2\boldsymbol{i}k} \end{pmatrix}, \; v_3 = \begin{pmatrix} 1 \\ \dfrac{e^{\boldsymbol{i}\omega_k}e^{-\boldsymbol{i}k} - \sqrt{p}}{\sqrt{1-p}} \\ \dfrac{e^{-\boldsymbol{i}\omega_k}e^{-\boldsymbol{i}k} - \sqrt{p}e^{-2\boldsymbol{i}k}}{\sqrt{1-p}} \\ \dfrac{\sqrt{p}e^{-3\boldsymbol{i}k} - e^{-\boldsymbol{i}\omega_k}e^{-2\boldsymbol{i}k}}{\sqrt{p}e^{-\boldsymbol{i}k} - e^{\boldsymbol{i}\omega_k}} \end{pmatrix},$$

$$v_4 = \left(1, \quad \frac{e^{-\boldsymbol{i}\omega_k}e^{-\boldsymbol{i}k} - \sqrt{p}}{\sqrt{1-p}}, \quad \frac{e^{\boldsymbol{i}\omega_k}e^{-\boldsymbol{i}k} - \sqrt{p}e^{-2\boldsymbol{i}k}}{\sqrt{1-p}}, \quad \frac{\sqrt{p}e^{-3\boldsymbol{i}k} - e^{\boldsymbol{i}\omega_k}e^{-2\boldsymbol{i}k}}{\sqrt{p}e^{-\boldsymbol{i}k} - e^{-\boldsymbol{i}\omega_k}} \right)^{\mathsf{T}}, \tag{4.3}$$

with their norm squared

$$\begin{aligned}\langle v_{1,2}|v_{1,2}\rangle &= \frac{4(1\mp\sqrt{p}\cos k)}{1-p},\\ \langle v_{3,4}|v_{3,4}\rangle &= \frac{4\left(1-p\cos^2 k\right)}{1+p-2p\cos^2 k\pm 2\sin k\sqrt{p(1-p\cos^2 k)}},\end{aligned}$$

where the alternating signs ($\pm$ and $\mp$) correspond to first/second indices. Recall that these will enter the calculations inverted, and that their numerators are simple factors that are also related to each other. The last (combined) expression can be manipulated into various forms, for example removing all k–dependence from the future denominator,

$$\begin{aligned}\langle v_{3,4}|v_{3,4}\rangle &= \frac{4\left(1-p\cos^2 k\right)}{(1-p)+2(1-p\cos^2 k)\pm 2\underbrace{\sqrt{(p-1)+(1-p\cos^2 k)}}_{\sqrt{p}\sin k}\sqrt{1-p\cos^2 k}}\\ &= \frac{4\left(1-p\cos^2 k\right)}{\left(\sqrt{(1-p\cos^2 k)-(1-p)}\pm\sqrt{(1-p\cos^2 k)}\right)^2} = \frac{4}{\left(\sqrt{1-\frac{1-p}{1-p\cos^2 k}}\pm 1\right)^2}\end{aligned}$$

To recover the coefficients from their Fourier transforms, we use

$$\begin{aligned}a_t(n) &= \frac{1}{2\pi}\int_0^{2\pi}\widehat{a}_t(k)e^{-\boldsymbol{i}\,k\,n}dk \qquad (4.4)\\ &= \frac{1}{2\pi}\int_0^{2\pi}e^{-\boldsymbol{i}\,k\,n}\Big[(\lambda_1)^t g_1(k)+\cdots+(\lambda_4)^t g_4(k)\Big]dk,\end{aligned}$$

where $g_i(k)$ are factors $\langle e_1|v_i\rangle/\langle v_i|v_i\rangle$. (Here $\langle e_1|v_i\rangle$ is the first coordinate of the eigenvector $|v_i\rangle$ in the standard basis in the coin space, $\{|e_i\rangle\}, i=1,\ldots,4$.) The remaining coefficients (b,c,d) are obtained the same way, with appropriate coordinates of the summed $|v_i\rangle$'s $(2,3,4)$.

Comments on the calculation What remains is to organize and calculate the above integrals. It is very helpful that they can be evaluated numerically with the efficiency which is completely acceptable. The analytical treatment can only seek asymptotic solutions, since the expressions raised to arbitrary power are much too complicated. This will involve the stationary phase method as the most appropriate technique here.

4.1.2 Coefficients inversion: $a_t(n)$

With notation $\omega_k = \cos^{-1}(\sqrt{p}\cos k)$ for the phase, our integral is:

$$a_t(n) = \frac{1}{2\pi}\int_0^{2\pi} dk\, e^{-\boldsymbol{i}\,k\,n}\left[\frac{1-p}{4(1-\sqrt{p}\cos k)} + (-1)^t\frac{1-p}{4(1+\sqrt{p}\cos k)}\right.$$
$$+ e^{+t(\,\boldsymbol{i}\,\omega_k)}\,\frac{1+p-2p\cos^2 k + 2(\sqrt{p}\sin k)\sqrt{1-p\cos^2 k}}{4\left(1-p\cos^2 k\right)}$$
$$\left.+ e^{-t(\,\boldsymbol{i}\,\omega_k)}\,\frac{1+p-2p\cos^2 k - 2(\sqrt{p}\sin k)\sqrt{1-p\cos^2 k}}{4\left(1-p\cos^2 k\right)}\right].$$

The function labels $g_i(k)$ introduced in Eq. (4.4), that we will use when discussing other coefficients, can be identified above for $a_t(n)$. Note that we expect this to be real: The eigenvalues are complex conjugate pairs, and since the first component of all $|v_i\rangle$ is 1, the above four integrals will form complex conjugate pairs. This can be seen directly only for the $a_t(n)$ coefficient. The exresssion involves different kinds of integrals, and we break it up as $a_t(n) = I_1 + I_2 + I_{t\omega_k}$, with

$$I_1 + I_2 = \frac{1-p}{8\pi}\int_0^{2\pi}\frac{e^{-\boldsymbol{i}\,k\,n}\,dk}{1-\sqrt{p}\cos k} + (-1)^t\,\frac{1-p}{8\pi}\int_0^{2\pi}\frac{e^{-\boldsymbol{i}\,k\,n}\,dk}{1+\sqrt{p}\cos k},$$

while the integral I_{t,ω_k} is a sum of the two integrals

$$I_\pm = \frac{1}{2\pi}\int_0^{2\pi} dk\, e^{-\boldsymbol{i}\,k\,n}\, e^{\pm t\,(\boldsymbol{i}\,\omega_k)}\,\frac{1+p-2p\cos^2 k \pm 2(\sqrt{p}\sin k)\sqrt{1-p\cos^2 k}}{4\left(1-p\cos^2 k\right)}.$$

These last integrals will need an asymptotic analysis, and the stationary phase method is suitable. Apart from being approached as they stand, the integrals can be manipulated, for example as,

$$I_{t,\omega_k} = \frac{1}{4\pi}\int_0^{2\pi} dk\, e^{-\boldsymbol{i}\,k\,n}\left[\frac{1+p-2p\cos^2 k}{\left(1-p\cos^2 k\right)}\cos(t\,\omega_k) + \boldsymbol{i}\,\frac{2(\sqrt{p}\sin k)\sqrt{1-p\cos^2 k}}{\left(1-p\cos^2 k\right)}\,\sin(t\,\omega_k)\right],$$

but note that $\omega_k = \cos^{-1}(\sqrt{p}\cos k)$ while t is an arbitrary parameter (time), so it is not clear whether this is beneficial. Above some factors of 2 were moved around. This can

be further simplified,

$$I_{t,\omega_k} = \frac{1}{4\pi}\int_0^{2\pi} dk\, e^{-\boldsymbol{i}\,k\,n}\left[\frac{p-1}{1-p\cos^2 k}\cos(t\,\omega_k) + 2\cos(t\,\omega_k) + \frac{2\sqrt{p}\,\sin k}{\sqrt{1-p\cos^2 k}}\sin(t\,\omega_k)\right].$$

The last fraction can be rewritten using $\sqrt{p}\sin k = \sqrt{p-p\cos^2 k} = \sqrt{(p-1)+(1-p\cos^2 k)}$, with some more cancellations, but we may not want to pursue integrals involving integration variable buried in $\cos\left[t\cos^{-1}(\sqrt{p}\cos k)\right]$. While this expression may well be of good use with other methods, it is better for our calculation to keep $t\omega_k$ in the exponent, working with the integrals

$$I_\pm = \frac{1}{8\pi}\int_0^{2\pi} dk\, e^{-\boldsymbol{i}\,k\,n}\, e^{\pm t\,(\boldsymbol{i}\,\omega_k)}\left[\frac{p-1}{1-p\cos^2 k} + 2 \pm \frac{2\sqrt{p}\sin k}{\sqrt{1-p\cos^2 k}}\right],\ \omega_k = \cos^{-1}(\sqrt{p}\cos k).$$

The integrals $I_1 + I_2$ are calculated (Appendix E.2) to

$$I_1 + I_2 = \left[1 + (-1)^{t+|n|}\right]\frac{\sqrt{1-p}}{4}\left(\frac{1-\sqrt{1-p}}{\sqrt{p}}\right)^{|n|}. \tag{4.5}$$

The results for these integrals are shown in Fig. (4.1). The first two integrals, involving time only via the $(-1)^t$ alternating factor, have a constant value, as discussed earlier and seen in Eq. (4.5). The integrals $I_{t,\omega_k} = I_3 + I_4$, shown as a function of position (sites) for a few times, have time dependence and show the expected (ballistic, $\sim t$) propagation.

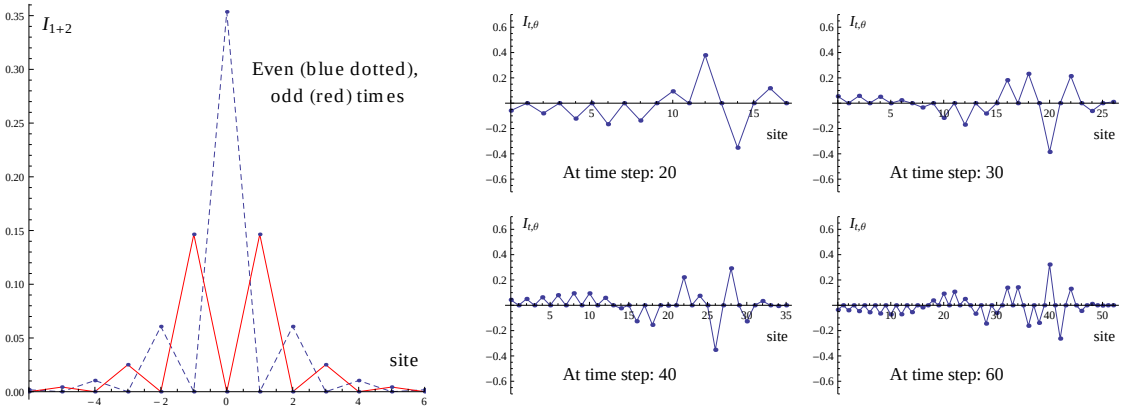

Figure 4.1: Integrals I_{1+2} (left) and I_{t,ω_k} (right), for the coefficient $a_t(n)$.

Adding up the integrals, with I_{t,ω_k} integrated numerically while I_{1+2} by Eq. (4.5), we get the coefficient $a_t(n)$, shown in Fig. (4.2). Note that the numerical integration can be substituted by numerical *evaluation*, giving the exact result, since the Fourier transform $\widehat{a}_t(k)$ is the generating function, what can be used to bypass the integration [72]. However, the result obtained here by numerical integration is good for all purposes.

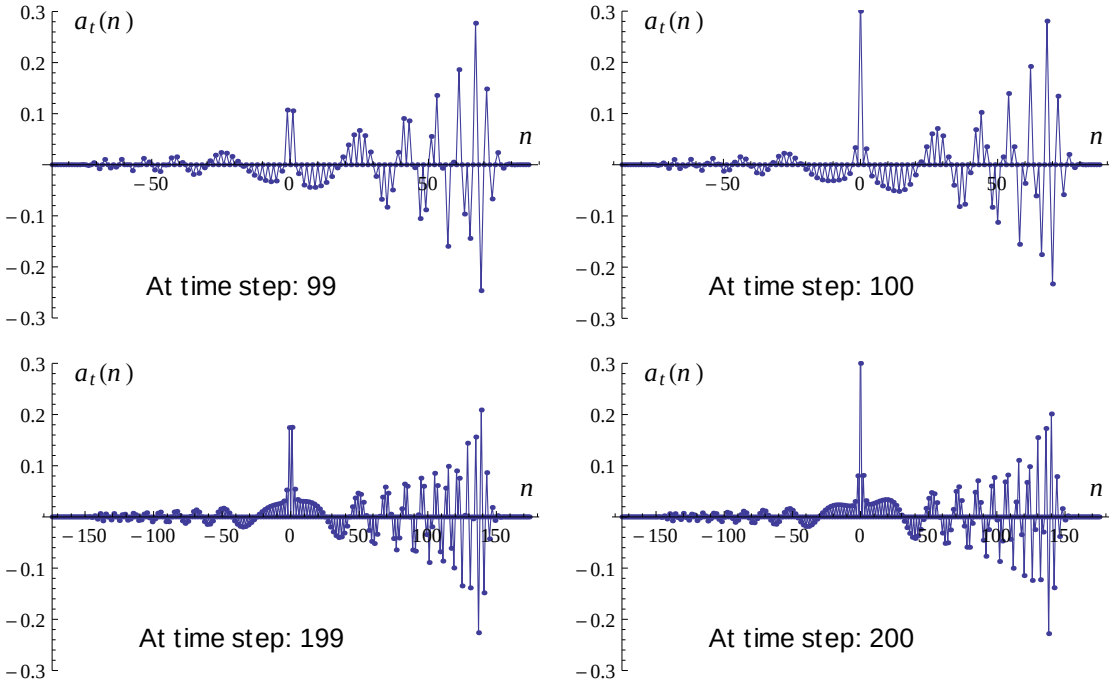

Figure 4.2: The coefficient $a_t(n)$ as a function of position (site), at some time-steps.

Next, we look at an analytical estimate of the asymptotic behaviour of I_{t,ω_k} factors of the coefficient. This involves integrals that immediately invoke some discussion,

$$I_{\pm} = \frac{1}{8\pi}\int_0^{2\pi} dk\, e^{-\boldsymbol{i}\,k\,n}\, e^{\pm t\,(\boldsymbol{i}\,\omega_k)}\left[\frac{p-1}{1-p\cos^2 k}+2 \pm \frac{2\sqrt{p}\sin k}{\sqrt{1-p\cos^2 k}}\right],\ \omega_k = \cos^{-1}(\sqrt{p}\cos k).$$

We use the stationary phase method in order to estimate their asymptotic behavior. In the spirit of the method, the exponent is expanded around its stationary point(s), where the largest contribution to the integral is built. This relies on the use of t as a large parameter, so the dominance of the stationary point contribution is magnified to

the point where the rest of the integral is negligible (formally $t \to \infty$). The parameter t is time, and so it is also physically desirable to consider it at large values. However, treating only the $\boldsymbol{i}t\omega_k$ exponent as relevant (and expanding ω_k) yields results that provide no indication of what value of the parameter (t) is 'large enough' for a given site (n).

Instead, it is possible to absorb the other exponent ($-\boldsymbol{i}kn$) into the function to be expanded, with the following reasoning. (Note that for the method to work the whole exponent to be expanded need be multiplied by a large parameter.) In the exponent we then obtain $\boldsymbol{i}t\left(-\frac{n}{t}k \pm \omega_k\right)$, and since there is good evidence that the peak propagates linearly with time, we can set $n = \alpha\, t$, where α is a fixed parameter. Then using the function $-\alpha k \pm \omega_k \equiv \Phi_{\pm}(\alpha, k)$ in the stationary phase expansion yields results that for every site (n) and the corresponding t should be a good approximation. So we work with the integrals

$$
\begin{aligned}
I_{t,\omega_k} = \frac{1}{8\pi} \Bigg\{ & \int_0^{2\pi} \frac{p-1}{1-p\cos^2 k} e^{\boldsymbol{i}\, t\left(-\frac{n}{t}k+\omega_k\right)} dk + \int_0^{2\pi} \frac{p-1}{1-p\cos^2 k} e^{\boldsymbol{i}\, t\left(-\frac{n}{t}k-\omega_k\right)} dk \\
& + \int_0^{2\pi} \frac{2\sqrt{p}\sin k}{\sqrt{1-p\cos^2 k}} e^{\boldsymbol{i}\, t\left(-\frac{n}{t}k+\omega_k\right)} dk - \int_0^{2\pi} \frac{2\sqrt{p}\sin k}{\sqrt{1-p\cos^2 k}} e^{\boldsymbol{i}\, t\left(-\frac{n}{t}k-\omega_k\right)} dk \\
& + \int_0^{2\pi} 2\, e^{\boldsymbol{i}\, t\left(-\frac{n}{t}k+\omega_k\right)} dk + \int_0^{2\pi} 2\, e^{\boldsymbol{i}\, t\left(-\frac{n}{t}k-\omega_k\right)} dk \Bigg\}.
\end{aligned}
$$

The stationary phase method is based on a set of theorems that establish the expansions of the exponent mentioned above, along with formulas that are obtained. (After the expansion the integrals can be calculated.) Very often the general theorem simplifies somewhat, as is the case in the most interesting regime of α in our integrals, to the form

$$
\begin{aligned}
I(t) \;&=\; \int_a^b f(k)\, e^{\boldsymbol{i}\, t\, \Phi(k)} dk \qquad (4.6) \\
&\sim\; f(k_s) e^{\boldsymbol{i} t \Phi(k_s)} \sqrt{\frac{2\pi}{t\,|\Phi''(k_s)|}}\, e^{\boldsymbol{i}\frac{\pi}{4}\mu}, \quad \mu = \operatorname{sgn}\left[\Phi''(k_s)\right].
\end{aligned}
$$

Here $k_s \in [a, b]$ is the stationary point of $\Phi(k)$, and then $f(k_s)$ and $\Phi''(k_s)$ are the values of $f(k)$ and $\Phi''(k)$ at k_s. Using now $\Phi_{\pm}(\alpha, k) \equiv -\alpha k \pm \omega_k$, where $\alpha \equiv \frac{n}{t}$, our integrals

can be written as

$$I_{t,\omega_k} = \frac{p-1}{8\pi}\left[\int_0^{2\pi} f_1(k)e^{\boldsymbol{i}\,t\,\Phi_+(\alpha,k)}dk + \int_0^{2\pi} f_1(k)e^{\boldsymbol{i}\,t\,\Phi_-(\alpha,k)}dk\right] \tag{4.7}$$
$$+\frac{\sqrt{p}}{4\pi}\left[\int_0^{2\pi} f_2(k)e^{\boldsymbol{i}\,t\,\Phi_+(\alpha,k)}dk - \int_0^{2\pi} f_2(k)e^{\boldsymbol{i}\,t\,\Phi_-(\alpha,k)}dk\right]$$
$$+\frac{1}{4\pi}\left[\int_0^{2\pi} e^{\boldsymbol{i}\,t\,\Phi_+(\alpha,k)}dk + \int_0^{2\pi} e^{\boldsymbol{i}\,t\,\Phi_-(\alpha,k)}dk\right] \quad = \; I_{t1} + I_{t2} + I_{t0},$$

where $f_1 = \dfrac{1}{1-p\cos^2 k}$, $f_2 = \dfrac{\sin k}{\sqrt{1-p\cos^2 k}}$, and (implied) $f_0 = 1$.

The stationary phase method in the quoted form now directly applies. Some aspects of the physical behavior of the quantum walk are directly reflected in the structure of these integrals, which is why we discuss that here. The later details of the calculation are moved out of the way to the Appendix F. We first need the stationary point (k_s) of the function in the exponent,

$$\frac{\partial\Phi_\pm}{\partial k} = -\alpha \pm \frac{\sqrt{p}\sin k}{\sqrt{1-p\cos^2 k}}, \quad \text{and} \tag{4.8}$$
$$\left.\frac{\partial\Phi_\pm}{\partial k}\right|_{k_s} = 0 \quad \Rightarrow \quad \sin k_s = \pm\sqrt{\frac{1-p}{p}}\frac{\alpha}{\sqrt{1-\alpha^2}},$$

where $\pm$ signs correspond to $\Phi_\pm$. The boundedness of the sine function implies that $-\sqrt{p} \le \alpha \le \sqrt{p}$, and we get different regimes with different physical behavior. It is seen that for $|\alpha| = \sqrt{p}$ we have one stationary point, $k_s = \pi/2$, while otherwise there are two, $k_{s1} \in (0, \frac{\pi}{2})$ and $k_{s2} \in (\frac{\pi}{2}, \pi)$ (for each of $\Phi_\pm$). Thus the integrals are broken into two, one over $(0, \frac{\pi}{2})$ and the other one over $(\frac{\pi}{2}, 2\pi)$ and each computed using Eq. (4.6). This estimates the asymptotic behaviour of integrals (4.7) for the regime $|\alpha| < \sqrt{p}$. The boundary case needs a slightly more elaborate treatment, see Appendix G.

For $|\alpha| > \sqrt{p}$ there is no (real) stationary point, and this indicates that the integral vanishes faster than any inverse polynomial (of t), thus the physical amplitude diminishes practically immediately.

The regime of most interest is clearly $|\alpha| \leq \sqrt{p}$. It turns out that the bounds need be treated separately since the stationary phase method gets a little more involved when $|\alpha| = \sqrt{p}$, which results in different behaviour. Note that $\alpha = n/t$ has (loosely) the meaning of the speed of propagation. As it is shown in Appendix G, for the maximal values of $|\alpha| = \sqrt{p}$ the decay of the amplitude ($\sim t^{1/3}$) is very different than in the rest of $|\alpha| \leq \sqrt{p}$ regime ($\sim t^{1/2}$); that is the very front of the process. The case $|\alpha| = \sqrt{p}$ refers to one particular point (n, t) and is not necessary for this analysis. We calculate and quote it for completeness.

For $|\alpha| \leq \sqrt{p}$ the form of the stationary phase method theorem quoted above applies, and the calculation goes through directly. One way to present results is to plot the values of the integral for a range of n at one fixed value of t; this gives the snapshot of the process in space at that time t. At this point, for the long and cumbersome calculation we refer to Appendix G, and here the results are given.

The integrals (4.7) give the non-stationary contribution to the coefficient $a_t(n)$. They are evaluated numerically, which together with I_{1+2} of Eq. (4.5) gives the coefficient shown in Fig. 4.2.

On the other hand, their analytical asymptotic at large t, in the regime $|\alpha = \frac{n}{t}| < \sqrt{p}$, established in Appendix G, is

$$I_{t,\omega_k} \sim \frac{1}{\sqrt{t}} \sqrt{\frac{2\pi}{|\omega_s''|}} \frac{(1+\alpha)^2}{4\pi} \cos\left(\Phi_{s1}^{+}\, t + \frac{\pi}{4}\right) \times \left[1 + (-1)^{t+n}\right],$$

where $\Phi_{s1}^{+} = \Phi_{+}(k{=}k_{s1})$, the value of the exponent $\Phi^{+} \equiv -\alpha k + \omega_k$ at the first stationary point k_{s1}, and $\omega_s'' = \omega''(k{=}k_s)$ (as ω'' is equal at both stationary points). It agrees nearly perfectly with the numerically evaluated one, see Fig. G.1, and this is a testimony of sorts to the method used.

The remaining coefficients are calculated in a very similar manner. They acquire an oscillating factor what results in a diminishing amplitude of the propagating fronts.

4.1.3 The coefficients $b_t(n)$, $c_t(n)$, and $d_t(n)$.

The behaviour of the remaining coefficients (b_t, c_t, and d_t) is of the exact same nature as for the a_t seen above (with decreasing peaks), and the representative plots are in Appendix H. Here we list results.

Coefficient $b_t(n)$ Using the relation for the evolution of Fourier components of the coefficients (4.2), we have for the generating function $\widehat{b}_t(k)$ and its inverse $b_t(n)$

$$\widehat{b}_t(k) = \sum_{i=1}^{4} \frac{(\lambda_i)^t}{\langle v_i|v_i\rangle}\langle e_2|v_i\rangle, \quad b_t(n) = \frac{1}{2\pi}\int_0^{2\pi} e^{-\boldsymbol{i}\,k\,n} \sum_{i=1}^{4} \frac{(\lambda_i)^t}{\langle v_i|v_i\rangle}\langle e_2|v_i\rangle,$$

where $\langle e_2|v_i\rangle$ is the second coefficient of $|v_i\rangle$ in Eq. (4.3). This leads to same types of integrals as for $a_t(n)$. By repeatedly reducing to the $I_{1,2}^{(a)}$ derivation we find

$$I_{1+2}^{(b)} = \frac{\left[1+(-1)^{t+n}\right]}{4}\left[\left(\frac{1-\sqrt{1-p}}{\sqrt{p}}\right)^{|n+1|} + \sqrt{p}\left(\frac{1-\sqrt{1-p}}{\sqrt{p}}\right)^{|n|}\right]. \tag{4.9}$$

With I_{1+2} of Eq. (4.9) and I_{t,ω_k} integrated numerically, we get the coefficient $b_t(n)$, shown in Fig. (H.1). This coefficient is real, as well.

Coefficient $c_t(n)$ Using the third coordinate $\langle e_3|v_i\rangle$ with

$$c_t(n) = \frac{1}{2\pi}\int_0^{2\pi} e^{-\boldsymbol{i}\,k\,n} \sum_{i=1}^{4} \frac{(\lambda_i)^t}{\langle v_i|v_i\rangle}\langle e_3|v_i\rangle$$

we obtain completely analogous integrals, with the stationary part yielding

$$I_{1+2}^{(c)} = \frac{\left[1+(-1)^{t+n}\right]}{4}\left[\left(\frac{1-\sqrt{1-p}}{\sqrt{p}}\right)^{|n+1|} - \sqrt{p}\left(\frac{1-\sqrt{1-p}}{\sqrt{p}}\right)^{|n+2|}\right]. \tag{4.10}$$

As previously, adding I_{t,ω_k} integrated numerically with I_{1+2} computed by Eq. (4.10), we get the coefficient $c_t(n)$, shown in Fig. (H.2). The coefficient is real.

Coefficient $d_t(n)$ Proceeding the same way,

$$d_t(n) = \frac{1}{2\pi}\int_0^{2\pi} e^{-\boldsymbol{i}\,k\,n} \sum_{i=1}^{4} \frac{(\lambda_i)^t}{\langle v_i|v_i\rangle}\langle e_4|v_i\rangle,$$

and noting that the coordinates $\langle e_4|v_{1,2}\rangle$ are the simple $e^{-2\boldsymbol{i}k}$, this reduces to

$$I_{1+2}^{(d)} = \left[1+(-1)^{t+n}\right]\frac{\sqrt{1-p}}{4}\left(\frac{1-\sqrt{1-p}}{\sqrt{p}}\right)^{|n+2|}, \tag{4.11}$$

the same expression as for $a_t(n)$ but centered around $n = -2$. Adding I_{t,ω_k} integrated numerically with I_{1+2} by Eq. (4.11), we get the (real) coefficient $d_t(n)$, shown in Fig. (H.3).

4.1.4 The probability

Finally, $|\psi(t,n)|^2 = |a_t(n)|^2 + |b_t(n)|^2| + |c_t(n)|^2 + |d_t(n)|^2$ is the probability as a function of time and position, which is our final result. In Fig. (4.3) this is shown for a few time steps.

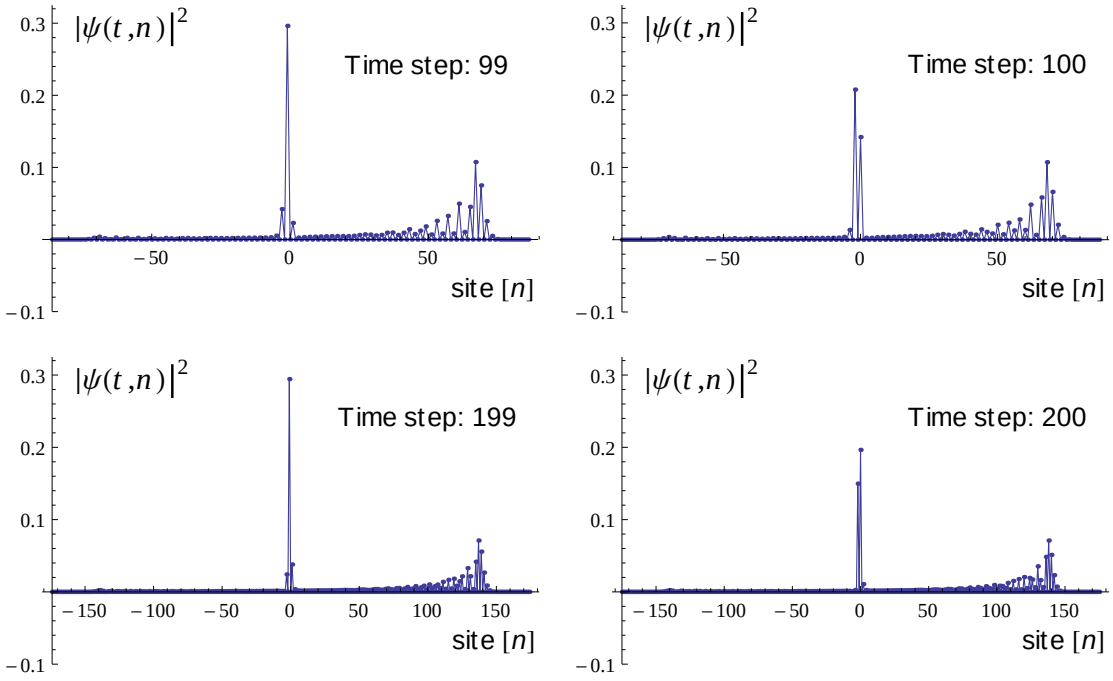

Figure 4.3: Probability $|\psi(t,n)|^2$ as a function of position (site), at some time-steps. The central peak is time-independent, and it is non-zero only very close to the center.

4.2 Discussion

The first feature of this walk is the central peak, which is also stationary due to the eigenvalue of 1. Normally quantum walks do not have anything like this, but here we are looking at a (quantum) walk for which we expect some classicality to show up. However,

it is not a priori clear what exactly to expect, and the strong time-independent central peak does not disappoint as the outcome. It also brings up interesting relation to some other noted work, discussed below.

The walk is seen to retain the ballistic propagation ($n \sim t$) typical of quantum walks in 1 dimension, as opposed to the diffusive one ($n \sim \sqrt{t}$) of classical random walks. The question comes to mind, at what point in the transition to classical behaviour is this lost? It would be beneficial to introduce some classical features (to manage the process more easily), while maintaining the quantum efficiency in exploring the state space.

We also see a practically complete directionality of the walk, where the left peak is tens of times smaller (G.1.2) than the right one already at mere 100 steps. This kind of asymmetry is seen in standard coined (memoryless-based) quantum walks as well and is dependent on the initial coin state, but it is never nearly as pronounced. A property like this can be extremely useful for algorithmic uses, since the walk can apparently be fully directed.

4.3 The results in the context of the literature

The framework presented in Chapters 2 and 3 is designed by analogy with classical memoried walks. One property of quantum walks constructed in that way is a certain directionality, an arrowed structure. The framework is distinct from other models, while some ideas based on, or in some ways related to, memory in walks had been seen in literature, as discussed in detail in Sec. 2.1.3. However, the use of this one-step-memory based framework on the binary tree (Ch. 3) had no precursors; there had simply been no explicit constructions of DTQW on the binary tree. In general, relation between unitarity and memory in cellular automata and quantum walks has been noted [13, 42], but to the best of our knowledge not explicitly investigated.

Our next step in the examination of memoried nature of this quantum process, of adding another level of correlation, revealed distinct behaviour of the walk discussed above. That already brings us into a closer contact with a body of work on broader aspects of DTQW, other than one-coin one-dimension algorithms-only efforts. Below we first review some work that is in principle loosely related to the two-step-memory walk presented in this Chapter, and then discuss a particular noted multi-coin model that comes much closer to our study.

This walk can *in principle* be related to studies of multi-dimensional DTQW, with one of the most well-known and earliest works [100]. However, such studies are explicitly concerned only with higher spatial dimensions (in the state space) and generally do not turn to a (possible) relation to correlation in walks. Another interest that is in principle somewhat similar are studies of correlation effects, such as [101]. Their "memory-dependent" DTQW means that explicit (coupled) memory agents are added to the Hamiltonian, as well as uncorrelated memory terms. This is clearly not what we do, but with particular choices in our formalism it can be related. Randomized coin is used in [102] and asymptotic behavior studied. This work is also concerned with correspondence of QW with classical random walks. It may be possible to relate it to explicit correlations under some conditions, but basic approach is very different. Finally we notice in passing that some studies involving quantum "multibaker" maps, for example [103], can be related to multiple coin formulation of DTQW.

On the other hand, our walk with extended correlation is at least partly a study of how such quantum walks can be related to classical processes. This implies a consideration of the "quantum–to–classical transition" as well, and this is a topic of constant interest, approached in a variety of ways. The most direct and thorough take on this problem for quantum walks is the well-known study by Brun, Carteret, and Ambainis from 2003 [81, 82, 104]. While their paper on effects of decoherence [82] does not directly relate to our work, the one with multiple coins [81] certainly does, in spite of its approach unrelated to memory or correlations in the walk. Interestingly, the paper obtains very similar results. Here we make a very brief and basic statement of related aspects of that work, for convenience.

The paper investigates the following scenario. Instead of acting with the coin by repeatedly using the same (unitary) operator, a "different coin" is used in subsequent steps. The coin can be replaced every time, or a certain number of coins can be used cyclically. The rational is that this should enable one to reproduce a classical random walk, if a new coin is used every time and then measurements performed so to average over the ensemble. Thus one can study a transition from quantum to classical behaviour. What a "different coin" means is critical and discussed in detail below. It is mentioned that this is equivalent to using multi-dimensional coins, but the paper does not examine various possibilities in such identification. In short, the main finding is that the ballistic propagation remains unless a coin is changed at every step, in which case one finds

classical behaviour. This well-quoted work has not been pursued directly, but related ideas have been examined and we first list some of them briefly, before discussing relation between [81] and our work.

Higher dimensional coins are mentioned in [73], in the context of the study of dependence of walks on initial conditions (the objective of that paper). A setup extremely interesting to us is used in [105], with multiple coins each having a history dependence (on the previous tosses of others). This paper comes closest to our interests. However, they use a particular model of memory (history), what results in the coin operator with explicit probabilities for which it is not at all clear how it relates to ours. More importantly, the paper does not pursue nor discuss effects of this on the quantum process it uses, but is rather concerned solely with implementing a so-called Parrondo game. This is a construct from classical probability in which two losing games are combined to obtain a wining one, that has had many (classical) applications. While this paper diverges from our direction right at the onset, and it has not been pursued further, it is interesting to see that our work can be used directly for studies of Parrondo effect in quantum computing, which recently has drawn attention and papers (for example, [75, 106]). Also interesting to us and implicitly related are studies of multiple coins that are entangled in particular ways, for example [107, 108]. This could be related in some way to spatial entanglement across our walk, which is a direction we plan to pursue. A variation of the multiple coin idea of [81] is also used for an entanglement measurement scheme in [109]. Now we comment specifically on how our work relates to [81] summarized above.

First we need to make precise the statement of the "new coin" introduced at steps. (Never made explicit in the paper!) A standard discrete time quantum walk with a 2-dimensional auxiliary (coin) space is a walk of a two-component state. By introducing a "different coin" the authors introduce (two) new components, so then their new state vector is a four-component state. This can be interpreted similarly as ours adding memory, as shown when setting up the problem in the beginning of this Chapter, which is one of the main reasons why we used the coin formalism.

However, their initial coin acted on the original two components, while the "new coin" will act *only on the new components*, in the newly introduced subspace. Every next coin that is introduced brings in its own subspace and stays restricted to it; their walk is fully separable, and if they actually wrote down this multidimensional coin it would be a block-diagonal operator, with two-by-two "coin" blocks. This is the reason why it can

be technically reduced to integrals for a normal 1d walk and solved (to an extent). Their walk would become directly related to ours if their coins were *exchanged* at every step, acting in each other's subspaces in turn; however, then none of their analysis could go through.

This difference is critical, making our walks *completely distinct processes*. In the language of the internal degree of freedom (coin), our walk has its coin components mixed, and there is no way to transform this away; the coin operator is easily seen to be irreducible. In the light of this, it is entirely unclear to us in what sense their walk examines a "transition to classical" since it does not at all relate to correlations of interference between components (or history), but rather adds a duplicate of a kind of the original walk with every new coin. Again, this is precisely why their decomposition works and the walk is reduced to a multiple of 1-dimensional walks. In the case of the limit of a new coin introduced at every step, the whole process is broken up into non-interfering parts, and it seems plausible that this may indeed be a classical process. (Even though their only justification is via comparison of the moments in that limit.) As for anything less than that, we find it unclear what exactly their process represents. It is certainly interesting, but it is also something different from our walk.

More interestingly, their (numerical) results for the two-coin case that are shown seem to agree very well with our result for the two-step memory. They certainly show exact same features, with a time-independent central peak that exists only very near the center and the ballistic propagation of the outside peaks (fronts). Since we have different walks, as discussed above, and our objectives and approaches to them are different, as discussed next, we find this agreement to be interesting and worth clarifying. We do not have answers yet, but we do now compare our work in some detail.

The objectives of the paper are clearly stated as comparison with classical moments to reveal whether the altered quantum walk becomes classical. While they find what they look for with a new coin at every step, the meaning of the process with partial replacement of coins is not discussed and is unclear, while interesting.

Our work is concerned with subtle alterations of quantum walks, asking what happens when one reaches somewhat deeper into correlations in a quantum process. In other words, we are not primarily studying the transition to classical behaviour, but rather a possible appearance of faint classical features, or any anomalies in general, in quantum walks. This may be of direct use for algorithmic purposes, as it would allow much greater

control over the process, and we certainly find it interesting as an explicit and detailed study of the quantum nature of the walk. (Of course, it *does* imply a study of the full transition as well.)

The difference is also very clear technically. We do not study enlarged internal space, nor multiple coins—we are specifically interested in correlations (over histories) and memory in a quantum process.[3] The process can be represented via an enlarged coin space as well, but the point is very different and this has explicit consequences. For example, the paper works with moments of the distribution, in order to compare them with known classical ones; the nature of coins is not relevant for that purpose, nor discussed. (It is simply Hadamard many times over.) Our analysis is focused on the properties of the amplitude (state), in the light of the explicit history in the process, and our "coin" (used as a formal implementation of the interchange framework for two-step memory) is very specific, constructed precisely to encode this.

Finally, we need to comment on statements in the work [105], briefly mentioned above, with the walk defined much as ours is to start with, but diverging in use from the beginning (toward a Parrondo game). That work mentions the paper [81] discussed above at length, finding the same basic difference. (They do not seem to identify it fully, perhaps because their own work is unrelated.)

Given the previous discussion, we believe that the work described in this Chapter is the first detailed and *explicit* examination of the quantum nature of DTQW and of their gradual transition toward classical features. This is only the first step in such a direction, and we plan to significantly extend and expand this effort.

In closing, we mention a recent suggestion for an implementation of a DTQW with a 4-dimensional coin [110], which so far has been at least noticed [111]. The scheme proposed in that paper should in principle be usable for implementing the walk described in this Chapter, and we find this an exciting possibility.

[3] Keeping tabs on history directly affects the path integral (its discrete form as used for these discrete nearest-neighbor processes), removing some interferences between paths and thus explicitly examining the quantum (unitary and so memoried) nature of the process. This is another aspect of the increased correlation that we plan to pursue further.

Chapter 5: Graph connections and network analysis with DTQW

5.1 Introduction: overview and significance

Quantum walks have been motivated by principles and approaches from the classical probability theory and its applications to stochastic processes across various sciences. While this is still an emerging field in quantum computing, by now quantum walks have been established as a well-rounded tool for construction of algorithms and are becoming a general investigative tool. However, the dramatic algorithmic benefits expected by analogy with classical uses of random walks are still awaited for, while quantum walks have not been established yet as a general tool either. Judged by the uses of classical stochastic techniques, we believe that quantum walks can benefit from stepping beyond current approaches. In the rest of this thesis we focus on such ideas, that are still in the initial stages of development in this field. In this Chapter we ask and solve a graph–matching question, and construct a conceptual framework for building networks that can be analyzed using this approach.

Network reconstruction or discovery—finding the structure/internals of a network—is one of the central problems in computer science and its modern applications. With access only to network's end nodes, classically it is a very difficult problem, as the state of a classical process on the end nodes is the same regardless of which connection it went over. On the other hand, because of superpositions in propagation, quantum states on end nodes can be manipulated to retrieve information about paths, for a suitably designed quantum process. This is where quantum walks can be very helpful.

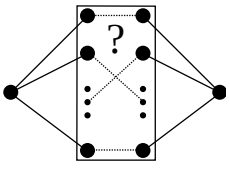

Consider a simple network formed by two graphs: each emanates from a single node, and they are connected via their leaves, but in an unknown manner. To start, consider the simplest case: All nodes connect directly, except for one pair which is transposed. We construct a discrete-time quantum walk over such a network, and identify the transposed node, thus the connection. It is critical that our approach uses the framework for discrete-time quantum walks described in the previous Chapters, that

draws its design from classical memoried random walks and thus does not need "coin" spaces. This solution has interesting and surprising features, that give rise to a conceptual procedure for building networks that can be analyzed using the same method. Here we outline some such ideas, and our work toward them that is discussed in this Chapter.

The method used for a single transposition can be directly generalized to multiple ones, and this translates into results for arbitrary permutations. Such a general solution has a direct potential to establish a new use for quantum walks, in network exploration and analysis, while solving a specific and difficult classical problem which we believe is slated to have important applications (that we still need to identify). Further development of the method involves more complex networks, and networks formed by joining more complex graphs. As it turns out, it is possible to construct networks of increasing complexity that can still be analyzed by the algorithms developed for the simple network outlined above, by virtue of the particular framework for DTQW [72] that we use.

This work brings together two general directions. The method used here is drawn from our framework, which is a different approach to DTQW, as discussed so far. Such methods have not been well explored yet, in our opinion mainly because quantum walks are still in rapid development and a number of standard stochastic approaches have simply not yet been utilized. We find it important for the development of quantum walks to employ methods alternative to standard coined walks, and to establish more flexible, and in the first place different, approaches.

On the other hand, the problem is also a starting point for a broader, long-term direction that we are pursuing. The main approaches in classical computing are mostly based on either Fourier transform or on random walks. It is very interesting that quantum mechanics and computation affords us to utilize analogous approaches together. For example, in the preliminary solution outlined above, a suitable mixing of components that allows the identification is achieved by placing Fourier and its inverse at the end nodes. Quantum walks are characterized by mixing of components, and in our framework we can simply use Fourier for this. For the moment this project is focused on the network discovery framework. However, we keep in mind (and observe) broader insights related to uses of Fourier transformation with quantum walks, aided by the use of our framework. A systematic exploration of this promising research direction has a potential for establishing a tool of unmatched power. It is without any analog in classical computational sciences, and as such is a natural prime target for examination in quantum computing.

5.1.1 Related work and research directions

The work described in this Chapter can be related to quantum process (or channel) tomography [1, 112, 113]. However, the problem we focus on has not been investigated in this context. Additionally, our broader intended work will be directed toward establishing a tool combining Fourier transformation and quantum walks, and this appears to be an unexplored direction. Nevertheless, quantum tomography is a broad field with varied results, and here we identify and review some of its connections to our work.

Quantum process/channel tomography (QPT) is mostly related to open systems; however, much of this work applies to processes not necessarily involving interaction with environment. There are various approaches, for example, "indirect" ones involving state tomography, standard [114, 115] and ancilla (entanglement) assisted process tomography [116–119], and "direct" characterization of quantum dynamics [120, 121]. Our work relates to the recently introduced framework for quantum networks [122]. Perhaps the most closely related aspect of QPT is channel discrimination [123–128]. (See "Subsequent work" [128, Ref.s 16–26] as well.) The key in our preliminary solution is the interference between different components in the DTQW (as explained below), supporting and extending [126]. Note that, in the terminology of DQP, we deal with a unitary channel [123, 124, 129], and we do not require a single access to it. Consistent with this, we do not need an ancilliary system [130], and can locally (without use of entanglement) discriminate the channel with arbitrary probability, in a fixed (and small) number of uses. We do not see how "adaptive strategies" would improve the discrimination, possibly providing an example for the study [130]. We should also point out that we do not discriminate between a pair of operators (but, rather, among many), while on the other hand a lot is known about the channel. In terms of algorithmic behavior and resource analysis [131], our approach utilizes particulars of the network we analyze; our preliminary results are obtained in a fixed number of measurements and we expect either sublinear or fixed-time general results, so general QPT estimates are not comparable.

We comment briefly on this relation in the next two sections, once we present our approach and current (preliminary) results. This problem can be seen as a specific realization of QPT. It also potentially adds to the discussion of entanglement vs. interference as a key resource in quantum computing [132], in particular given how entanglement of the state of the walk evolves over the network, seen and commented in Sec. 5.2. However,

at this stage we do not plan to specifically pursue its role in the DQP context.

Different aspects of this problem are related to graph theory, and to various fields in computer science. Our problem deals with the mismatch in graph enumeration, and to an extent it is related to graph matching and similarity. In the field of pattern recognition, for example, similar problems were studied using both continuous- and discrete-time quantum walks [133, 134].

It may be interesting to note that one of the well known results in algebraic problems in quantum computing, establishing Fourier transforms over symmetric groups [135], while not directly related to our work in some sense brings together our two objectives.

This study is made possible by the use of our memory-motivated framework for DTQW. The main intended algorithmic uses and expectations of the interchange framework are related to the property of walks to effectively explore the state space, analogously to classical walks, what can be utilized by the explicitly memoried evolution. However, there are other various benefits of the 'arrowed' structure, specifically discussed in the next section.

5.2 Network analysis and discovery

Finding information about the structure of networks is an important problem in modern applications of computer science. With classical approaches it is not possible to learn anything about network internals while having access only to its outside modes. Quantum mechanical superpositions, on the other hand, encode this information in the final states, after a process has traversed the network. We use a DTQW built with the interchange framework extensively discussed earlier. This also provides examples related to various process tomography questions, and supports study of entanglement and its flow over the network. We approach the problem with a simple example, of two graphs with an unknown permutation of edges that connect them, as in Fig. 5.1.

Consider two graphs: end-node 0 (left) connected to nodes $\{1, 2, \ldots, n\}$, and end-node $0'$ (right) connected to nodes $\{1', 2', \ldots, n'\}$. The graphs are connected in the middle, but it is not known how: Their middle nodes may meet directly ($1 \leftrightarrow 1'$, etc), or be permuted in some unknown way. This can be stated in terms of graph labeling—the nodes connect directly but their respective labels are mismatched. For clarity, focus on the case where there may be one transposition (say, $1 \leftrightarrow 2'$ and $2 \leftrightarrow 1'$), while all other

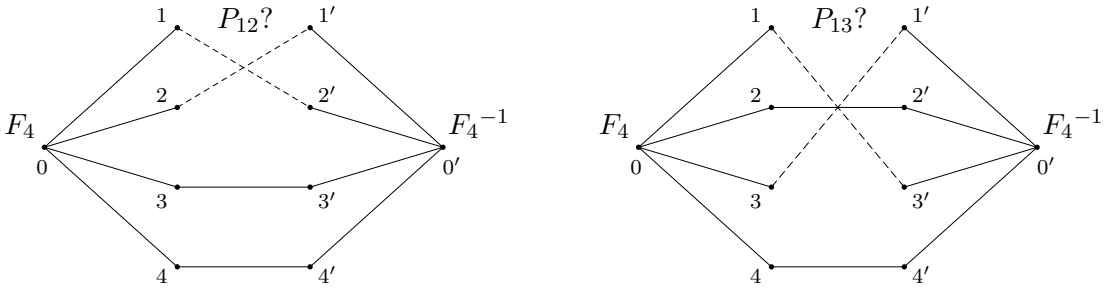

Figure 5.1: Nodes connected in an unknown manner. Shown are possible permutations $(1\,2) \to (2\,1)$ vs. $(1\,3) \to (3\,1)$.

nodes connect directly. We need to determine the transposition, if there is one.

We set up a DTQW on this structure, using the interchange framework. It is useful to think of the walk as the arrow $(|i\rangle \otimes |j\rangle)$ proceeding along the graph, at each step being first reversed by $\widehat{X}$, and then (the originating state) acted upon by U_j for that site. For the operators in the corner vertices we choose Fourier and its inverse, and reduced to their nearest-neighbor subspaces,

$$U_0^{\text{red}} \;=\; F_4 \;=\; \begin{bmatrix} 1 & 1 & 1 & 1 \\ 1 & i & -1 & -i \\ 1 & -1 & 1 & -1 \\ 1 & -i & -1 & i \end{bmatrix}, \qquad U_{0'}^{\text{red}} \;=\; {F_4}^{-1} \;=\; {F_4}^{*}.$$

(This is by no means the only option. For example, the 4-dimensional Hadamard operators can be used as well, resulting in walks with different properties, which generally bring in less complexity but are easier to analyze.) The U_j operators at all other sites need to facilitate forward steps, acting after the state has been reversed, so in their nearest-neighbor subspaces, $U_{i/i'}^{\text{red}} = \left[\begin{smallmatrix} 0 & 1 \\ 1 & 0 \end{smallmatrix}\right]$, for $i = \{1, \ldots, n\}$.

We trace step by step one full cycle on this graph, starting from a sharp state. For concreteness, we start with $|\psi_{\text{init}}\rangle \equiv |\psi_0\rangle = |0\rangle \otimes |3\rangle$, think of a graph with 4 vertices, and consider the only transposition to be $P_{12} = (12) \to (21)$, shown on the Fig. 5.1. However, this does not deprive us of generality, and we also show evolution for a general graph with (any) one unknown transposition.

Step 1. With $U_3^{\rm red} = \left[\begin{smallmatrix} 0 & 1 \\ 1 & 0 \end{smallmatrix}\right]$ in the subspace $\{|0\rangle, |3'\rangle\}$, we have:

$$|\psi_0\rangle = |0\rangle \otimes |3\rangle \xrightarrow{\widehat{X}} |3\rangle \otimes |0\rangle \xrightarrow{\widehat{U}=|3\rangle\langle 3|\otimes U_3} |3\rangle \otimes |3'\rangle = |\psi_1\rangle.$$

Note that in general there may be a permutation on the way, as 3 may be connected to a vertex $\sigma(3) \neq 3'$. Thus in general, $|0\rangle \otimes |3\rangle \to |3\rangle \otimes |\sigma(3)'\rangle = |3\rangle \otimes P_\sigma^{'}|3\rangle$. We use the notation $P_\sigma^{'}$ to stress that the permutation $P_\sigma^{'}|i\rangle$ produces a primed state $|\sigma(i)'\rangle$.

Step 2. The walk proceeds to the other corner, $U_{3'}^{\rm red} = \left[\begin{smallmatrix} 0 & 1 \\ 1 & 0 \end{smallmatrix}\right]$ in subspace $\{|3\rangle, |0'\rangle\}$, and

$$|\psi_1\rangle = |3\rangle \otimes |3'\rangle \xrightarrow{\widehat{X}} |3'\rangle \otimes |3\rangle \xrightarrow{\widehat{U}=|3'\rangle\langle 3'|\otimes U_{3'}} |3'\rangle \otimes |0'\rangle = |\psi_2\rangle.$$

In general, when $\sigma(3) \neq 3'$, we have $|\psi_1\rangle = |3\rangle \otimes |\sigma(3)'\rangle \to |\sigma(3)'\rangle \otimes |0'\rangle = |\psi_2\rangle$.

Step 3. Now $U_{0'} = F_4^{-1}$, and the state will get mixed. The step proceeds as

$$|\psi_2\rangle = |3'\rangle \otimes |0'\rangle \xrightarrow{\widehat{X}} |0'\rangle \otimes |3'\rangle \xrightarrow{\widehat{U}=|0'\rangle\langle 0'|\otimes U_{0'}} |0'\rangle \otimes F_4^{-1}|3'\rangle = |\psi_3\rangle.$$

Again, in a general case, when the walk starts along a permuted connection,

$$|\psi_2\rangle = |\sigma(3)'\rangle \otimes |0'\rangle \to |0'\rangle \otimes F_4^{-1}|\sigma(3)'\rangle = |0'\rangle \otimes F_4^{-1}P_\sigma^{'}|3\rangle = |\psi_3\rangle.$$

Step 4. At this point, it gets more complicated: now we have a superposition $|\psi_3\rangle$ in which some states will propagate over permuted connections and some will not. The state at the next step is entangled, and cannot anymore be presented in a form with operators acting on only one state in the product. (However, this property is restored at the next step, when the graph gets collected again into the corner node.)

$$|\psi_3\rangle = |0'\rangle \otimes F_4^{-1}P_\sigma^{'}|3\rangle \xrightarrow{\widehat{X}} F_4^{-1}P_\sigma^{'}|3\rangle \otimes |0'\rangle = \sum_{\{i'\}} a_{i'}|i'\rangle \otimes |0'\rangle$$
$$\xrightarrow{\sum \Pi_j \otimes U_j} \sum_{\{i'\}} a_{i'}|i'\rangle \otimes U_{i'}|0'\rangle = \sum_{\{i'\}} a_{i'}|i'\rangle \otimes |\sigma^{-1}(i)\rangle = |\psi_4\rangle,$$

since $U_{i'}$ send states via the inverse permutation to $\sigma^{-1}(i)$. Note that the sum above is

over both $\{i\}$ and $\{i'\}$ indices, $|\psi_3\rangle = a_{1'}|1'\rangle \otimes |\sigma^{-1}(1)\rangle + \cdots$, where $a_{i'}$ coefficients are given by action of Fourier transformation.

Step 5. The walk proceeds, reaching the corner node,

$$|\psi_4\rangle = \sum_{i'} a_{i'}|i'\rangle \otimes |\sigma^{-1}(i)\rangle \xrightarrow{\widehat{X}} \sum_{i'} |\sigma^{-1}(i)\rangle \otimes a_{i'}|i'\rangle \xrightarrow{\sum |j\rangle\langle j| \otimes U_j} \sum_{i'} |\sigma^{-1}(i)\rangle \otimes a_{i'}U_i|i'\rangle.$$

Here all U_i send $|i'\rangle$ states into $|0\rangle$, and we get

$$|\psi_5\rangle = \sum_{i'} a_{i'}|\sigma^{-1}(i)\rangle \otimes |0\rangle = \sum_{i'} a_{i'}P_\sigma^{-1}|i'\rangle \otimes |0\rangle = P_\sigma^{-1}\left(F_4^{-1}P_\sigma^{'}|3\rangle\right) \otimes |0\rangle.$$

The state is given by action of all operators on one qubit, $|\psi_5\rangle = P_\sigma^{-1}F_4^{-1}P_\sigma^{'}|3\rangle \otimes |0\rangle$.

Step 6. In the last step the walk gets turned around at the corner node:

$$|\psi_5\rangle = P_\sigma^{-1}F_4^{-1}P_\sigma^{'}|3\rangle \otimes |0\rangle \xrightarrow{\widehat{X}} |0\rangle \otimes P_\sigma^{-1}F_4^{-1}P_\sigma^{'}|3\rangle \xrightarrow{|0\rangle\langle 0| \otimes U_0} |0\rangle \otimes F_4P_\sigma^{-1}F_4^{-1}P_\sigma^{'}|3\rangle = |\psi_{\text{final}}\rangle.$$

Thus the final state after one pass is obtained by an action of one operator on the second state in the product. With an initial state at the corner being an arbitrary linear superposition of states like the one considered above, $|\psi_0\rangle = |0\rangle \otimes \sum b_i|i\rangle$, we have in general

$$|\psi_i\rangle \xrightarrow{\text{cycle}} |\psi_f\rangle = \left(\mathbb{I} \otimes F_4P_\sigma^{-1}F_4^{-1}P_\sigma\right)|\psi_i\rangle \equiv \left(\mathbb{I} \otimes \mathcal{C}_\sigma\right)|\psi_i\rangle, \quad \mathcal{C}_\sigma = F_4P_\sigma^{-1}F_4^{-1}P_\sigma. \quad (5.1)$$

Here we introduced the graph operator $\mathcal{C}_\sigma$ (which is a group commutator, as discussed below). Note that with pure transpositions $P_\sigma^{-1} = P_\sigma$. For the walk that starts along an untransposed connection, the operator simplifies to $\mathcal{C} \to \mathbb{G}_\sigma = F_4P_\sigma^{-1}F_4^{-1}$ (as $P_\sigma = \mathbb{I}$). Note that this describes the general case as well (when there may be a transposition on the initial connection), since the last P_σ can be understood as modifying the initial state (irrelevant for the calculation), and the rest of the formalism applies using $\mathbb{G}$. We will be considering the full $\mathcal{C}$ commutator in generalizations of this problem, but for the permutation identification we use $\mathbb{G}$.

We emphasize at this point that the size of the graphs does not affect the calculation,

either. In other words, this formalism fully applies to a graph with n vertices, along with the obtained commutator structure of the effective graph operator. The question of multiple transpositions is a different matter, of course. However, once this is discussed below it is seen that the size of the graph does not affect that generalization either.

It is interesting and useful that the graph action is entirely in the second state of the product, and that the action of the whole graph is given by a compact operator, reduced to the dimension $n \times n$, in the subspace of neighbors nearest to end-nodes. Then the first finding is immediate. With a permutation we get a superposition, while when there is no permutation, the initial state does not change ($\mathbb{G}_\sigma = \mathbb{I}$), thus: Finding out whether there is a permutation (an error in the line, for example) is a matter of determining whether in the end we receive the initial state back, what is accomplished very easily.

It may be informative to show the graph/network operators for the case of one transposition, for $n = 4$. With P_σ being the standard matrix representation of the permutation operator, for possible transpositions $\sigma = \{12, 13, 14, 23, 24, 34\}$, we have for all $\mathbb{G}_\sigma = F_4 P_\sigma F_4^{-1}$ operators

$$\mathbb{G}_{12} = \tfrac{1}{2}\begin{bmatrix} 2 & 0 & 0 & 0 \\ 0 & 1 & -1+\boldsymbol{i} & \boldsymbol{i} \\ 0 & -1-\boldsymbol{i} & 0 & -1+\boldsymbol{i} \\ 0 & -\boldsymbol{i} & -1-\boldsymbol{i} & 1 \end{bmatrix}, \quad \mathbb{G}_{13} = \tfrac{1}{2}\begin{bmatrix} 1 & 0 & 0 & 0 \\ 0 & 0 & 0 & -1 \\ 0 & 0 & 1 & 0 \\ 0 & -1 & 0 & 0 \end{bmatrix},$$

$$\mathbb{G}_{14} = \tfrac{1}{2}\begin{bmatrix} 2 & 0 & 0 & 0 \\ 0 & 1 & -1-i & -\boldsymbol{i} \\ 0 & -1+\boldsymbol{i} & 0 & -1-\boldsymbol{i} \\ 0 & \boldsymbol{i} & -1+\boldsymbol{i} & 1 \end{bmatrix}, \quad \mathbb{G}_{23} = \tfrac{1}{2}\begin{bmatrix} 2 & 0 & 0 & 0 \\ 0 & 1 & 1+\boldsymbol{i} & -\boldsymbol{i} \\ 0 & 1-\boldsymbol{i} & 0 & 1+\boldsymbol{i} \\ 0 & \boldsymbol{i} & 1-\boldsymbol{i} & 1 \end{bmatrix},$$

$$\mathbb{G}_{24} = \tfrac{1}{2}\begin{bmatrix} 1 & 0 & 0 & 0 \\ 0 & 0 & 0 & +1 \\ 0 & 0 & 1 & 0 \\ 0 & +1 & 0 & 0 \end{bmatrix}, \quad \mathbb{G}_{34} = \tfrac{1}{2}\begin{bmatrix} 2 & 0 & 0 & 0 \\ 0 & 1 & 1-i & \boldsymbol{i} \\ 0 & 1+\boldsymbol{i} & 0 & 1-\boldsymbol{i} \\ 0 & -\boldsymbol{i} & 1+\boldsymbol{i} & 1 \end{bmatrix}.$$

Another interesting observation is that, for sharp initial states, there are classes of transpositions which yield sharp final states with identical probabilities (ie. with equal coefficients with opposite signs), while others form classes with very closely related superpositions in the final states. For example, this is readily seen on the columns of operators shown above, in particular for P_{13} and P_{24}. It will be interesting to understand why this

is so, how general this class structure is, and to identify such classes for graphs of size 2^k, as this will provide some insight into the nature of Fourier transformation's coupling with a quantum walk. For practical purposes, one can use particular initial superpositions, in which case all transpositions yield unique and distinguishable final states.

Knowing the exact action of all transpositions allows one to classify how each acts on any initial state, for example computationally. Then we can craft such initial superpositions so to get the final state that permits efficient analysis. In particular, when the final state is a superposition of only a few (ideally two) basis states, we can determine with a fixed number of measurements all transpositions, to a desired precision. In most cases, a rather small number of measurements will resolve the operator.

For example, we identify the initial state $|\psi_0\rangle = (1/\sqrt{6})\left(|2\rangle + (2+\boldsymbol{i})|3\rangle\right)$ that allows very efficient identification of all possible transpositions in $n = 4$ case, along with a number of other such two-state combinations. We also established computationally that very similar input combinations yield final states with only a few components, thus resolvable very efficiently, for various (larger) sizes of graphs. There are clear indications that for graphs of any size it is possible to find initial states such that the final states are superpositions of a small number of components. Note that with reasonably sparse final states it is always possible to efficiently identify the operator: Successive (adaptive) measurements narrowing down components' frequencies very soon resolve the state to a desired precision. At this point many results of quantum state tomography can be applied as well, what we plan to incorporate in specific algorithms.

These are practical results, even as they are still limited to the initial stage of identifying a single transposition. It is in principle straightforward to extend this to cases with multiple transpositions. Products of the Fourier operator and a permutation matrix seen above, $F_4 P_\sigma$, form an operator with a rearrangement of rows and columns of the original Fourier. Further such products (with additional P_σ) then result in operators of the same structure, which will allow construction of suitable initial states by a similar algorithm, thus identifying an arbitrary permutation.

The above algorithm concludes with a computational determination of the input state that allows efficient identification of the final state. These are results that form a solid basis for the further development of this problem. However, analytical analysis will be much more interesting. The first task is to develop an analytical algorithm for construction of initial superposition states such that the obtained final states allow an

efficient analysis. (Given the regularities in the operator structure, and our preliminary findings, there is a distinct possibility for fixed-time algorithms.) This can be done efficiently computationally for graphs of any order, but analytical understanding will shed light on properties of Fourier gates in quantum walks, and will allow to ultimately extend the complexity of networks analyzed.

There are strong indications that it is always possible to tell apart different graph operators $F_4 P_\sigma^{-1} F_4^{-1} P_\sigma$. They generally produce final states with coefficients of the form $\sum \alpha_i \omega^i / n$ where $\alpha \in \mathbb{Z}$ and ω being simple root of unity. Input states with coefficients *not* belonging to this extension of $\mathbb{Z}$ (which is $\frac{1}{n}\mathbb{Z}[\omega]$) lead to output states with independent sets of coefficients, and are thus resolvable. We expect to be able to determine a general form of the needed initial states by an algebraic analysis of the product of general forms of the initial and final states, using the above observation. On the basis of this property it is also expected that initial states can be found such that there are very few surviving coefficients in the final state, so that the final states have very few components. Then one would expect a sublinear or even a fixed-time algorithm for identifying operators.

Following this, multiple transpositions need be handled. In principle, this is a straightforward extension of the described procedure. As discussed, allowing multiple σ does not change our treatment of the evolution, and the graph acts again by way of $\mathbb{G}$ that acts on one state in the product. Analytical analysis of the relation between the (suitably) mixed initial and final states should proceed in an analogous fashion. Having in place an analytical algorithm developed for suitable initial states for a single transposition should provide a direct roadmap. Note that, in terms of practical outcomes, these tasks are straightforward to accomplish using software for symbolic calculation (for example, MATHEMATICA). Such findings can also guide analytical treatments.

5.2.1 Complex networks with interchange framework for DTQW

We now discuss further planned work on this problem, beyond identifying a permutation in the network connections. It is an example of one aspect of of our framework for DTQW, which makes it possible to approach the problem described below. By construction, the U_j operators that mix components thus making the obtained process an analog of a random walk, act in the state space (not in auxiliary spaces), also controlling evolution. This helps technically, as many structures of interest have turned out to be

difficult to treat with "coin" spaces. However, perhaps more importantly, this also allows us to model behavior of various networks (in line with [122] for example), as there is no limitation on what operator one may choose for U_j, at any one site. Thus a comparably simple graph may be used to encode complex behavior or structure, by choosing suitable U_j at its appropriate vertices, and running a walk over it.[1] Having quantum walks at one's disposal for such studies is certainly promising. What is really helpful is to have the above procedure that can be used to analyze classes of networks of increasing complexity. A very simple example is the placement of Fourier and its inverse in the corners of the simple network we study so far. Since this is one of the main directions for extension of our current work, we offer a few examples of how increasingly more complex networks can be formed so to permit the same type of analysis as above.

Consider a network such as one shown on Fig. 5.2. As seen in the figure, the graph operator has the same structure as in our initial example, where $A^{-1}F_4^{-1}A$ again performs a basis change on the inverse Fourier, and the resulting $\mathcal{C}$ will bear very similar algebraic regularities as the operator for our initial simple network.

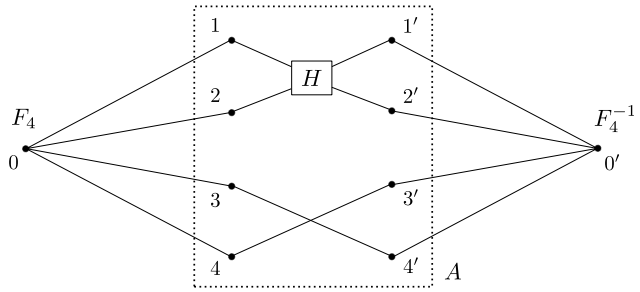

$$A = \begin{array}{c} \\ 1 \\ 2 \\ 3 \\ 4 \end{array} \begin{array}{c} \begin{array}{cccc} 1' & 2' & 3' & 4' \end{array} \\ \left[\begin{array}{cc|cc} \multicolumn{2}{c|}{\multirow{2}{*}{H}} & & \\ & & & \\ \hline & & 0 & 1 \\ & & 1 & 0 \end{array}\right] \end{array},$$

Figure 5.2: An example of forming a more complex network. The graph operator $\mathcal{C} = F_4 A^{-1} F_4^{-1} A$ has the same structure as in (5.1). The operator H shown in the upper half is Hadamard, but the framework we use to construct discrete-time quantum walks can facilitate any (unitary) operator.

We show Hadamard, since we observed that its interaction with Fourier has very interesting properties, and because of its canonical role in quantum computing. However, any operator can be facilitated equally well with the interchange framework. As long as the block structure of the effective middle-of-the-network operator is retained, the

[1] We emphasize that it is in our view crucial that the "coin" U_j is at the same time the operator that acts in the state space and drives the evolution.

resulting graph operator clearly allows approach by a variety of well-studied algebraic techniques. It should be emphasized that efficient input states can readily be found computationally.

Note that the above block A need not be of this particular structure, for the developed formalism to hold. Observe that we went from group commutators of the form $\mathcal{C}_\sigma = F_n P_\sigma^{-1} F_n^{-1} P_\sigma$, where σ were transpositions, to the same commutators for arbitrary permutations. The next step was to consider commutators of the form $\mathcal{C} = F_n A^{-1} F_n^{-1} A$, for arbitrary $A \in SU(n)$. Finally, by placing a general operator $B \in SU(n)$ and B^{-1}, instead of Fourier operators, in the nodes $0'$ and 0 leads us to a general commutator of the form $B^{-1}A^{-1}BA$. Thus the network discovery problem is reduced to analyzing the group commutators, which gives us a robust and well-developed tool for the analysis.

In this framework, we consider the following general problem. Let $G = \{g_1, g_2, \ldots, g_d\}$ be a given group, and let $A_{g_1}, \ldots, A_{g_d}$ be a certain representation of this group in $SU(n)$. Then, we wish to study the network discovery problem via group commutators $B^{-1}A_{g_j}^{-1}BA_{g_j}$. Note that in the case considered in the example in the preceding section, the group G was S_n and $B = F_n^{-1}$. A preliminary comparison to the corresponding classical case yields possibilities for significant algorithmic improvements.

We also note that it is natural to continue constructing considerably more complex and general networks with interesting applications potential, which still allow efficient analysis along the same lines.

The above technique can be used to compare graph labelings, and identify mismatches: We can join two graphs for which we need to be able to compare labelings, and run the above procedure over them. The further developments of this approach can make it suitable for somewhat more general questions related to graph comparisons.

5.3 Summary and current work

To conclude this Chapter we now summarize findings and the expected development of this work. The starting point was a question about how two graphs connect. By the courtesy of particular features of the interchange framework we are able to construct a walk that very directly answers this question in its simplest form.

As it turns out, in the process an interesting property is established as well: A graph acts on a walk in a very compact way, and this can be encoded in one operator. Further,

this operator has the structure of a group commutator.

These findings present a platform for the following developments. First, it is seen that the structure of the problem (of identifying the graph operator) can be reduced to the identification of the final states, where methods and results of the quantum state tomography can then be used if needed. On the other hand, it is also clear that the problem can be effectively analyzed computationally, and for some questions of interest directly solved that way.

The properties of graphs that utilize this walk allow for a clear roadmap for generalizing the problem as well, and in various directions. They also give rise to mathematical developments, that seem to be promising for a complex network analysis. In summary, we plan to pursue the following.

- Complete the multiple transpositions and arbitrary permutation algorithm.
- Use the group commutator properties of $SU(n)$ to analyze the discussed network discovery approaches. Next, develop the comparison to the corresponding classical randomized algorithms.
- Explore deeper algebraic properties, and free-group connections. Also, compare this quantum walk algorithms to the corresponding classical randomized algorithms over group structures. This may connect to the problem discussed in the next Chapter, of walks on non-Abelian structures.
- In the study of propagation properties of DTQW modeled on Markov chains with longer memory, discussed in detail in the Chapter 4, we observed that unlike the classical case these quantum walks do not include replicas of shorter memory quantum walks, thus they are very different process in nature. This hinted at a potential of greater speedup, because of the larger number of parameters that control its propagation, allowing greater flexibility over the design of such walks. These properties motivate similar ideas for the problem at hand, since the freedom to construct network elements should allow us to tweak their properties as needed for algorithmic purposes. This is an intriguing possibility and should be investigated.

Chapter 6: Walk on the symmetric group, "quantum card shuffling"

6.1 Introduction

Algorithms relating to algebraic problems are of widely recognized interest in quantum computing [136]. On the other hand, the next stage in uses of classical stochastic approaches, going beyond Markov chains (random walks on graphs), are precisely walks on algebraic structures. The prime and classic example of such a problem is "card shuffling," a walk on the rich non-Abelian permutation (symmetric) group. This problem for quantum walks had been recognized [14, 137] and attempted with CTQW [138]. However, the approach taken was via the representation theory, which is known in the classical probability to be too narrow to be effective for this problem [139].

We construct a DTQW on the permutation group using a standard method: Based on the action of a (unitary) "coin" operator in an additional space, (unitary) steps in the group space are taken, resulting in a (quantum) walk over group elements. We use general techniques for the eigenvalue problem of the combined "coin" and permutation operators, utilizing regularities in the block structure. We have reached the preliminary stage with solutions for a few low-dimensional cases. The next stage is to integrate them into a more general solution, what will yield the first step in this deep and far-reaching, while very challenging problem.

This Chapter is devoted to the initial efforts along these lines, and is thus different from the preceding ones. The unifying theme is a quest for development of approaches that draw on more advanced techniques known in the classical probability theory. It should be emphasized that much of the specific (partial and/or incomplete) results shown in the sections below present work in progress. Here we first comment on some general aspects of the problem.

Much more can be learned about quantum walks on graphs, and they can be utilized further. Still, it is by no means too early to put concentrated effort into studying quantum walks on non-Abelian structures, since this is the next natural step that quantum walks need to take. Unitary walks on non-Abelian groups are challenging, but they are

approachable by general and standard mathematical techniques. The reward is an access to problems of much greater complexity, which we believe is precisely what is needed in the current state of development of quantum walks, as well as for quantum computing in general. Quantum walks need to produce successful algorithms, but in our opinion they need more to become fully established as a versatile tool that can be used to approach problems of greater variety and complexity. We believe that this problem is one of the suitable starting points.

Our work on this problem relates to the field (of algebraic problems) that in general clearly has a deep significance in quantum computing, and that has the potential to utilize some particular strengths of quantum walks. This comes with a price: It is a difficult subject, and much of mathematics for it in quantum computing has not yet been mapped out. Not much work has been done on this problem, with the very few (notable!) examples now introduced.

The problem of quantum walks on the permutation group was suggested in [14, 137], and was approached by Gerhardt and Watrous in 2003 [138], using continuous time walks. As mentioned before, we are not aware of other related work in this area, and in particular of any attempts using DTQW for any non-Abelian structures. This is somewhat surprising, since "card shuffling" is certainly the next level in uses of stochastic methods, and quantum walks are only to be expected to follow this trend. Here we briefly describe the related work by Gerhard and Watrous [138].

The authors study properties of CTQW restricted to n-cycles on S_n. They use a specific case of transpositions as group generators for the Cayley graph, on which their CTQW is constructed. With transpositions there are various symmetries in the character structure, and the representation theory can be utilized; this is the method exclusively used in the paper. It is established that the limiting distribution of the walk is not uniform, and for a particular (alternating) case of transpositions they obtain the lower bound of how much the limiting distribution departs from the uniform. Many questions "remain unanswered" and points of interest identified, but we have not seen any directed follow up studies.

It should be noted that the case of transpositions is practically the only case on S_n for which one expects the representation theory to be useful for classical walks on the permutation group [139], and quantum walks are only worse in this sense. In more general settings characters do not posses the same useful symmetries, and representation

theory becomes too narrow. Nevertheless, study in this work is interesting and insightful, and we readily confirm some of their basic findings.

The work presented in this Chapter appears to have no direct precursors, apart from the recognition of the problem [14, 137], and the study using CTQW [138], discussed above. The more general mathematical techniques that we use are best introduced along with the explicit descriptions, in the next section. We conclude this introduction with a few comments, and an overview of our approach.

Random walks on the permutation group, or "card shuffling," is among the most important classical stochastic approaches. The richness of the non-Abelian symmetric group lends itself to modeling of complex phenomena, while it also quickly leads to rather complicated problems, and transcends into studies of classical processes on more general algebraic structures. The challenge of studying such quantum processes is no lesser, but the benefits can be expected to even outweigh the classical uses.

We approach the problem from one specific, but by no means trivial case, of "top-to-random" shuffle. Classically, this is a stochastic process where the top card of the deck is moved to a random slot in the deck. In order to construct a corresponding quantum process, let us restate it as follows. An n-dimensional "coin" is tossed (uniformly random choice among n possibilities is made), and based on its outcome ($1 \leq k \leq n$) the "top" card of the deck is replaced to that (outcome's) position. For a uniformly distributed choice (fair coin), the top card has the probability $1/n$ of being in any one position in the deck (including the chance of staying on top), while the deck itself upon each shuffle has the probability of $1/n!$ of being in any one distinct configuration (permutation).

Quantum walks are processes with properties which still have not been fully understood, and walks on a non-Abelian group require a very careful approach. We first describe basics of the evolution of a discrete-time quantum walk constructed in analogy with the classical "top-to-random card shuffling."

6.2 DTQW on S_n: Analogy of top-to-random classical card shuffling

Consider a collection of n distinct elements (states), a "deck of cards." A state of the deck is described by $|\psi\rangle = |c_1\rangle \otimes |c_2\rangle \otimes \cdots \otimes |c_n\rangle$, an element of the Hilbert space $\mathcal{H}^D$, where $D = n!$ and where the card at each position i, $|c_i\rangle$, is a $\lceil \log_2(n) \rceil$-long binary string (qubit system), as needed for its identification. Each configuration of cards in the

deck is an element of the symmetric (permutation) group S_n.

In order to facilitate the mixing of components characteristic of a "quantum walk," we use the standard method, with an additional "coin" space, here necessarily of dimension n. Then the full state we work with is

$$|\psi\rangle = |q\rangle \otimes |\psi\rangle = |q\rangle \otimes |c_1\rangle \otimes |c_2\rangle \otimes \cdots \otimes |c_n\rangle, \quad |q\rangle = \sum_{i=1}^{n} a_i |i\rangle,$$

in the product space $\mathcal{H}^C \otimes \mathcal{H}^D \cong \mathbb{C}^n \otimes \mathbb{C}^{n!}$, which is thus of total dimension $n \times n!$. For clarity we will sometimes omit the direct tensor product signs, and write either of

$$|c_1\rangle \otimes |c_2\rangle \otimes \cdots \otimes |c_n\rangle \equiv |c_1\rangle|c_2\rangle \cdots |c_n\rangle \equiv |c_1\, c_2\, \cdots\, c_n\rangle.$$

The evolution is specified by

$$|\psi_t\rangle = \widehat{U}^t |\psi_0\rangle, \quad \widehat{U} = \widehat{V}(\widehat{C} \otimes I), \quad \widehat{V} = \prod_{j=0}^{n-1} \Pi_j \otimes \widehat{V}_j, \text{ with } \Pi_j = |j\rangle\langle j|,$$

and where $\widehat{C}, \widehat{V}_j$ are unitary. The operator C acts in its "coin" space, in general on an n-component superposition state $|q\rangle$. For each component present in this state after the action of C, the operator V acts on $|\psi\rangle$, moving the card: if the coin "shows k" (k-th component of $|q\rangle$ is non-zero), the card c_1 is moved to the k-th position,

$$\langle k|q\rangle \neq 0 \quad \Rightarrow \quad \widehat{V}_k \colon |\psi_t\rangle = |c_1\rangle|c_2\rangle \cdots |c_n\rangle \;\rightarrow\; |c_2\rangle \cdots |c_k\rangle|c_1\rangle|c_{k+1}\rangle \cdots |c_n\rangle = |\psi_{t+1}\rangle.$$

Thus a new configuration (permutation) is generated with each step, and we have a quantum (unitary) walk over the permutation group elements. The general state can also be written as

$$\psi_t = \sum_{i,\sigma \in S_n} \alpha_i(t)\, |i\rangle \otimes |\sigma\big(0 \cdots (n-1)\big)\rangle, \quad \sum_i |\alpha_i(t)|^2 = 1.$$

Here $\sigma\big(0 \cdots (n-1)\big)$ is a permutation of n elements, enumerated from 0 to $n-1$. As introduced above, we focus on a subset of S_n, restricting the walk to always moving the first card. This is an analogy with "top-to-random" classical card shuffling.

It is generally useful when studying quantum walks to obtain an analog of a classical

limiting distribution, and with it an analog of a mixing time of the walk. In quantum walks the main method of finding the limiting distribution is by spectral analysis, ie. by solving the eigenproblem of the relevant operators. We approach this by generic analysis of the symmetries and block-structure of the evolution operator. As stated in the introduction, we do not expect the representation theory to be useful, since characters will not have the symmetries that they enjoy in restricted cases of walks on S_n (mainly, those generated by transpositions). We approach the problem by study of low-dimensional cases, in order to more easily identify regularities in the operator structure and come up with a preliminary algorithm for block-decomposition.

6.2.1 Beginnings: Quantum walk on S_2 and S_3

The case of a two-card shuffle (S_2) is trivial, working like walks on $\mathbb{Z}^n$. Still, we found it useful to come up with an analysis of the eigenvalue problem which turned out to be a good template for the 3-card (S_3) construction. In S_2 the representation theory approach worked, as expected with abundant symmetries.

The S_3 case, the first non-Abelian dimension, clearly shows an inadequacy of the representation theory. On the other hand, the generic block structure of the complete evolution operator provides guidelines for identification of eigenvectors. Here we sketch the ideas behind this approach, which we also expect to yield a general algorithm. Note that in the following various different block-decompositions are possible and useful, and we utilize two different ones.

The walk can be represented on the Cayley graph $\Gamma = \Gamma(S_n, G)$ of S_n, where G is the generating set of the graph. A generator is an element of S_n that determines which nodes are connected by an edge and what direction that edge has. For instance, for $\Gamma = \Gamma(S_3, \{\pi_1, \pi_2, \pi_3\})$, the Cayley graph that we consider for the 3-card case, the generators correspond to the three different ways the top card can be placed into the deck, ie. $\pi_1 = id, \pi_2 = (12), \pi_3 = (231)$. We use for our coin a symmetric-acting operator

$$C = \frac{1}{\sqrt{3}} \begin{bmatrix} 1 & a & a \\ a & 1 & a \\ a & a & 1 \end{bmatrix}, \quad \text{where } a = e^{2\pi \boldsymbol{i}/3},$$

and then write the evolution operator in the following block-form

$$U = V(C \otimes I) = \frac{1}{\sqrt{3}} \left[\begin{array}{c|c|c} I & & \\ \hline & R_2 & \\ \hline & & R_3 \end{array}\right] \left[\begin{array}{c|c|c} I & aI & aI \\ \hline aI & I & aI \\ \hline aI & aI & I \end{array}\right] = \frac{1}{\sqrt{3}} \left[\begin{array}{c|c|c} I & aI & aI \\ \hline aR_2 & R_2 & aR_2 \\ \hline aR_3 & aR_3 & R_3 \end{array}\right],$$

where R_2 and R_3 correspond to applying generators π_1 and π_2 to the group,

$$R_2 = \left[\begin{array}{c|c|c} X & & \\ \hline & X & \\ \hline & & X \end{array}\right], \quad X = \begin{bmatrix} 0 & 1 \\ 1 & 0 \end{bmatrix},$$

and R_3 is a six-by-six matrix that implements the action of the π_3 generator. Symmetries in such block-diagonal structure suggest a general form for eigenvectors, and allow for algebraic observations and analysis. However, there are various useful other decompositions. The following (further) decomposition of R_2 and R_3 provides guidelines,

$$R_2 = \begin{bmatrix} 0 & X \\ X & 0 \end{bmatrix} \quad \text{and} \quad R_3 = \begin{bmatrix} S & 0 \\ 0 & S \end{bmatrix},$$

with X and S being

$$X = \begin{bmatrix} 0 & 0 & 1 \\ 0 & 1 & 0 \\ 1 & 0 & 0 \end{bmatrix}, \qquad S = \begin{bmatrix} 0 & 1 & 0 \\ 0 & 0 & 1 \\ 1 & 0 & 0 \end{bmatrix}.$$

This suggests to look for an eigen-structure of the form $\sum_{i=1}^{3} |\alpha_i\rangle \otimes |v_i\rangle$, where $|\alpha_i\rangle$ are $6d$ while $|v_i\rangle$ are in $3d$, since

$$\{v_1, v_2, v_3\} = \frac{1}{\sqrt{3}} \left\{ \begin{pmatrix} 1 \\ 1 \\ 1 \end{pmatrix}, \begin{pmatrix} 1 \\ a \\ a^2 \end{pmatrix}, \begin{pmatrix} 1 \\ a^2 \\ a \end{pmatrix} \right\}$$

are an eigenbasis of S and are cycled through by X. Using U on this algebraically yields insight and parts of the spectrum. It leads us to the invariant vectors in the original

($R_{2,3}$) $6d$ subspace,

$$\frac{1}{\sqrt{6}}\begin{pmatrix}\pm 1\\ \pm 1\\ \pm 1\\ 1\\ 1\\ 1\end{pmatrix},\quad \frac{1}{\sqrt{6}}\begin{pmatrix}\pm(1+1)\\ \pm(a^2+a)\\ \pm(a+a^2)\\ (1+1)\\ (a^2+a)\\ (a+a^2)\end{pmatrix},\quad \frac{1}{\sqrt{6}}\begin{pmatrix}\pm(a^2+1)\\ \pm(1+a^2)\\ \pm(a+a)\\ (a^2+1)\\ (1+a^2)\\ (a+a)\end{pmatrix},$$

where entries remind of the origin in the eigenbasis of the generator R_3. (They simplify via $a^2+a+1=0$, since $a=e^{2\pi \boldsymbol{i}/3}$.) The first set are the $6d$ components of eigenvectors of the full operator. Much more importantly, combinations of $\{|v_i\rangle\}$, guided by lessons from the 2-card case, lead to certain 3×3 matrices that produce eigenvalues.

The main points that came up in this procedure can be summarized as follows.

- Eigenvalues come from the 'coin' operator, and in a curious way.
- Rows of the coin operator are multiplied by consequtive roots of unity.
- The eigenvalues of the obtained matrices are eigenvalues of the full $\widehat{U}$.
- This works for various coins too, and it works in the 2-card case as well. It may be a crucial part of a more general procedure.

For the S_3 case the eigenvalues are

$$\Big\{\, e^{-\frac{\pi \boldsymbol{i}}{6}},\, e^{\frac{\pi \boldsymbol{i}}{2}},\, e^{-\frac{7\pi \boldsymbol{i}}{18}},\, e^{\frac{\pi \boldsymbol{i}}{18}},\, e^{\frac{13\pi \boldsymbol{i}}{18}},\\ -\Big(\tfrac{\sqrt{11}}{4}+\tfrac{\sqrt{3}}{12}\Big)-\Big(\tfrac{\sqrt{33}}{12}-\tfrac{1}{4}\Big)\boldsymbol{i},\, \Big(\tfrac{\sqrt{11}}{4}-\tfrac{\sqrt{3}}{12}\Big)+\Big(\tfrac{\sqrt{33}}{12}+\tfrac{1}{4}\Big)\boldsymbol{i}\,\Big\}.$$

We can then obtain (most of) the remaining 3d eigenvectors, resulting in (nearly all) full eigenvectors. (Resolving a few 'black spots' is in progress.) The degeneracies seen above allow for interesting averaging schemes, what in turn allows us to derive limit theorems and "Cesàro averages." This is a particular kind of convergence rates used for quantum walks, which we now define.

Processes such as quantum walks do not have stationary distributions. Thus their limiting behaviour is studied in different ways, and one of standard notions is that of Cesàro averages,

$$\widetilde{f}(T) = \frac{1}{T}\sum_{k=1}^{T} f(k).$$

A natural parameter for k above is most often time. One way to use this is to pick T randomly and work with sequences of averages obtained, for very large T's (formally $T \to \infty$). Often *that* will converge to some limiting value.

One of our findings above was that, unlike in the classical case, the limiting distribution for Cesàro averages turn out to be a distribution other than the uniform, and that it also depends highly on the initial state. This is in agreement with the similar observations in [14] (for S_n) and [138] (for S_3), for both discrete- and continuous-time quantum walks, respectively. Thus, the limit law properties being of interest have yet to be derived. We also observed that if Cesàro averages are modified in a certain way, in the case of S_3, they yield the uniform limit law.

This pattern is one of the first objectives for further investigation, since any feasible averaging scheme would be of great interest for quantum walks in general. It is possible that a modification necessary in non-Abelian problems may be suitable in other areas but are harder to come up with or simply have not been noticed. In the problem investigated here, we can reasonably conjecture that the same modification of the Cesàro average (that we observed for S_3) will yield the uniform limit law in the general case of S_n.

Note that this method of decomposing U, as well as the form of the matrices, is inferred from the (much) simpler 2-card case.

6.2.2 Toward a quantum walk on S_n

The above is interesting because the general S_n case permits the same kind of a block-diagonal decomposition. To demonstrate this we will use the inverse-lexicographical ordering of permutations $\{\sigma_1, \ldots, \sigma_{n!}\}$. For eample, for S_3, this gives:

$$\sigma_1 = (321), \sigma_1 = (231), \sigma_1 = (312), \sigma_1 = (132), \sigma_1 = (213), \sigma_1 = (123).$$

Now consider the following (Cartesian) product decomposition of $\mathcal{H}^D$ for each k,

$$\mathcal{H}^D = \mathcal{H}_{k,1} \times \mathcal{H}_{k,2} \times \cdots \times \mathcal{H}_{k,\frac{n!}{k!}} \ , \tag{6.1}$$

each of them having dimension of $k!$. Each of these subspaces is invariant under the k-th generator,

$$\pi_k = \begin{pmatrix} 1 & 2 & 3 & \cdots & k & k+1 & \cdots & n \\ k & 1 & 2 & \cdots & k-1 & k+1 & \cdots & n \end{pmatrix}.$$

This corresponds to placing the top card in the k-th slot, so the rest of the deck remains unchanged. Now the block symmetry structure comes from the following observation. The above decomposition of $\mathcal{H}^D$ for the case $k-1$ splits the space into k-times more invariant subspaces,

$$\mathcal{H}^D = \mathcal{H}_{k-1,1} \times \mathcal{H}_{k-1,2} \times \cdots \times \mathcal{H}_{k-1,\frac{n!}{(k-1)!}}.$$

In the language of card-shuffling, the number of configurations with unchanged bottom $(n-k)$ cards is k-times smaller than the number of configurations with unchanged bottom $(n-k+1)$ cards. This also means that each of the elements of Eq. (6.1) is further split into k subspaces, consecutively further decomposing the space,

$$\begin{aligned}
\mathcal{H}_{k,1} &= \mathcal{H}_{k-1,1} && \times \cdots \times \mathcal{H}_{k-1,k} && \text{(first } k\text{)} \\
\mathcal{H}_{k,2} &= \mathcal{H}_{k-1,k+1} && \times \cdots \times \mathcal{H}_{k-1,2k} && (k+1 \text{ to } 2k) \\
&\cdots \\
\mathcal{H}_{k,j} &= \mathcal{H}_{k-1,(j-1)k+1} && \times \cdots \times \mathcal{H}_{k-1,jk} && (j\text{-th group of } k) \\
&\cdots
\end{aligned}$$

This establishes the following block-diagonal structure, mentioned above,

$$V = \begin{bmatrix} \boxed{\text{I}} & & & \\ & \boxed{R_2} & & \\ & & \ddots & \\ & & & \boxed{R_n} \end{bmatrix}, \qquad \begin{array}{l} \text{where each } R_k \text{ is block-diagonal itself,} \\ \text{having } \dfrac{n!}{k!} \text{ blocks of size } k!\times k! \text{ each.} \end{array}$$

This scaffolding of block-diagonal elements means that, from the bottom right corner, blocks on the diagonal are of increasing size, by k times each. For example, for S_4, we have the following block decomposition: the R_4 is represented as one block, R_3 has 4 diagonal blocks each of size 6×6, R_2 has 12 blocks each of dimension 2×2, and R_1 is the identity matrix (24 blocks of 1).

These successive decompositions result in a structure strikingly similar to the one solved in S_3 case. Our current work revolving around S_4 indicates that a process of manipulating the eigenvector symmetries to solve the eigenproblem, slightly adjusted from the one developed in the S_3 case, will work on S_n.

6.3 Summary and planned work

In this Chapter we presented our beginning efforts toward building a quantum walk on the permutation group, with the solution for the first non-Abelian case of S_3. This low-dimensional problem allowed us to identify and utilize various symmetries in the block diagonal decompositions of the evolution operator that should be directly transferable to higher dimensions. Here we outline the immediate goals of algorithmic nature and the future development of the problem.

Having obtained the full solutions, we will proceed to the assessment of algorithmic behavior and performance. The quantitites of interest in this regard are the probabilistic limit laws for Cesàro type averages, and the corresponding convergence rates, ie. quantum-walk analogs of mixing times. Limit laws and mixing times are fundamental notions in probability theory, stochastic processes and their applications. In classical computing mixing times represent running times of a randomized algorithm (see for example [140, 141] and references therein), and in the case of quantum walks the corresponding notion carries the same significance. Note that the full analysis of even the S_3 case alone would be very meaningful in this sense.

We now summarize the expected further development of this research.

- Use block-diagonalization and other spectral and probabilistic techniques for deriving the limit laws for Cesàro averages of probabilistic frequencies for the above stated example of "quantum card shuffling" and related quantum walks on non-

Abelian group structures. Two other examples could represent quantum card shuffling via random transpositions, and the one done by the neighboring transpositions.

- Modify Cesàro averages to obtain uniform limit laws, according to our conjecture that such finding in the S_3 case generalizes to S_n.

- Study convergence rates for both above limit laws (original and uniform with modified averaging). That is, find the corresponding mixing times.

- We note that $2I + R_2 + \cdots + R_n$ is the adjacency matrix for Cayley graph of S_n generated by $\{\pi_1 = id, \pi_2, \ldots, \pi_n\}$. (The adjacency matrix for a graph is the construct used to define continuous-time quantum walks.) We will use this observation to attempt to link continuous-time quantum walks that are based on the adjacency and graph Laplacian matrices to the above discrete-time quantum walk on S_n.

  Relation of any kind between continuous- and discrete-time quantum walks would be a major advancement in the field [15, 16]. It is interesting that it may well be possible to meaningfully pursue this elusive target for walks on non-Abelian structures!

Chapter 7: Conclusions

We have described here a study of ideas in the field of discrete-time quantum walks, that mostly relate to varied uses of a particular framework that we introduced (Ch. 2). This formalism is very different form the standard coined approach. In addition, while there are a few other related constructions, such as the memory-based Szegedy's and the scattering walk, the described interchange framework offers their combined ideas and is unifying of them (sec. 2.1.3).

Specifically, the formalism does not need coin spaces, and the walks are both "mixed" and driven by one local operator (sec. 2.1.2). It explicitly refers to the memory in the walk (by using the product of state spaces) and at the same time acts as a scattering operator (by driving the walk locally from each site). These are the combined properties of the Szegedy and scattering walk (sec. 2.1.3). The construction (or choice) of this operator is not constrained by anything other than unitarity, and in most cases it is very simple. (For example, see each of the non-trivial problems treated in Chapters 3–5.)

We believe that the above properties of this framework make it very suitable for a capable general algorithmic tool useful for varied problems, and we discussed this throughout. As a concrete support of this statement, we can so far offer the following.

The framework has been used to construct and solve a DTQW on the semi-infinite binary tree (Ch. 3), which is a problem of undisputed interest yet unsolved previously. It was also used to build and solve a quantum walk with deeper memory/history (Ch. 4), providing the first explicit study of the well-known question of how quantum walks may develop classical features (sec. 4.3). In a yet different direction, we solve a simple-looking problem with matching graphs, which is nevertheless not possible to solve classically in that form (sec. 5). The arrowed and coinless properties of the framework are crucial in this (sec. 5.2), and also raise a possibility for surprising generalizations. But beyond algorithms-related directions, we wish to study questions related to more fluid and flexible uses of quantum walks, roughly belonging to two kinds of quests.

Quantum walks should be useful as a general tool for exploration of physics. Our initial effort along these lines is the study of effects of tracing the history in the walk

(Ch. 4), a problem for which our framework is tailor made. While we used the coin formalism for easier comparison, it should be emphasized that the very specific form of the coin operator came from the targeted discussion of the memory in the walk. We find this work and results worthy of seriously extended studies.

In terms of general uses of quantum walks, it is intriguing and promising to explore the possibility of combining quantum walks with the Fourier transformation, since it is possible in quantum computing to bring together the two main classical approaches (sec. 5.1). The mixing of components is a defining property of quantum walks. With the introduced framework this can be done very conveniently with the Fourier as an evolution operator, by simply placing it on graph nodes (sec. 5.2). While one can choose a Fourier "coin" as well, in the coin approach this is separated from the shift operator that drives the evolution, it raises questions about the nature of the necessary coin space, and altogether has a very different meaning. (A few papers with the "Fourier coin" that we have seen have not established specific results and have not been pursued.)

It is in our opinion critical for actually pursuing the idea of the combined use of these methods to have Fourier interact with the walk, by mixing the components *and* evolving the state. We have laid out a detailed approach along the lines of such ideas in the network discovery and analysis context (sec. 5.2.1), following the approach developed for the simpler problem of matching graphs (sec. 5.2).

Finally, we started a study of walks on the permutation group S_n (Ch. 6). This follows our belief that quantum walks can take the next step, as guided by the development of the corresponding classical disciplines, toward uses on non-Abelian structures.

In closing, we offer a one-paragraph summary of the work discussed in this dissertation. We presented a framework for discrete-time quantum walks based on memoried classical walks which unifies other approaches. We used it to construct and solve walks on a binary tree and with increased explicit memory/history, as well as on a network with glued graphs. We approached questions of the memoried nature of the quantum evolution, while also looking at a possibility of algorithmically useful alterations to quantum walks. As an extension of a simple-network discovery procedure, we identify a conceptual framework for construction of increasingly complex networks that can be efficiently analyzed by the approach conceived in the original case. We identify ideas for development and directions for further study, which we believe are all interesting questions to pursue.

Bibliography

[1] M. A. Nielsen and I. L. Chuang. *Quantum Computation and Quantum Information* (Cambridge University Press, 2000).

[2] T. D. Ladd, F. Jelezko, R. Laflamme, Y. Nakamura, C. Monroe, and J. L. O/'Brien. Quantum computers. Nature **464**, 45–53 (2010). URL http://dx.doi.org/10.1038/nature08812.

[3] J. Preskill. Lecture notes on quantum computation (2011). URL http://www.theory.caltech.edu/~preskill/ph219/index.html#lecture. See linked pages for earlier years for useful pointers to papers.

[4] D. Gottesman. An introduction to quantum error correction and fault-tolerant quantum computation (2009). http://arxiv.org/abs/0904.2557.

[5] J. Preskill. Quantum computing and the entanglement frontier (Oct 2011). Rapporteur talk at the 25th Solvay Conference on Physics ("The Theory of the Quantum World"), http://arxiv.org/abs/1203.5813.

[6] P. W. Shor. Algorithms for quantum computation: discrete logarithms and factoring. In *Proceedings of the Symposium on the Foundations of Computer Science*, 124–134 (IEEE Computer Society Press, New York, 1994). URL http://dx.doi.org/10.1109/SFCS.1994.365700.

[7] M. Mosca. Quantum algorithms (2008). http://arxiv.org/abs/0808.0369.

[8] M. M. Wolf, F. Verstraete, M. B. Hastings, and J. I. Cirac. Area laws in quantum systems: Mutual information and correlations. Phys. Rev. Lett. **100**, 070502 (2008). URL http://dx.doi.org/10.1103/PhysRevLett.100.070502.

[9] J. Eisert, M. Cramer, and M. B. Plenio. *Colloquium*: Area laws for the entanglement entropy. Rev. Mod. Phys. **82**, 277–306 (2010). URL http://dx.doi.org/10.1103/RevModPhys.82.277.

[10] R. Horodecki, P. Horodecki, M. Horodecki, and K. Horodecki. Quantum entanglement. Rev. Mod. Phys. **81**, 865–942 (2009). URL http://dx.doi.org/10.1103/RevModPhys.81.865.

[11] L. Amico, R. Fazio, A. Osterloh, and V. Vedral. Entanglement in many-body systems. Rev. Mod. Phys. **80**, 517–576 (2008). URL http://dx.doi.org/10.1103/RevModPhys.80.517.

[12] E. Farhi and S. Gutmann. Quantum computation and decision trees. Phys. Rev. A **58**, 915–928 (1998). URL http://dx.doi.org/10.1103/PhysRevA.58.915.

[13] D. A. Meyer. From quantum cellular automata to quantum lattice gases. J. Stat. Phys. **85**, 551–574 (1996). URL http://dx.doi.org/10.1007/BF02199356.

[14] D. Aharonov, A. Ambainis, J. Kempe, and U. Vazirani. Quantum walks on graphs. In *Proceedings of the 33rd Annual ACM Symposium on Theory of Computation*, STOC '01, 50–59 (ACM, New York, 2001). URL http://dx.doi.org/10.1145/380752.380758.

[15] A. M. Childs. On the relationship between continuous- and discrete-time quantum walk. Commun. Math. Phys. **294**, 581–603 (2009). URL http://dx.doi.org/10.1007/s00220-009-0930-1.

[16] F. W. Strauch. Connecting the discrete- and continuous-time quantum walks. Phys. Rev. A **74**, 030301 (2006). URL http://dx.doi.org/10.1103/PhysRevA.74.030301.

[17] Y. Aharonov, L. Davidovich, and N. Zagury. Quantum random walks. Phys. Rev. A **48**, 1687–1690 (1993). URL http://dx.doi.org/10.1103/PhysRevA.48.1687.

[18] S. Godoy and S. Fujita. A quantum random-walk model for tunneling diffusion in a 1d lattice. a quantum correction to Fick's law. J. Chem. Phys. **97**, 5148 (1992). URL http://dx.doi.org/10.1063/1.463812.

[19] J. Watrous. Quantum simulations of classical random walks and undirected graph connectivity. J. Comput. Syst. Sci. **62**, 376–391 (2001). URL http://dx.doi.org/10.1006/jcss.2000.1732.

[20] A. Ambainis, E. Bach, A. Nayak, A. Vishwanath, and J. Watrous. One-dimensional quantum walks. In *Proceedings of the 33rd Annual ACM Symposium on Theory of Computation*, STOC '01, 37–49 (ACM, New York, 2001). URL http://dx.doi.org/10.1145/380752.380757.

[21] J. Kempe. Quantum random walks: an introductory overview. Contemp. Phys. **44**, 307 (2003). http://arxiv.org/abs/quant-ph/0303081v1.

[22] V. M. Kendon. A random walk approach to quantum algorithms. Phil. Trans. R. Soc. A **364**, 3407–3422 (2006). URL http://dx.doi.org/10.1098/rsta.2006.1901.

[23] A. M. Childs, R. Cleve, E. Deotto, E. Farhi, S. Gutmann, and D. A. Spielman. Exponential algorithmic speedup by a quantum walk. In *Proceedings of the 35th Annual ACM Symposium on Theory of Computation*, STOC '03, 59–68 (ACM, New York, 2003). URL http://dx.doi.org/10.1145/780542.780552.

[24] A. M. Childs, L. J. Schulman, and U. V. Vazirani. Quantum algorithms for hidden nonlinear structures. In *Foundations of Computer Science, 2007 (FOCS '07). 48th Annual IEEE Symposium*, 395–404 (2007). URL http://dx.doi.org/10.1109/FOCS.2007.18.

[25] N. Shenvi, J. Kempe, and K. B. Whaley. Quantum random-walk search algorithm. Phys. Rev. A **67**, 052307 (2003). URL http://dx.doi.org/10.1103/PhysRevA.67.052307.

[26] A. M. Childs and J. Goldstone. Spatial search by quantum walk. Phys. Rev. A **70**, 022314 (2004). URL http://dx.doi.org/10.1103/PhysRevA.70.022314.

[27] A. M. Childs and J. Goldstone. Spatial search and the dirac equation. Phys. Rev. A **70**, 042312 (2004). URL http://dx.doi.org/10.1103/PhysRevA.70.042312.

[28] S. Aaronson and A. Ambainis. Quantum search of spatial regions. Theory of Computing **1**, 4779 (2005). Conference version: FOCS'03, pp.200-209 (2003).

[29] A. Ambainis, J. Kempe, and A. Rivosh. Coins make quantum walks faster. Proc. 16th ACM-SIAM Symposium on Discrete Algorithms (SODA) 1099–1108 (2005). http://arxiv.org/abs/quant-ph/0402107.

[30] A. Ambainis. Quantum walk algorithm for element distinctness. SIAM Journal on Computing **37**, 210–239 (2007). URL http://dx.doi.org/10.1137/S0097539705447311.

[31] F. Magniez, A. Nayak, J. Roland, and M. Santha. Search via quantum walk. ACM Symposium on Theory of Computing (ACM New York) 575–584 (2007). http://arxiv.org/abs/quant-ph/0608026.

[32] E. Farhi, J. Goldstone, and S. Gutmann. A quantum algorithm for the hamiltonian nand tree. Theory Comput. **4**, 169–190 (2008). URL http://dx.doi.org/10.4086/toc.2008.v004a008.

[33] A. Ambainis, A. M. Childs, B. W. Reichardt, R. Špalek, and S. Zhang. Every NAND formula of size N can be evaluated in time $n^{1/2+o(1)}$ on a quantum computer. In *IEEE Symposium on Foundations of Computer Science (FOCS)*, 363–372 (2007). http://arxiv.org/abs/quant-ph/0703015.

[34] A. Ambainis. A nearly optimal discrete query quantum algorithm for evaluating NAND formulas. http://arxiv.org/abs/0704.3628.

[35] B. W. Reichardt and R. Špalek. Span-program-based quantum algorithm for evaluating formulas. In *ACM Symposium on Theory of Computing (ACM, New York)*, 103–112 (2008). http://arxiv.org/abs/0710.2630.

[36] A. Ambainis. Quantum walks and their algorithmic applications. International Journal of Quantum Information **1**, 507–518 (2003). URL http://arxiv.org/abs/quant-ph/0403120.

[37] V. Kendon. Decoherence in quantum walks – a review. Math. Struct. Comp. Sci. **17**, 1169 (2007). URL http://dx.doi.org/10.1017/S0960129507006354.

[38] A. M. Childs. Universal computation by quantum walk. Phys. Rev. Lett. **102**, 180501 (2009). URL http://dx.doi.org/10.1103/PhysRevLett.102.180501.

[39] N. B. Lovett, S. Cooper, M. Everitt, M. Trevers, and V. Kendon. Universal quantum computation using the discrete-time quantum walk. Phys. Rev. A **81**, 042330 (2010).

[40] A. M. Childs, D. Gosset, and Z. Webb. Universal computation by multi-particle quantum walk. http://arxiv.org/abs/1205.3782v1.

[41] Y. Shikano, K. Chisaki, E. Segawa, and N. Konno. Emergence of randomness and arrow of time in quantum walks. Phys. Rev. A **81**, 062129 (2010). URL http://dx.doi.org/10.1103/PhysRevA.81.062129.

[42] X. Martin, D. O'Connor, and R. D. Sorkin. Random walk in generalized quantum theory. Phys. Rev. D **71**, 024029 (2005). URL http://dx.doi.org/10.1103/PhysRevD.71.024029.

[43] O. Mülken, A. Blumen, T. Amthor, C. Giese, M. Reetz-Lamour, and M. Weidemüller. Survival probabilities in coherent exciton transfer with trapping. Phys. Rev. Lett. **99**, 090601 (2007). URL http://dx.doi.org/10.1103/PhysRevLett.99.090601.

[44] A. Thilagam. Grover-like search via a Frenkel-exciton trapping mechanism. Phys. Rev. A **81**, 032309 (2010). URL http://dx.doi.org/10.1103/PhysRevA.81.032309.

[45] T. Kitagawa, M. S. Rudner, E. Berg, and E. Demler. Exploring topological phases with quantum walks. Phys. Rev. A **82**, 033429 (2010). URL http://dx.doi.org/10.1103/PhysRevA.82.033429.

[46] C. M. Chandrashekar, R. Srikanth, and R. Laflamme. Optimizing the discrete time quantum walk using a su(2) coin. Phys. Rev. A **77**, 032326 (2008). URL http://dx.doi.org/10.1103/PhysRevA.77.032326.

[47] L. Lehman, V. Zatloukal, G. K. Brennen, J. K. Pachos, and Z. Wang. Quantum walks with non-abelian anyons. Phys. Rev. Lett. **106**, 230404 (2011). URL http://dx.doi.org/10.1103/PhysRevLett.106.230404.

[48] T. Oka and H. Aoki. Ground-state decay rate for the zener breakdown in band and mott insulators. Phys. Rev. Lett. **95**, 137601 (2005). URL http://link.aps.org/doi/10.1103/PhysRevLett.95.137601.

[49] T. Oka, N. Konno, R. Arita, and H. Aoki. Breakdown of an electric-field driven system: A mapping to a quantum walk. Phys. Rev. Lett. **94**, 100602 (2005). URL http://link.aps.org/doi/10.1103/PhysRevLett.94.100602.

[50] R. J. Sension. Biophysics: Quantum path to photosynthesis. Nature **446**, 740–741 (2007). URL http://dx.doi.org/10.1038/446740a.

[51] M. Mohseni, P. Rebentrost, S. Lloyd, and A. Aspuru-Guzik. Environment-assisted quantum walks in photosynthetic energy transfer. J. Chem. Phys. **129**, 174106 (2008). URL http://dx.doi.org/10.1063/1.3002335.

[52] M. S. Rudner and L. S. Levitov. Topological transition in a non-hermitian quantum walk. Phys. Rev. Lett. **102**, 065703 (2009). URL http://link.aps.org/doi/10.1103/PhysRevLett.102.065703.

[53] O. Mülken and A. Blumen. Continuous-time quantum walks: Models for coherent transport on complex networks. Phys. Rept. **502**, 37 (2011). URL http://www.sciencedirect.com/science/article/pii/S0370157311000184.

[54] A. Ahlbrecht, V. B. Scholz, and A. H. Werner. Disordered quantum walks in one lattice dimension. Journal of Mathematical Physics **52**, 102201 (2011). URL http://dx.doi.org/10.1063/1.3643768.

[55] A. Ahlbrecht, A. Alberti, D. Meschede, V. B. Scholz, A. H. Werner, and R. F. Werner. Bound molecules in an interacting quantum walk (2011). http://arxiv.org/abs/1105.1051.

[56] C. A. Ryan, M. Laforest, J. C. Boileau, and R. Laflamme. Experimental implementation of a discrete-time quantum random walk on an NMR quantum-information processor. Phys. Rev. A **72**, 062317 (2005). URL http://dx.doi.org/10.1103/PhysRevA.72.062317.

[57] H. Schmitz, R. Matjeschk, C. Schneider, J. Glueckert, M. Enderlein, T. Huber, and T. Schaetz. Quantum walk of a trapped ion in phase space. Phys. Rev. Lett. **103**, 090504 (2009). URL http://dx.doi.org/10.1103/PhysRevLett.103.090504.

[58] M. Karski, L. Förster, J.-M. Choi, A. Steffen, W. Alt, D. Meschede, and A. Widera. Quantum walk in position space with single optically trapped atoms. Science **325**, 174 (2009). URL http://dx.doi.org/10.1126/science.1174436.

[59] F. Zähringer, G. Kirchmair, R. Gerritsma, E. Solano, R. Blatt, and C. F. Roos. Realization of a quantum walk with one and two trapped ions. Phys. Rev. Lett. **104**, 100503 (2010). URL http://dx.doi.org/10.1103/PhysRevLett.104.100503.

[60] P. Xue, B. C. Sanders, and D. Leibfried. Quantum walk on a line for a trapped ion. Phys. Rev. Lett. **103**, 183602 (2009). URL http://dx.doi.org/10.1103/PhysRevLett.103.183602.

[61] R. Matjeschk, C. Schneider, M. Enderlein, T. Huber, H. Schmitz, J. Glueckert, and T. Schaetz. Experimental simulation and limitations of quantum walks with trapped ions. New J. Phys. **14**, 035012 (2012). URL http://dx.doi.org/10.1088/1367-2630/14/3/035012.

[62] A. Schreiber, K. N. Cassemiro, V. Potoček, A. Gábris, P. J. Mosley, E. Andersson, I. Jex, and C. Silberhorn. Photons walking the line: A quantum walk with adjustable coin operations. Phys. Rev. Lett. **104**, 050502 (2010). URL http://dx.doi.org/10.1103/PhysRevLett.104.050502.

[63] M. A. Broome, A. Fedrizzi, B. P. Lanyon, I. Kassal, A. Aspuru-Guzik, and A. G. White. Discrete single-photon quantum walks with tunable decoherence. Phys. Rev. Lett. **104**, 153602 (2010). URL http://dx.doi.org/10.1103/PhysRevLett.104.153602.

[64] A. Peruzzo, M. Lobino, J. Matthews, N. Matsuda, A. Politi, K. Poulios, X.-Q. Zhou, Y. Lahini, N. Ismail, K. Wörhoff, Y. Bromberg, Y. Silberberg, M. G. Thompson, and J. L. OBrien. Quantum walks of correlated photons. Science **329**, 1500 (2010). URL http://dx.doi.org/10.1126/science.1193515.

[65] A. Schreiber, K. N. Cassemiro, V. Potoček, A. Gábris, I. Jex, and C. Silberhorn. Decoherence and disorder in quantum walks: From ballistic spread to localization. Phys. Rev. Lett. **106**, 180403 (2011). URL http://dx.doi.org/10.1103/PhysRevLett.106.180403.

[66] H. B. Perets, Y. Lahini, F. Pozzi, M. Sorel, R. Morandotti, and Y. Silberberg. Realization of quantum walks with negligible decoherence in waveguide lattices. Phys.

Rev. Lett. **100**, 170506 (2008). URL http://dx.doi.org/10.1103/PhysRevLett.100.170506.

[67] L. Sansoni, F. Sciarrino, G. Vallone, P. Mataloni, A. Crespi, R. Ramponi, and R. Osellame. Two-particle bosonic-fermionic quantum walk via integrated photonics. Phys. Rev. Lett. **108**, 010502 (2012). URL http://dx.doi.org/10.1103/PhysRevLett.108.010502.

[68] J. C. F. Matthews, K. Poulios, J. D. A. Meinecke, A. Politi, A. Peruzzo, N. Ismail, K. Wörhoff, M. G. Thompson, and J. L. O'Brien. Simulating quantum statistics with entangled photons: A continuous transition from bosons to fermions. http://arxiv.org/abs/1106.1166.

[69] A. Aspuru-Guzik and P. Walther. Photonic quantum simulators. Nature Physics **8**, 285–291 (2012). URL http://dx.doi.org/10.1038/nphys2253.

[70] P. P. Rohde, A. Fedrizzi, and T. C. Ralph. Entanglement dynamics and quasi-periodicity in discrete quantum walks. J. Mod. Opt. **59**, 710–720 (2012). URL http://dx.doi.org/10.1080/09500340.2012.660204. Special issue.

[71] G. 't Hooft. Dimensional reduction in quantum gravity (1993). Also in *Salam-festschrift*, edited by A. Alo, J. Ellis, and S. Randjbar-Daemi, (World Scientific, Singapore, 1993)., http://arxiv.org/abs/gr-qc/9310026.

[72] Z. Dimcovic, D. Rockwell, I. Milligan, R. M. Burton, T. Nguyen, and Y. Kovchegov. Framework for discrete-time quantum walks and a symmetric walk on a binary tree. Phys. Rev. A **84**, 032311 (2011). URL http://dx.doi.org/10.1103/PhysRevA.84.032311.

[73] B. Tregenna, W. Flanagan, R. Maile, and V. Kendon. Controlling discrete quantum walks: coins and initial states. New Journal of Physics **5**, 83 (2003). URL http://dx.doi.org/10.1088/1367-2630/5/1/383.

[74] A. Romanelli, A. C. Schifino, R. Siri, G. Abal, A. Auyuanet, and R. Donangelo. Quantum random walk on the line as a markovian process. Physica A **338**, 395 – 405 (2004). URL http://dx.doi.org/10.1016/j.physa.2004.02.061.

[75] D. A. Meyer and H. Blumer. Parrondo games as lattice gas automata. J. Stat. Phys. **107**, 225 – 239 (2002). URL http://dx.doi.org/10.1007/BF02199356.

[76] N. Konno. Limit theorems and absorption problems for one-dimensional correlated random walks. Stochastic Models **25**, 28–49 (2009).

[77] M. Szegedy. Quantum speed-up of Markov chain based algorithms. In *Proceedings of the 45th Annual IEEE Symposium on Foundations of Computer Science*, 32–41 (IEEE Computer Society, Washington, DC, 2004). URL http://portal.acm.org/citation.cfm?id=1032645.1033158.

[78] M. Hillery, J. Bergou, and E. Feldman. Quantum walks based on an interferometric analogy. Phys. Rev. A **68**, 032314 (2003). URL http://dx.doi.org/10.1103/PhysRevA.68.032314.

[79] E. Feldman and M. Hillery. Scattering theory and discrete-time quantum walks. Phys. Lett. A **324**, 277 – 281 (2004). URL http://www.sciencedirect.com/science/article/pii/S0375960104003275.

[80] D. Reitzner, M. Hillery, E. Feldman, and V. Bužek. Quantum searches on highly symmetric graphs. Phys. Rev. A **79**, 012323 (2009). URL http://dx.doi.org/10.1103/PhysRevA.79.012323.

[81] T. A. Brun, H. A. Carteret, and A. Ambainis. Quantum walks driven by many coins. Phys. Rev. A **67**, 052317 (2003). URL http://dx.doi.org/10.1103/PhysRevA.67.052317.

[82] T. A. Brun, H. A. Carteret, and A. Ambainis. Quantum random walks with decoherent coins. Phys. Rev. A **67**, 032304 (2003).

[83] J. Košík, V. Bužek, and M. Hillery. Quantum walks with random phase shifts. Phys. Rev. A **74**, 022310 (2006). URL http://dx.doi.org/10.1103/PhysRevA.74.022310.

[84] M. Mc Gettrick. One-dimensional quantum walks with memory. Quantum Inf. Comput. **10**, 0509 (2010).

[85] N. Konno and T. Machida. Limit theorems for quantum walks with memory. Quantum Inf. Comput. **10**, 1004 (2010).

[86] F. Magniez, A. Nayak, J. Roland, and M. Santha. Search via quantum walk. http://arxiv.org/abs/quant-ph/0608026v3.

[87] A. Gábris, T. Kiss, and I. Jex. Scattering quantum random-walk search with errors. Phys. Rev. A **76**, 062315 (2007). URL http://dx.doi.org/10.1103/PhysRevA.76.062315.

[88] J. Košík and V. Bužek. Scattering model for quantum random walks on a hypercube. Phys. Rev. A **71**, 012306 (2005). URL http://dx.doi.org/10.1103/PhysRevA.71.012306.

[89] M. Hillery, D. Reitzner, and V. Bužek. Searching via walking: How to find a marked clique of a complete graph using quantum walks. Phys. Rev. A **81**, 062324 (2010). URL http://dx.doi.org/10.1103/PhysRevA.81.062324.

[90] E. Feldman, M. Hillery, H.-W. Lee, D. Reitzner, H. Zheng, and V. Bužek. Finding structural anomalies in graphs by means of quantum walks. Phys. Rev. A **82**, 040301 (2010). URL http://dx.doi.org/10.1103/PhysRevA.82.040301.

[91] A. Rosmanis. Quantum snake walk on graphs. Phys. Rev. A **83**, 022304 (2011). URL http://dx.doi.org/10.1103/PhysRevA.83.022304.

[92] N. Linden and J. Sharam. Inhomogeneous quantum walks. Phys. Rev. A **80**, 052327 (2009). URL http://dx.doi.org/10.1103/PhysRevA.80.052327.

[93] Y.-Y. Shi, L.-M. Duan, and G. Vidal. Classical simulation of quantum many-body systems with a tree tensor network. Phys. Rev. A **74**, 022320 (2006). URL http://dx.doi.org/10.1103/PhysRevA.74.022320.

[94] P. Rebentrost, M. Mohseni, I. Kassal, S. Lloyd, and A. Aspuru-Guzik. Environment-assisted quantum transport. New J. Phys. **11**, 033003 (2009). URL http://dx.doi.org/10.1088/1367-2630/11/3/033003.

[95] P. Silvi, V. Giovannetti, S. Montangero, M. Rizzi, J. I. Cirac, and R. Fazio. Homogeneous binary trees as ground states of quantum critical hamiltonians. Phys. Rev. A **81**, 062335 (2010). URL http://dx.doi.org/10.1103/PhysRevA.81.062335.

[96] P. A. MacMahon. *Combinatorial Analysis, Vols. 1 and 2* (Cambridge University Press, 1915).

[97] M. Štefaňák, I. Jex, and T. Kiss. Recurrence and Pólya number of quantum walks. Phys. Rev. Lett. **100**, 020501 (2008). URL http://dx.doi.org/10.1103/PhysRevLett.100.020501.

[98] M. Štefaňák, T. Kiss, and I. Jex. Recurrence properties of unbiased coined quantum walks on infinite d -dimensional lattices. Phys. Rev. A **78**, 032306 (2008). URL http://dx.doi.org/10.1103/PhysRevA.78.032306.

[99] M. J. Cantero, L. Moral, F. A. Grünbaum, and L. Velázquez. Matrix-valued Szegő polynomials and quantum random walks. Commun. Pure Appl. Math. **63**, 464–507 (2010). URL http://dx.doi.org/10.1002/cpa.20312.

[100] T. D. Mackay, S. D. Bartlett, L. T. Stephenson, and B. C. Sanders. Quantum walks in higher dimensions. Journal of Physics A: Mathematical and General **35**, 2745 (2002). URL http://dx.doi.org/10.1088/0305-4470/35/12/304.

[101] J. B. Stang, A. T. Rezakhani, and B. C. Sanders. Correlation effects in a discrete quantum random walk. Journal of Physics A: Mathematical and Theoretical **42**, 175304 (2009). URL http://dx.doi.org/10.1088/1751-8113/42/17/175304.

[102] A. Ahlbrecht, H. Vogts, A. H. Werner, and R. F. Werner. Asymptotic evolution of quantum walks with random coin. Journal of Mathematical Physics **52**, 042201 (2011). URL http://link.aip.org/link/?JMP/52/042201/1.

[103] D. K. Wójcik and J. R. Dorfman. Diffusive-ballistic crossover in 1d quantum walks. Phys. Rev. Lett. **90**, 230602 (2003). URL http://dx.doi.org/10.1103/PhysRevLett.90.230602.

[104] T. A. Brun, H. A. Carteret, and A. Ambainis. Quantum to classical transition for random walks. Phys. Rev. Lett. **91**, 130602 (2003). URL http://dx.doi.org/10.1103/PhysRevLett.91.130602.

[105] A. P. Flitney, D. Abbott, and N. F. Johnson. Quantum walks with history dependence. Journal of Physics A: Mathematical and General **37**, 7581 (2004). URL http://dx.doi.org/10.1088/0305-4470/37/30/013.

[106] C. Chandrashekar and S. Banerjee. Parrondo's game using a discrete-time quantum walk. Physics Letters A **375**, 1553–1558 (2011). URL http://dx.doi.org/10.1016/j.physleta.2011.02.071.

[107] S. E. Venegas-Andraca, J. L. Ball, K. Burnett, and S. Bose. Quantum walks with entangled coins. New Journal of Physics **7**, 221 (2005). URL http://dx.doi.org/10.1088/1367-2630/7/1/221.

[108] C. Liu and N. Petulante. One-dimensional quantum random walks with two entangled coins. Phys. Rev. A **79**, 032312 (2009). URL http://dx.doi.org/10.1103/PhysRevA.79.032312.

[109] J. Endrejat and H. Büttner. Entanglement measurement with discrete multiple-coin quantum walks. Journal of Physics A: Mathematical and General **38**, 9289 (2005). URL http://dx.doi.org/10.1088/0305-4470/38/42/008.

[110] C. S. Hamilton, A. Gábris, I. Jex, and S. M. Barnett. Quantum walk with a four-dimensional coin. New Journal of Physics **13**, 013015 (2011). URL http://dx.doi.org/10.1088/1367-2630/13/1/013015.

[111] L. Marrucci, E. Karimi, S. Slussarenko, B. Piccirillo, E. Santamato, E. Nagali, and F. Sciarrino. Spin-to-orbital conversion of the angular momentum of light and its classical and quantum applications. Journal of Optics **13**, 064001 (2011). URL http://dx.doi.org/10.1088/2040-8978/13/6/064001.

[112] G. M. D'Ariano and P. Lo Presti. Characterization of quantum devices. In M. J. A. Paris and J. Řeháček (editors), *Quantum State Estimation*, vol. 649 of *Lecture Notes in Physics*, 297 (Springer, New York, 2004).

[113] L. M. Artiles, R. D. Gill, and M. I. Gută. An invitation to quantum tomography. J. Roy. Statist. Soc. B **67**, 109–134 (2005). URL http://dx.doi.org/10.1111/j.1467-9868.2005.00491.x.

[114] I. L. Chuang and M. A. Nielsen. Prescription for experimental determination of the dynamics of a quantum black box. J. Mod. Opt. **44**, 2455 (1997). arXiv:quant-ph/9610001v1.

[115] J. F. Poyatos, J. I. Cirac, and P. Zoller. Complete characterization of a quantum process: The two-bit quantum gate. Phys. Rev. Lett. **78**, 390–393 (1997). URL http://link.aps.org/doi/10.1103/PhysRevLett.78.390.

[116] G. M. D'Ariano and P. Lo Presti. Quantum tomography for measuring experimentally the matrix elements of an arbitrary quantum operation. Phys. Rev. Lett. **86**, 4195–4198 (2001). URL http://link.aps.org/doi/10.1103/PhysRevLett.86.4195.

[117] G. M. D'Ariano and P. Lo Presti. Imprinting complete information about a quantum channel on its output state. Phys. Rev. Lett. **91**, 047902 (2003). URL http://link.aps.org/doi/10.1103/PhysRevLett.91.047902.

[118] D. W. Leung. Choi's proof as a recipe for quantum process tomography. J. Math. Phys. **44**, 528–533 (2003). URL http://dx.doi.org/10.1063/1.1518554.

[119] J. B. Altepeter, D. Branning, E. Jeffrey, T. C. Wei, P. G. Kwiat, R. T. Thew, J. L. O'Brien, M. A. Nielsen, and A. G. White. Ancilla-assisted quantum process tomography. Phys. Rev. Lett. **90**, 193601 (2003). URL http://link.aps.org/doi/10.1103/PhysRevLett.90.193601.

[120] M. Mohseni and D. A. Lidar. Direct characterization of quantum dynamics. Phys. Rev. Lett. **97**, 170501 (2006). URL http://link.aps.org/doi/10.1103/PhysRevLett.97.170501.

[121] M. Mohseni and D. A. Lidar. Direct characterization of quantum dynamics: General theory. Phys. Rev. A **75**, 062331 (2007). URL http://link.aps.org/doi/10.1103/PhysRevA.75.062331.

[122] G. Chiribella, G. M. D'Ariano, and P. Perinotti. Theoretical framework for quantum networks. Phys. Rev. A **80**, 022339 (2009). URL http://link.aps.org/doi/10.1103/PhysRevA.80.022339.

[123] A. Acín. Statistical distinguishability between unitary operations. Phys. Rev. Lett. **87**, 177901 (2001). URL http://link.aps.org/doi/10.1103/PhysRevLett.87.177901.

[124] G. M. D'Ariano, P. Lo Presti, and M. G. A. Paris. Using entanglement improves the precision of quantum measurements. Phys. Rev. Lett. **87**, 270404 (2001). URL http://link.aps.org/doi/10.1103/PhysRevLett.87.270404.

[125] R. Duan, Y. Feng, and M. Ying. Perfect distinguishability of quantum operations. Phys. Rev. Lett. **103**, 210501 (2009). URL http://link.aps.org/doi/10.1103/PhysRevLett.103.210501.

[126] R. Duan, Y. Feng, and M. Ying. Entanglement is not necessary for perfect discrimination between unitary operations. Phys. Rev. Lett. **98**, 100503 (2007). URL http://link.aps.org/doi/10.1103/PhysRevLett.98.100503.

[127] J. Watrous. Distinguishing quantum operations having few Kraus operators. Quantum Inf. Comput. **8**, 819 (2008). arXiv:0710.0902v3.

[128] M. Piani and J. Watrous. All entangled states are useful for channel discrimination. Phys. Rev. Lett. **102**, 250501 (2009). URL http://dx.doi.org/10.1103/PhysRevLett.102.250501.

[129] A. M. Childs, J. Preskill, and J. Renes. Quantum information and precision measurement. J. Mod. Opt. **47**, 155 (2000). arXiv:quant-ph/9904021v2.

[130] A. W. Harrow, A. Hassidim, D. W. Leung, and J. Watrous. Adaptive versus nonadaptive strategies for quantum channel discrimination. Phys. Rev. A **81**, 032339 (2010). URL http://link.aps.org/doi/10.1103/PhysRevA.81.032339.

[131] M. Mohseni, A. T. Rezakhani, and D. A. Lidar. Quantum-process tomography: Resource analysis of different strategies. Phys. Rev. A **77**, 032322 (2008). URL http://link.aps.org/doi/10.1103/PhysRevA.77.032322.

[132] D. A. Meyer. Sophisticated quantum search without entanglement. Phys. Rev. Lett. **85**, 2014–2017 (2000). URL http://dx.doi.org/10.1103/PhysRevLett.85.2014.

[133] D. Emms, E. Hancock, and R. Wilson. Graph matching using the interference of continuous-time quantum walks. Pattern Recognition **42**, 995 (2009).

[134] D. Emms, E. Hancock, and R. Wilson. A correspondence measure for graph matching using the discrete quantum walk. In F. Escolano and M. Vento (editors), *Graph-Based Representations in Pattern Recognition*, vol. 4538 of *Lecture Notes in Computer Science (LNCS)*, 81–91 (Springer, 2007). URL http://dx.doi.org/10.1007/978-3-540-72903-7_8.

[135] R. Beals. Quantum computation of Fourier transforms over symmetric groups. In *Proceedings of the 29th Annual ACM Symposium on the Theory of Computation (STOC '97)*, 48–53 (ACM Press, New York, 1997).

[136] A. M. Childs and W. van Dam. Quantum algorithms for algebraic problems. Rev. Mod. Phys. **82**, 1–52 (2010). URL http://dx.doi.org/10.1103/RevModPhys.82.1.

[137] C. T. A. Ahmadi, R. Belk and C. Wendler. Mixing in continuous quantum walks on graphs. Quant. Inf. Comput. **3**, 611 (2003).

[138] H. Gerhardt and J. Watrous. Continuous-time quantum walks on the symmetric group. In *Approximation, randomization, and combinatorial optimization (APPROX)*, vol. 2764, 290–301 (2003). arXiv:quant-ph/0305182v1.

[139] P. Diaconis. *Group Representations in Probability and Statistics* (Institute of Mathematical Statistics, 1988).

[140] Y. Kovchegov, P. T. Otto, and M. Titus. Mixing times for the mean-field blume-capel model via aggregate path coupling. J. Stat. Phys. **144**, 1009 (2011). URL http://dx.doi.org/10.1007/s10955-011-0286-8.

[141] K. Bradford and Y. Kovchegov. Adiabatic times for markov chains and applications. J. Stat. Phys. **143**, 955 (2011). URL http://dx.doi.org/10.1007/s10955-011-0219-6.

[142] R. Wong. *Asumptotic Approximations of Integrals* (Academic Press, 1989).

[143] N. Bleistein and R. A. Handelsman. *Asymptotic expansions of integrals* (Dover, 1986).

[144] Y. Kovchegov. Orthogonality and probability: beyond nearest neighbor transitions. Elect. Comm. in Probab. **14**, 90 (2009). URL http://www.math.washington.edu/~ejpecp/ECP/viewarticle.php?id=2078&layout=abstract.

[145] Y. Kovchegov. Orthogonality and probability: mixing times. Elect. Comm. in Probab. **15**, 59 (2010). URL http://www.math.washington.edu/~ejpecp/ECP/viewarticle.php?id=2171&layout=abstract.

APPENDICES

Appendix A: Spectral analysis of classical random walks

A.1 Spectral analysis of a 1d memoryless classical random walk

To introduce the study of the spectral structure of the quantum walk, start with the spectral analysis of a classical walk on the chain with identified ends, with N sites. We want to solve the spectral problem for the Markov tensor acting on vectors in this space of N dimensions: $vP = \lambda v$, where v takes coordinates on each site, $v = \big(v(0), v(1), \ldots, v(N-1)\big)$. Given the action of Markov operator P, that moves the state in either direction with probabilities of p or $(1-p)$, we have for any vector

$$P \,:\, v \;\mapsto\; \big(\;\ldots,\; \underbrace{p\,v(j-1) + (1-p)\,v(j+1)}_{j-\text{th coordinate}},\;\ldots\;\big)$$

This suggests that vP can be written as a superposition of two vectors, having the coordinates of v shifted around, to the left for one and to the right for the other:

$$vP = p\;\underbrace{\Big(v(N-1), v(0),\;\ldots,\;v(N-2)\Big)}_{v's \text{ coordinates, shifted right by one ...}} + (1-p)\;\underbrace{\Big(v(1),\;\ldots,\;v(N-1), v(0)\Big)}_{\text{... and shifted left by one.}} \qquad \text{(A.1)}$$

For an eigenvector this gives for the j-th coordinate: $p\,v(j-1) + (1-p)\,v(j+1) = \lambda v(j)$.

Action of the Markov tensor on the states on the circle is a (stochastic) permutation, and its spectral structure can be obtained using properties of cyclic groups. This makes the use of representations straightforward. The N sites on the circle can be identified by the roots of unity, $w^k = e^{\frac{2\pi i}{N}k}$ $(k = 0, \ldots, N-1)$. Using $a = w^k$ $(w = e^{2\pi i/N})$ simplifies Eq. (A.1)) to

$$\Big(1, a, a^2, \ldots, a^{N-1}\Big)\,P = p\,a^{-1}\,\Big(1, a, \ldots, a^{N-1}\Big) + (1-p)\,a\,\Big(1, a, \ldots, a^{N-1}\Big),$$

what is $vP = \big(pa^{-1} + (1-p)a\big)\,v$, and this shows that $\big(1, a, a^2, \ldots, a^{N-1}\big)$ is an

eigenvector, with an eigenvalue of $\lambda = pa^{-1} + (1-p)a$. Putting back $a = w^k$ we have

$$\lambda_k = pw^{-k} + (1-p)w^k, \quad \text{with } k\text{-th eigenvector: } \big(1,\, w^k,\, w^{2k},\, \ldots,\, w^{(N-1)\,k}\big).$$

Selecting a fixed k then chooses a particular representation, in which the group operation is to move (left or right) to the next k-th site. (For example, if $N \equiv k \pmod 0$, then $\mathbb{Z}_N \to \mathbb{Z}_{N/k}$ and $\mathbb{Z}_{N/k}$ is permuted onto itself under group action.) So we have all eigenvalues and eigenvectors,

$$|v_k\rangle = \sum_j a^j |j\rangle = (1, a, a^2, \ldots) = (1, w^k, w^{2k}, \ldots),\ k = 0, \ldots, N-1.$$

The spectral analysis can be carried out using Fourier transform too, and as it will be useful later it is introduced here. The k-th coordinate of the Fourier transform of v, with $v(j) \equiv v_j$, can be written as

$$\hat{v}(k) = \sum_j a^j v_j, \quad \text{with coefficient } a = w^k = e^{\frac{2\pi i}{N}k}.$$

The Fourier transformation $v \mapsto \hat{v}$, on the column-vector, $\hat{v} = F\,v$, is

$$\begin{bmatrix} \hat{v}_0 \\ \hat{v}_1 \\ \vdots \\ \\ \hat{v}_{N-1} \end{bmatrix} = \begin{bmatrix} 1 & 1 & 1 & 1 & \cdots \\ 1 & w & w^2 & w^3 & \cdots \\ 1 & w^2 & w^4 & w^6 & \cdots \\ 1 & w^3 & w^6 & w^9 & \cdots \\ \vdots & & & & \end{bmatrix} \begin{bmatrix} v_0 \\ v_1 \\ \vdots \\ \\ v_{N-1} \end{bmatrix} \tag{A.2}$$

To solve the recursion relation $p\,v_{j-1} + (1-p)\,v_{j+1} = \lambda v_j$, obtained from $vP = \lambda v$ for the j-th coordinate, apply the expansion $\hat{v}(k) = \sum w^{kj} v_j$ to it, by multiplying by w^{kj} and summing, using $\sum w^{jk} v_{j-1} = w^k \sum w^{(j-1)k} v_{j-1}$ and re-enumerating indices. We get

$$\big(pw^k + (1-p)w^{-k}\big)\hat{v}_k = \lambda\,\hat{v}_k \quad \Rightarrow \quad \big(pw^k + (1-p)w^{-k} - \lambda\big)\hat{v}_k = 0, \quad \forall k$$

Solutions for λ for each k are unique, so this directly determines eigenvectors, as $\hat{v}_k \neq 0$,

while other coordinates have to be zero for that k. Thus we have

$$\lambda_{N-k} = pw^k + (1-p)w^{-k} \;=\; \cos\left(\frac{2\pi k}{N}\right) + i\,(2p-1)\sin\left(\frac{2\pi k}{N}\right). \qquad \text{(A.3)}$$

A note on indexing. These eigenvalues appear to be different from the result obtained using representations; but they still list the same set of eigenvectors, corresponding to same eigenvalues, so the results agree. The rest is a matter of labeling them and, while not necessary, it is sensible to have the indexing agree: in the inverse space the circle is traversed in the opposite direction, and then the eigenvalues can be indexed with $(-k)$. This can be seen via the Fourier transform of v, taken as inverse to the above transform of $\hat{v}$

$$vP = \lambda v \quad \Leftrightarrow \quad \left(\sum w^{-kj}\hat{v}_j\right) P \;=\; \lambda\left(\sum w^{-kj}\hat{v}_j\right),$$

and $a = w^{-k}$. Then we also have λ_{N-k}, since it wraps around (or can use λ_{-k}).

The k-th eigenvector in the inverse space is just the k-th coordinate vector. The eigenvector v_k is then found using the inverse of the above Fourier transformation, $v_k = F^{-1}\hat{v}_k$, which is applied to the k-th coordinate vector, and v_k is given by the k-th column of the F^{-1} matrix, $v_k = \left(1, w^{-k}, w^{-2k}, \ldots, w^{-(N-1)k}\right)^{\mathsf{T}}$. Remember that $a = w^{-k}$. Note that the eigenvalues of Eq. (A.3) lie on an ellipse.

A.2 Eigen-problem of a persistent walk via Fourier transformation

To approach the persistent walk, we present it as a walk on the enlarged space of states, and use the Fourier transform of the recursion relation stemming from the Markov action. The space of states, and the evolution, are constructed as follows.

For each site we assign two coordinates, corresponding to the possibilities that the walk is directed left or right. Then the space dimension is $2N$, with a vector being: $v = (\ \ldots, v_i^R, v_i^L, \ldots\ )$, where v_i^R labels the 'right-moving' possibility, and v_i^L is when the walk is moving to the left. Across every pair of indices $(i, i+1)$ we have thus associated two vectors: v_i^R: $(i, i+1)$ and v_i^L: $(i+1, i)$. We now establish rules for how to index the transition from a site to another, based on whether the direction changed or not:

1. the walk came to i from the left (moving to the right) and *switched* the direction,

now moving to the right: $v_i^R \to v_i^L$, with probability $(1-p)$

2. the walk came to i from the left (moving to the right) and *continued* in the same direction: $v_{i-1}^R \to v_i^R$, with probability p

When the direction changes the state is associated with the same site, $v_i^R \to v_i^L$; when the direction is maintained the next neighbor is involved and the index changes, $v_{i+1}^L \to v_i^L$. With this we have:

$$vP = \lambda v \quad \Rightarrow \quad \begin{array}{rcl} \lambda\, v_i^R &=& p\, v_{i-1}^R \;+\; (1-p)\, v_i^L \\ \lambda\, v_i^L &=& (1-p)\, v_i^R \;+\; p\, v_{i+1}^L \end{array}$$

Notation is simplified considerably by introducing $a_i \equiv v_i^R$ and $b_i \equiv v_i^L$ for right/left modes

$$\begin{array}{rcl} \lambda\, a_i &=& p\;\; a_{i-1} + (1-p)\, b_i \\ \lambda\, b_i &=& (1-p)\, a_i \quad + \quad p\;\; b_{i+1} \end{array} \tag{A.4}$$

In exactly the same way like in the memoryless case, this is solved using its Fourier transform (and change index to j): multiply by w^{kj} and sum over j starting from $(j=0)$. Using

$$\sum_{j=0} w^{kj} a_{j-1} \;=\; w^k \sum_{j=0}^{N-1} w^{k(j-1)} a_{j-1} \;=\; w^k \sum_{j=1}^{N} w^{k(j-1)} a_{j-1} \;=\; w^k \sum_{j=0}^{N-1} w^{kj} a_j = w^k \hat{a}_k$$

the above recursion relations give, for Fourier transforms

$$\begin{array}{rcl} \lambda\, \hat{a}_k &=& p\, w^k\, \hat{a}_k + (1-p)\, \hat{b}_k \\ \lambda\, \hat{b}_k &=& (1-p)\, \hat{a}_k + \;\; p\, w^{-k}\, \hat{b}_k \end{array}$$

Now this eigenvalue problem can be represented in the matrix form

$$\begin{bmatrix} pw^k - \lambda & 1-p \\ 1-p & pw^{-k} - \lambda \end{bmatrix} \begin{bmatrix} \hat{a}_k \\ \hat{b}_k \end{bmatrix} \;=\; 0 \tag{A.5}$$

Note that vectors $\{\hat{a}_k, \hat{b}_k\}$ represent dynamics at site k. For them to be non-zero the

matrix must be singular, and the solutions to this characteristic equation are:

$$\lambda \;=\; p\,\cos\left(\frac{2\pi k}{N}\right) \pm \sqrt{p^2\,\cos^2\left(\frac{2\pi k}{N}\right) - (2p-1)}$$

Here $2p-1=0$ when the walk is unbiased ($p=1/2$), and we recover the standard random walk's $\lambda = \cos(2\pi k/N) = \frac{1}{2}w^k + \frac{1}{2}w^{-k}$.

Putting this solution back in Eq. (A.5) we can solve for the relation between $\hat{a}_k$ and $\hat{b}_k$, and get the pair of eigenvectors in the inverse space, associated with site k

$$\begin{bmatrix}\hat{a}_k\\ \hat{b}_k\end{bmatrix}_{1,2} \;=\; -\Big[\;\underbrace{\frac{\pm\sqrt{\left(p\cos\frac{2\pi k}{N}\right)^2-(2p-1)}+i\,p\,\sin\left(\frac{2\pi k}{N}\right)}{1-p}}_{c_1^{(k)}\text{ and }c_2^{(k)}},\quad 1\;\Big]^{\mathsf{T}}$$

To return from the inverse space, note that the Fourier transforms were taken independently, and we apply F^{-1} of Eq. (A.2) separately to the 'vectors' of left and right moving components, $\hat{a}_k$ and $\hat{b}_k$. We can say $v^R_{k1,2} = c_{k_{1,2}}\left(\,\ldots\,w^{-jk}\,\ldots\,\right)$ and $v^L = \left(\,\ldots\,w^{-jk}\,\ldots\,\right)$; the full eigenvectors are:

$$v_1^{(k)} = \Big(\underbrace{-1,}_{c_1^k(j=0)}\;1,\ldots,\underbrace{c_1^{(k)}w^{-jk},w^{-jk},}_{j-\text{th}\;\;\text{right,left}}\ldots\Big),\;\; v_2 = \Big(\underbrace{+1,}_{c_2^k(j=0)}\;1,\ldots,c_2^{(k)}w^{-jk},w^{-jk},\ldots\Big) \tag{A.6}$$

where the coefficients are: $c_{1,2}^{(k)} \;=\; \dfrac{\pm\sqrt{\left(p\cos\frac{2\pi k}{N}\right)^2-(2p-1)}+i\,p\,\sin\left(\frac{2\pi k}{N}\right)}{1-p}$.

Note the structure of the expression under the root: when $p^2\cos^2(2\pi k/N) > 2p-1$, then $\left|c_{1,2}^{(k)}\right|^2 = 1$ and the normalization of v requires $1/\sqrt{2N}$. This appears to hold strictly for all p only in the $k=0$ representation ($k=0,1,\ldots,N-1$), when $c_{1,2}^{(k=0)} = \pm 1$. Behavior of this expression for some representations is shown on Fig. (A.1).

To understand the eigenvectors, consider the action of P on, say, right-moving mode (a). With $vP=\lambda v$, as per Eq. (A.4), acting on either vector of Eq. (A.6)

$$\lambda\,c_k\,w^{-jk} = c_k\,p\,w^{-(j-1)k} + (1-p)\,w^{-jk},\quad \text{or:}\quad \lambda w^{-jk} = w^k p\,w^{-jk} + \frac{(1-p)}{c_k}\,w^{-jk}$$

The behavior of the eigenvector under the action of the operator P can be seen as:

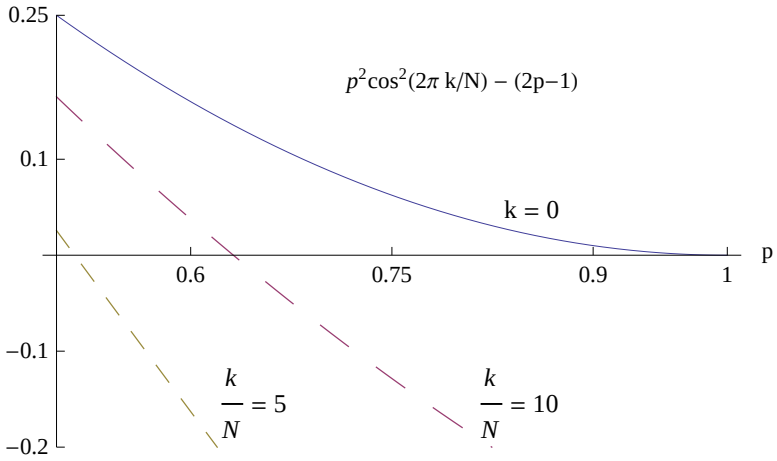

Figure A.1: The expression $p^2\cos^2(2\pi k/N) - (2p-1)$, affecting eigenvalues

moving to the right (w^k) with probability p, or changing the direction (when the site doesn't change) with probability $(1-p)$. The $1/c_k$ factor determines the relative 'weight' in the mix of the left and right moving vectors composing the eigenvector.

Appendix B: Standard coined 1-d DTQW and its spectral problem

The construction in [14] is introduced on a d-regular graph with n vertices, with an example of a circle. Here we review it in the same way. The state is constructed on the following direct product of two spaces. The first subspace, $\mathcal{H}_A$, is the 'coin space,' an auxiliary Hilbert space spanned by d states labeled $|a\rangle$; an unitary operator acting in this space represents a 'coin toss.' The second is the space of vertices, $\mathcal{H}_V$, spanned by n states $|v\rangle$. The complete evolution operator acts in the space $\mathcal{H}_A \otimes \mathcal{H}_V$ as

$$U\left(|a\rangle \otimes |v\rangle\right) \;=\; S \cdot (C \otimes I)\left(|a\rangle \otimes |v\rangle\right)$$

In the case of a cycle with n nodes, for the coin toss one can use the Hadamard transform

$$C \;=\; H = \frac{1}{\sqrt{2}} \begin{bmatrix} 1 & 1 \\ 1 & -1 \end{bmatrix}$$

and after its action the graph (circle) is then shifted by the operator S. Then the walk is a repeated application of the operator $U = S \cdot (C \otimes I)$. An implementation for S on a cycle, following up on the action of the 'coin toss' C, is

$$S \;=\; |\uparrow\rangle\langle\uparrow| \otimes \sum_j |j+1\rangle\langle j| \;+\; |\downarrow\rangle\langle\downarrow| \otimes \sum_j |j-1\rangle\langle j| \tag{B.1}$$

The first factor in each term selects the part of the state that is either in the 'up' or 'down' direction (following the action of the coin on this register), then the second projector shifts that state accordingly. Here is an example of the action of operator U, assuming the initial state of $|a\rangle = [\,1,\,0\,]^{\mathsf{T}}$ and $|v\rangle = (\,1,\,w^k,\,w^{2k},\,\dots\,)^{\mathsf{T}}$

$$S \cdot (C \otimes I) \begin{bmatrix} 1 \\ 0 \end{bmatrix} \otimes \begin{bmatrix} 1 \\ \vdots \\ w^{jk} \\ \vdots \end{bmatrix} \;=\; S \cdot \frac{1}{\sqrt{2}} \begin{bmatrix} 1 & 1 \\ 1 & -1 \end{bmatrix} \begin{bmatrix} 1 \\ 0 \end{bmatrix} \otimes \begin{bmatrix} 1 \\ \vdots \\ w^{jk} \\ \vdots \end{bmatrix} \;=\; S \cdot \frac{1}{\sqrt{2}} \begin{bmatrix} 1 \\ 1 \end{bmatrix} \otimes \begin{bmatrix} 1 \\ \vdots \\ w^{jk} \\ \vdots \end{bmatrix}$$

Using $(1,\,1)^{\mathsf{T}} = (1,\,0)^{\mathsf{T}} + (0,\,1)^{\mathsf{T}}$ we get two terms, transparent under the action of the 'selection projectors' of S of Eq. (B.1); with the shift operators' action, the new state is

$$U\left(|a\rangle \otimes |v\rangle\right) = \frac{1}{\sqrt{2}} \left(\begin{bmatrix} 1 \\ 0 \end{bmatrix} \otimes \begin{bmatrix} w^{(N-1)k} \\ 1 \\ \vdots \end{bmatrix} + \begin{bmatrix} 0 \\ 1 \end{bmatrix} \otimes \begin{bmatrix} w^{k} \\ \vdots \\ 1 \end{bmatrix} \right)$$

Factoring w^{-k} and w^{k} from the shifted $|v\rangle$'s, and using the cyclic property $w^{Nk} = 1$, we have

$$U\left(|a\rangle \otimes |v\rangle\right) = \frac{1}{\sqrt{2}} \left(w^{-k} \begin{bmatrix} 1 \\ 0 \end{bmatrix} \otimes |v\rangle \;+\; w^{k} \begin{bmatrix} 0 \\ 1 \end{bmatrix} \otimes |v\rangle \right) \;=\; \frac{1}{\sqrt{2}} \begin{bmatrix} w^{-k} \\ w^{k} \end{bmatrix} \otimes |v\rangle \qquad \text{(B.2)}$$

Note that the choice of fixed and equal factors in H yields an unbiased walk; we show below that this is exactly a special case of a memoried walk.

In order to see how the eigenproblem is approached, rewrite this in a more general fashion. Apply U to 'state of the coin' $|c\rangle = \sum c_a |a\rangle$, with $|a\rangle$ being the coordinate vectors in the coin space $\mathcal{H}_A$; the state vector in the space of vertices is $|v\rangle$. Then

$$U|c,v\rangle = S \cdot (C \otimes I)\left(|c\rangle \otimes |v\rangle\right) \;=\; S \cdot \left(C|c\rangle \otimes |v\rangle\right) \;=\; S \cdot \left(\sum_{a=1}^{d} c_a |a\rangle \otimes |v\rangle \right)$$

The matrix S can in general be constructed as

$$S = \sum_{a=1}^{d} \Pi_a \otimes S_a = \sum_{a=1}^{d} |a\rangle\langle a| \otimes S_a, \quad \text{where } S_a \text{ is the shift along } a.$$

Then, given that the operators above act in the product spaces only

$$U|c,v\rangle = \sum_{a=1}^{d} |a\rangle\langle a| \otimes S_a \cdot \left(\sum_{a=1}^{d} c_a |a\rangle \otimes |v\rangle \right) \;=\; \sum_{a=1}^{d} c_a |a\rangle \otimes S_a |v\rangle$$

The shift performed by S_a is the group action, $S_a|v\rangle = \chi(g_a^{-1})|v\rangle$, and we have

$$U|c,v\rangle = \left(\sum_{a=1}^{d} \chi(g_a^{-1})\, c_a |a\rangle \right) \otimes |v\rangle$$

It is now clear that for $|c, v\rangle$ to be an eigenvector, $\sum_{a=1}^{d} \chi(g_a^{-1})\, c_a |a\rangle$ has to be invariant under C, in other words it has to be the eigenvector of the coin operator C. This means that the operator for which we need eigenvectors can be written as

$$H_k = \Lambda_k \cdot C, \quad \text{where} \quad \Lambda_k(a,a) = \mathrm{diag}\{\, \chi(g_a^{-1}) \,\}$$

For the cycle, this is

$$H_k \;=\; \Lambda_k \cdot C \;=\; \begin{bmatrix} w^k & 0 \\ 0 & w^{-k} \end{bmatrix} \cdot \begin{bmatrix} \frac{1}{\sqrt{2}} & \frac{1}{\sqrt{2}} \\ \frac{1}{\sqrt{2}} & -\frac{1}{\sqrt{2}} \end{bmatrix} \;=\; \begin{bmatrix} \frac{w^k}{\sqrt{2}} & \frac{w^k}{\sqrt{2}} \\ \frac{w^{-k}}{\sqrt{2}} & -\frac{w^{-k}}{\sqrt{2}} \end{bmatrix}$$

As the construction of H_k includes the action of S, this matrix *is* a representation of the whole operator U, in the coordinate basis seen in Eq. (B.2).

Appendix C: Collected results involving Fourier transform

C.1 Converting sums to integrals using Fourier transform

Here we show the following identity used in text,

$$\sum_{k=0}^{m-1}(\alpha\beta)^k\binom{m}{k+1}\binom{m}{k} \;=\; \frac{1}{2\pi}\int_0^{2\pi}\left(1+\alpha e^{ix}\right)^m\left(1+\beta e^{-ix}\right)^m\frac{e^{-ix}}{\alpha}dx.$$

The powers under the integral can be written via the binomial expansion, and labeling the right-hand side by I,

$$\begin{aligned} I \;&= \frac{1}{2\pi\alpha}\int_0^{2\pi}\left[\sum_{n=0}^{m}\binom{m}{n}\left(\alpha e^{\boldsymbol{i}\,x}\right)^n\right]\times\left[\sum_{k=0}^{m}\binom{m}{k}\left(\beta e^{-\boldsymbol{i}\,x}\right)^k\right]e^{-\boldsymbol{i}\,x}\,dx \\ &= \frac{1}{2\pi\alpha}\int_0^{2\pi}\left[\sum_{n,k=0}^{m}\alpha^n\beta^k\binom{m}{n}\binom{m}{k}\right]e^{\boldsymbol{i}\,x\,(n-k-1)}\,dx. \end{aligned}$$

Now given that $\frac{1}{2\pi}\int_0^{2\pi}e^{\boldsymbol{i}\,a\,x}dx=\delta_{0,a}$, and that we have $e^{\boldsymbol{i}\,x\,(a-1)}$ under the integral,

$$\begin{aligned} I \;&= \frac{1}{2\pi\alpha}\sum_{k=0}^{m}\sum_{n=0}^{m}\alpha^n\beta^k\binom{m}{n}\binom{m}{k}\int_0^{2\pi}e^{\boldsymbol{i}\,x\,(n-k-1)}\,dx \\ &= \frac{1}{\alpha}\sum_{k=0}^{m}\sum_{n=0}^{m}\alpha^n\beta^k\binom{m}{n}\binom{m}{k}\delta_0(n-k-1), \end{aligned}$$

only the $n-k-1=0$ term (in one of the two sums) survives (after) the integration. Thus $n=k+1$, while we retain the sum over k. With the factor of 2π absorbed by the definition of the delta function and the 'extra' power in $\alpha^n=\alpha^{k+1}$ canceled by the one in the denominator we get the left hand side of the identity.

C.2 Inverse Fourier transform via Laurent expansion and Residue theorem

We start with the definition of the z transform,

$$\widehat{H}(z) = \sum_{t=0}^{\infty} H(t) z^t, \quad |z| < 1$$

and divide every term in this expansion by the power $m+1$.

$$\frac{\widehat{H}(z)}{z^{m+1}} = \frac{H(0)}{z^{m+1}} + \frac{H(1)}{z^m} + \cdots + \frac{H(m)}{z} + H(m+1) + \cdots ,$$

Now via Residue theorem,

$$\frac{1}{2\pi \boldsymbol{i}} \oint\limits_{|z|=r<1} \frac{\widehat{H}(z)}{z^{m+1}} dz = H(m),$$

what establishes the needed expression.

Another way to look at it, useful for certain kinds of the following integration, is via the Fourier of it. With $z = re^{\boldsymbol{i}\theta}$, $r < 1$,

$$\widehat{H}(re^{\boldsymbol{i}\theta}) e^{-\boldsymbol{i}m\theta} = \cdots + r^m \widehat{H}(m) + r^{m+1} H(m+1) e^{\boldsymbol{i}\theta} + \cdots ,$$

and now we have

$$\frac{1}{2\pi} \int_0^{2\pi} \frac{\widehat{H}(re^{\boldsymbol{i}\theta})}{r^m e^{\boldsymbol{i}m\theta}} d\theta = H(m).$$

This expression is suitable for direct integration around poles, for example.

Appendix D: Analysis of a 4–th order characteristic equation

The characteristic equation we obtain is

$$\lambda^4 - \left(\sqrt{p}\, e^{\boldsymbol{i}\, k} + \sqrt{q}\, e^{-\boldsymbol{i}\, k}\right) \lambda^3 + \left(\sqrt{p}\, e^{-\boldsymbol{i}\, k} + \sqrt{q}\, e^{\boldsymbol{i}\, k}\right) \lambda - 1 = 0.$$

Note the condition $|\lambda| = 1$, since λ is an eigenvalue of a unitary operator. This equation can be processed into a simpler form using either of the following two manipulations.

- Multiply twice by λ^*, obtaining $\lambda^2 - a\lambda = (\lambda^2 - a\lambda)^*$, where * denotes complex conjugation, and $a = \sqrt{p}\, e^{\boldsymbol{i}\, k} + \sqrt{q}\, e^{-\boldsymbol{i}\, k}$. This states that the complex number on the left has to be real.

- Divide by λ^2, and reorganize

  $$\lambda^2 - \lambda^{-2} - \sqrt{p}\left(e^{\boldsymbol{i}\, k}\lambda - (e^{\boldsymbol{i}\, k}\lambda)^{-1}\right) - \sqrt{q}\left(-e^{\boldsymbol{i}\, k}\lambda - (e^{-\boldsymbol{i}\, k}\lambda)^{-1}\right) = 0,$$

  then recognizing $\lambda = e^{\boldsymbol{i}\, \theta}$ we obtain

  $$\sin(2\theta) - \sqrt{p}\sin(\theta + k) - \sqrt{q}\sin(\theta - k) = 0,$$

  what can be interpreted as a relation on the imaginary part of a complex number,

  $$\mathfrak{Im}\left(e^{2\boldsymbol{i}\, \theta} - \sqrt{p}e^{\boldsymbol{i}(\theta+k)} - \sqrt{q}e^{\boldsymbol{i}(\theta-k)}\right) = 0.$$

In both cases we get the following statement, with its formal expression

$$\lambda^2 - \left(\sqrt{p}e^{\boldsymbol{i}\, k} + \sqrt{q}e^{-\boldsymbol{i}\, k}\right) \lambda \in \mathbb{R} \quad \Leftrightarrow \quad \lambda^2 - \left(\sqrt{p}e^{\boldsymbol{i}\, k} + \sqrt{q}e^{-\boldsymbol{i}\, k}\right) \lambda - \rho = 0, \quad \rho \in \mathbb{R}.$$

Here ρ may be any real number, but the solution must satisfy $|\lambda| = 1$. This allows the following,

$$\lambda_{1,2} = \frac{\sqrt{p}e^{\boldsymbol{i}\,k} + \sqrt{q}e^{-\boldsymbol{i}\,k} \pm \sqrt{\left(\sqrt{p}e^{\boldsymbol{i}\,k} + \sqrt{q}e^{-\boldsymbol{i}\,k}\right)^2 + 4\rho}}{2}, \quad \text{with} \quad |\lambda| = 1, \tag{D.1}$$

so with ρ such that

$$\left| \frac{\sqrt{p}e^{\boldsymbol{i}\,k} + \sqrt{q}e^{-\boldsymbol{i}\,k} \pm \sqrt{\left(\sqrt{p}e^{\boldsymbol{i}\,k} + \sqrt{q}e^{-\boldsymbol{i}\,k}\right)^2 + 4\rho}}{2} \right| = 1. \tag{D.2}$$

Solving Eq. (D.2) for ρ and using this in Eq. (D.1) yields the eigenvalues. However, finding an expression for ρ is algebraically exceedingly cumbersome, and would certainly lead to an unmanageable inversion. We will fall back to the case $p = q$, of equal probabilities governing left- and right-moving modes. This is also a physically more appropriate case to look at first.

Appendix E: Collected results on various integration

E.1 Laplace integral (method)

Find asymptotic behaviour of the integral $I = \int_L f(t)e^{-kt}dt$ when $k \to \infty$. (This goes after a change of variables in a problem of interest, s.t. $t = 0$ at the saddle.) Take

$$f(t) = f(0) + f'(0)t + \cdots = \sum_{j=0}^{\infty} \frac{f^{(j)}(0)}{j!} t^j, \quad \text{so that} \quad I \sim \sum_{j=0}^{\infty} \frac{f^{(j)}(0)}{j!} \int_0^a t^j e^{-kt} dt.$$

Here $a \in \mathbb{R}$ and small, and the saddle point contribution dominates. Now treat the integral with $kt = y$, and so $dt = dy/k$ and $t^j = y^j/k^j$,

$$I \sim \sum_{j=0}^{\infty} \frac{f^{(j)}(0)}{j!} \int_0^{ka\to\infty} \frac{y^j}{k^j} e^{-y} \frac{dy}{k} = \sum_{j=0}^{\infty} \frac{f^{(j)}(0)}{j!} \int_0^{\infty} y^j e^{-y} \frac{dy}{k^{j+1}}, \quad k \to \infty,$$

For analytic $f(t)$, have $I \sim \sum\limits_{j=0}^{\infty} \frac{1}{k^{j+1}} f^{(j)}(0)$ since $\int_0^\infty y^j e^{-y} dy = \Gamma(j+1) = j!$. Note: if there is, for example, $\sqrt{t} f(t)$, can't expand the $\sqrt{t}$ and we have

$$I \sim \sum_{j=0}^{\infty} \frac{1}{k^{j+1}} \frac{f^{(j)}(0)}{j!} \int_0^{\infty} y^{j+\frac{1}{2}} e^{-y} dy.$$

E.2 Integrals $I_{1,2}$ for $a_t(\ell)$

The first two integrals involved in $a_t(\ell)$ are calculated directly. For

$$I_1 = \frac{1}{2\pi} \int_0^{2\pi} dk \, \frac{e^{-\boldsymbol{i}k\ell}}{|v_1|^2} = \frac{1-p}{8\pi} \int_0^{2\pi} \frac{e^{-\boldsymbol{i}\,k\,\ell}\, dk}{1 - \sqrt{p}\cos k} = \frac{1-p}{8\pi} \int_0^{2\pi} \frac{\left(e^{-\boldsymbol{i}\,k}\right)^{\ell} dk}{1 - \sqrt{p}\,\frac{e^{\boldsymbol{i}k} + e^{-\boldsymbol{i}k}}{2}}$$

use $e^{-\boldsymbol{i}k} = z$, and we have $d(e^{-\boldsymbol{i}k}) = -\boldsymbol{i}e^{-\boldsymbol{i}k}dk = dz \Rightarrow dk = \boldsymbol{i}z^{-1}dz$, where the new contour is $|z| = 1$ (on a unit circle), going around clock-wise (corresponding to $k \in [0, 2\pi]$

with $z = e^{-\boldsymbol{i}k}$). Consider ℓ as positive for now. With $\left(e^{-\boldsymbol{i}\,k}\right)^{\ell} = z^{\ell}$ we have

$$\begin{aligned} I_1 = \; & \boldsymbol{i}\,\frac{1-p}{8\pi}\oint\limits_{|z|=1}\frac{z^{\ell-1}dz}{1-\frac{\sqrt{p}}{2}\,(z+z^{-1})} = \boldsymbol{i}\,\frac{1-p}{8\pi}\oint\limits_{|z|=1}\frac{z^{\ell}dz}{z-\frac{\sqrt{p}}{2}\,(z^2+1)} \\ = \; & -\boldsymbol{i}\,\frac{2}{\sqrt{p}}\frac{1-p}{8\pi}\oint\limits_{|z|=1}\frac{z^{\ell}dz}{z^2-\frac{2}{\sqrt{p}}z+1} \\ = \; & -\frac{\boldsymbol{i}}{4\pi}\,\frac{1-p}{\sqrt{p}}\oint\limits_{|z|=1}\frac{z^{\ell}dz}{\left[z-\left(\frac{1}{\sqrt{p}}+\sqrt{\frac{1}{p}-1}\right)\right]\left[z-\left(\frac{1}{\sqrt{p}}-\sqrt{\frac{1}{p}-1}\right)\right]}. \end{aligned}$$

This is calculated by the Residue theorem, $I_1 = -2\pi\boldsymbol{i}\sum_i \mathrm{Res}_i f(z_i)$. The minus sign corresponds to clock-wise direction along the contour. Of the two poles (solutions to $z^2 - \frac{2}{\sqrt{p}}z + 1 = 0$) one is inside the circle since they multiply to give 1. A simple asymptotic analysis ($p \to 0$ and $p \to 1$) shows that the solution with the $-$ sign is inside the unit circle, $z_2 = \frac{1}{\sqrt{p}} - \sqrt{\frac{1}{p}-1}$, and

$$\begin{aligned} I_1 = \; & -\frac{\boldsymbol{i}}{4\pi}\,\frac{1-p}{\sqrt{p}} \times \big[-2\pi\boldsymbol{i}\,\mathrm{Res} f(z_2)\big], \qquad \mathrm{Res}\, f(z_2) \;=\; \lim_{z\to z_2}(z-z_2)\frac{z^{\ell}}{(z-z_1)(z-z_2)} \\ = \; & -\left(\frac{1-p}{2\sqrt{p}}\right)\frac{(z_2)^{\ell}}{\left[z_2-\left(\frac{1}{\sqrt{p}}+\sqrt{\frac{1}{p}-1}\right)\right]} \;=\; -\left(\frac{1-p}{2\sqrt{p}}\right)\frac{\left(\frac{1}{\sqrt{p}}-\sqrt{\frac{1}{p}-1}\right)^{\ell}}{\left(\frac{1}{\sqrt{p}}-\sqrt{\frac{1}{p}-1}\right)-\left(\frac{1}{\sqrt{p}}+\sqrt{\frac{1}{p}-1}\right)} \\ = \; & \frac{\sqrt{1-p}}{4}\left(\frac{1}{\sqrt{p}}-\sqrt{\frac{1}{p}-1}\right)^{\ell} \;=\; \frac{\sqrt{1-p}}{4}\left(\frac{1-\sqrt{1-p}}{\sqrt{p}}\right)^{\ell} \end{aligned}$$

For $p = 1/2$, we have $I_1(\ell) = \frac{1}{4\sqrt{2}}\left(\sqrt{2}-1\right)^{\ell}$. The difference for I_2 is that in the denominator we have $z^2 + \frac{2}{\sqrt{p}}z + 1$, and without an overall minus sign. Now $z_{1,2} = -\frac{1}{\sqrt{p}} \pm \sqrt{\frac{1}{p}-1}$ are the poles, with roles swapped and a minus sign relative to the I_1 case, and we get

$$I_2 = (-1)^t\,\frac{1-p}{4\sqrt{1-p}}\left(-\frac{1}{\sqrt{p}}+\sqrt{\frac{1}{p}-1}\right)^{\ell} \;=\; (-1)^t\,\frac{\sqrt{1-p}}{4}\left(\frac{1}{\sqrt{p}}-\sqrt{\frac{1}{p}-1}\right)^{\ell} \times (-1)^{\ell},$$

with the $(-1)^t$ factor restored. Thus our first two integrals are

$$I_{1+2} = \left[1 + (-1)^{t+\ell}\right] \frac{\sqrt{1-p}}{4} \left(\frac{1-\sqrt{1-p}}{\sqrt{p}}\right)^{|\ell|},$$

where I formalized my expectation that the value of the integral should be symmetric w.r.t. $\ell = 0$, by writing $|\ell|$ instead.

Appendix F: Integral in Ch. 3 (steepest descent method)

Integrals suitable for analysis by the steepest descent method are typically of the form [142, 143]

$$I(k) = \int_C f(\omega)\, e^{k\Phi(\omega)}\, d\omega. \tag{F.1}$$

We use Eq. (3.11), where the exponent will be formed from powers of z. As z is always squared we first change variables via $z^2 = \xi$. Accounting for the double winding,

$$I(t;n) = 2 \times \frac{1}{2} \oint_{|\sqrt{\xi}|=r} \frac{\left[\frac{\widehat{g}(\xi)}{\xi} - \sqrt{3}\right]^n}{1 - \widehat{g}(\xi)} \frac{1}{\xi} \frac{d\xi}{\xi^{\frac{t-n}{2}}}.$$

We now use $\widehat{g}(\xi)/\xi = \omega$, to transfer some of the integrand's complexity into the exponent,

$$\frac{\widehat{g}(\xi)}{\xi} = \omega, \quad \xi = \varphi(\omega) = a\sqrt{3}\, \frac{\omega - \frac{1}{\sqrt{3}}}{(\omega + \frac{1}{\sqrt{3}})(\omega - \frac{2}{\sqrt{3}})}.$$

Carrying out the substitution, we have

$$I(t;n) = \oint_{|\sqrt{\varphi}|=r} \frac{(\omega - \sqrt{3})^n}{(1 - \omega\,\varphi)} \frac{\varphi\prime}{\varphi}\, \varphi^{-\frac{t-n}{2}}\, d\omega, \tag{F.2}$$

in the form (F.1), with $\varphi^{-\frac{t-n}{2}} = e^{\frac{t-n}{2}\log(\varphi^{-1})}$, and

$$f = \frac{(\omega - \sqrt{3})^n}{(1 - \omega\,\varphi)} \frac{\varphi\prime}{\varphi}, \quad \Phi = -\log\varphi, \quad k = \frac{t-n}{2}. \tag{F.3}$$

Keeping φ'/φ will be useful. Consider the critical points. A pole of order $\frac{t-n+2}{2}$ is at $\varphi = 0 \Rightarrow \omega_p = 1/\sqrt{3}$. Two simple poles are at $-\frac{1}{\sqrt{3}}$, $\frac{2}{\sqrt{3}}$. The logarithm's branch point is at $\varphi = 1$, and since this is not at $\omega_p = 1/\sqrt{3}$, what the contour must enclose, we can take any convenient branch. Two simple saddle points are

$$(\log\varphi)\prime = 0 \;\Rightarrow\; \omega_{s1/s2} = \frac{1 \pm \boldsymbol{i}\sqrt{2}}{\sqrt{3}} = e^{\pm \boldsymbol{i}\arctan\sqrt{2}}.$$

The main contribution to this integral comes from saddle points. A branch of the original integration contour $|\sqrt{\varphi}| = r$ can be chosen (via r) for use with steepest descent paths. There are no issues with deforming the contour, as no critical points are in the way, any branch of the logarithm is good, and $k = \frac{t-n}{2} \in \mathbb{Z}$ (Fig. F.1).

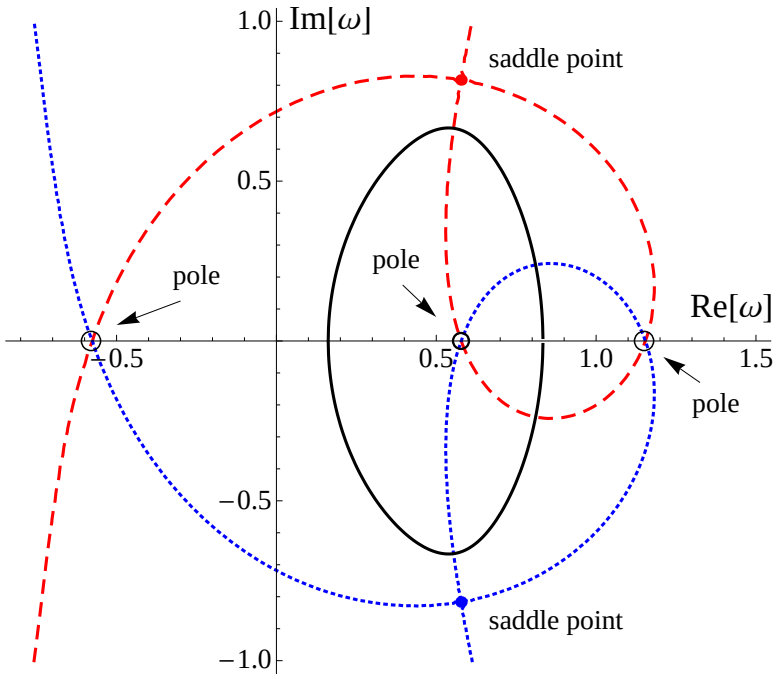

Figure F.1: Original integration contour (solid black), steepest descent paths (dashed red and dotted blue), and critical points.

In the steepest descent method decreasing orders of contribution are computed mostly via expansion around saddles. (There are theorems and formulas for the first–order contribution, but here it is zero.) Around ω_s we have $\Phi(\omega) = \Phi(\omega_s) + \frac{1}{2!}\big[\Phi(\omega)\big]''_{\omega_s}(\omega - \omega_s)^2 + o(\omega^2)$, and the usual change of variables $\Phi(\omega) - \Phi(\omega_s) = -y$ gives

$$\omega = \mp b\sqrt{y} + \omega_s, \quad b = \sqrt{\frac{2}{\big[\log\varphi(\omega)\big]''_{\omega=\omega_s}}}, \tag{F.4}$$

where y is zero at the saddle and real along the steepest descent path. We used $\sqrt{(\log\varphi^{-1})''} = \boldsymbol{i}\sqrt{(\log\varphi)''}$. Now $y = \log\big[\varphi(\omega)/\varphi(\omega_s)\big]$ and $dy = \big[\varphi(\omega)'/\varphi(\omega)\big]\,d\omega$,

and with $\varphi(\omega) = \varphi(\omega_s)\, e^y$ the integral of Eqs. (F.2) and (F.3) becomes

$$I(k) \sim e^{k\Phi(\omega_s)} \oint \frac{\left[\omega(y) - \sqrt{3}\right]^n}{1 - \omega(y)\, \varphi(\omega_s)\, e^y}\, e^{-ky}\, dy. \tag{F.5}$$

Now we can directly expand around $y = 0$ (to any order), restricting integration to the line along the steepest descent path, close to saddles. The signs in Eq. (F.4) correspond to the opposite directions from the saddle; we label $+/-$ as "R/L." Substituting $\omega(y)$ and expanding,

$$I \sim A\, \varphi_s^{-k} \int_0^\delta \left(1 \pm B\, \sqrt{y}\,\right)\, e^{-ky}\, dy, \quad \delta \sim o(1),$$
$$A = \frac{\left[\omega_s - \sqrt{3}\right]^n}{1 - \omega_s\, \varphi_s}, \; B = \left(\frac{b\, \varphi_s}{1 - \omega_s \varphi_s} + \frac{b}{\omega_s - \sqrt{3}}\, n\right).$$

For compactness we use $\varphi_s \equiv \varphi(\omega_s) = e^{i\lambda_s}$, with $\lambda_{s1} = \arctan\left[(9\sqrt{3}+8\sqrt{2})/23\right]$, $\lambda_{s2} = \arctan\left[(9\sqrt{3}-8\sqrt{2})/23\right] - \pi$. Note that $A(n) \sim (\sqrt{2})^n$, as $\omega_s - \sqrt{3} = \sqrt{2}e^{i\gamma_s}$, with $\gamma_{s1/s2} = \mp\left[\arctan(1/\sqrt{2}) - \pi\right] \equiv \mp(\gamma - \pi)$, and we will extract π later. The integral is dominated around ω_s ($\delta \approx 0$), so it can be formally extended, $\delta \to \infty$, and we get $I \sim A \int_0^\infty \left(1 \pm B\sqrt{y}\right)\, e^{-ky}\, dy$. This results in

$$I_{R/L}\,(k; n) \;\sim\; A_n \left(\frac{1}{k} \pm \frac{\sqrt{\pi}}{2}\, \frac{B_n}{k\sqrt{k}}\right)\, \varphi(\omega_s)^{-k}.$$

Subtracting contributions along opposite directions, the first non–zero order for either saddle is

$$I_s \sim (\sqrt{2})^n\, e^{i\,\gamma_s n}\, (a_s + d_s\, n)\, \frac{e^{-i\,\lambda_s k}}{k\sqrt{k}}.$$

We broke up the $A_n B_n$ term found in $I_R - I_L$, to show the structure of n dependence, where $a_s = \frac{b\,\varphi_s\sqrt{\pi}}{(1-\omega_s\varphi_s)^2}$ and $d_s = \frac{b\,\sqrt{\pi}}{(1-\omega_s\varphi_s)(\omega_s-\sqrt{3})}$ are of order ~ 1. Here we extract π from γ_s, and will use $e^{i\gamma_s} = (-1)e^{\mp i\gamma}$. Contributions for saddles are subtracted (for consistency of $\pm\sqrt{y}$ directions) and, with $c_{s,n} \equiv a_s + d_s n$, we get Eq. (3.12).

The full expansion of the integral (F.5) results in nested sums of a Gamma function. This cannot capture the peak of the amplitude though, and is not needed for our asymptotic analysis, so we do not pursue it here.

Appendix G: Integrals in Ch. 4 (stationary phase method)

The integrals for inverting the Fourier transform of the coefficients are most efficiently treated with the stationary phase method (see, for example, [142, 143]), whose main ideas were discussed in text. Here we go through the integration for $a_t(n)$ in detail; calculation for other coefficients follows suit, and the results are shown in a more condensed manner. We use the form for the stationary point k_s from Eq. (4.8), which is the same for all integrals in all coefficients, and reproduce it here for convenience:

$$\frac{\partial \Phi_\pm}{\partial k} = -\alpha \pm \frac{\sqrt{p}\sin k}{\sqrt{1-p\cos^2 k}}, \quad \left.\frac{\partial \Phi_\pm}{\partial k}\right|_{k_s} = 0 \;\Rightarrow\; \sin k_s = \pm\sqrt{\frac{1-p}{p}}\frac{\alpha}{\sqrt{1-\alpha^2}}. \tag{G.1}$$

Recall that $\Phi_\pm = -\alpha k \pm \omega_k$, where the frequency $\omega_k = \cos^{-1}\left(\sqrt{p}\cos k\right)$, and $\alpha \equiv \frac{n}{t}$.

G.1 Inverting $\widehat{a}_t(k)$ to find asymptotic of $a_t(n)$

Our target are integrals (4.7). It is readily seen that $\Phi''_\pm(k_s) \neq 0$ and that functions $f_{1,2}$ have zero-th order term in expansion around k_s, so we can use the somewhat simplified form of the main theorem, given in Eq. (4.6) for the regime $|\alpha| < \sqrt{p}$ (see discussion in text for different regimes). Again, it is given here as well, for convenience:

$$I(t) = \int_a^b f(k)\, e^{\boldsymbol{i}\, t\, \Phi(k)} dk \;\sim\; f(k_s) e^{\boldsymbol{i} t \Phi(k_s)} \sqrt{\frac{2\pi}{t\,|\Phi''(k_s)|}}\, e^{\boldsymbol{i}\frac{\pi}{4}\mu},\; \mu = \operatorname{sgn}\left[\Phi''(k_s)\right]. \tag{G.2}$$

However, when $|\alpha| = \sqrt{p}$ the second derivative of the exponent at the stationary point is zero, and we use the more general form of the theorem.

G.1.1 Stationary phase for $-\sqrt{p} + \epsilon \leq \alpha \leq \sqrt{p} - \epsilon$

The formula (G.2) applied to integrals (4.7) now operates with the following functions and their expansions. (For now they are separated into $\alpha \gtrless 0$ regimes, but later we find

that this is not necessary.)

$$\alpha > 0. \quad \text{For } \Phi_\pm(\alpha,k)\colon f_1(k_s) = \frac{1-\alpha^2}{1-p},\ f_2(k_s) = \pm\frac{\alpha}{\sqrt{p}}. \quad \Phi''_\pm(k_s) = \pm(1-\alpha^2)\sqrt{\frac{p-\alpha^2}{1-p}}$$

$$\alpha < 0. \quad \text{For } \Phi_\pm(\alpha,k)\colon f_1(k_s) = \frac{1-\alpha^2}{1-p},\ f_2(k_s) = \mp\frac{\alpha}{\sqrt{p}}. \quad \Phi''_\pm(k_s) = \mp(1-\alpha^2)\sqrt{\frac{p-\alpha^2}{1-p}}$$

The stationary points are inverted from the expression (G.1), and for Φ_+ we label them k^+_{s1} and $k^+_{s2} = \pi - k^+_{s1}$, while for Φ_- they are k^-_{s1} and $k^-_{s2} = \pi + k^-_{s1}$. Also note that $k^-_{s1} = -k^+_{s1}$ so we can reduce all these to one (we use k^+_{s1}), what is convenient for later,

$$k^+_{s1} = \text{Arcsin}\left(\sqrt{\frac{1-p}{p}}\frac{\alpha}{\sqrt{1-\alpha^2}}\right), \quad k^+_{s2} = \pi - k^+_{s1}, \quad k^-_{s1} = -k^+_{s1}, \quad k^-_{s2} = \pi + k^+_{s1}.$$

Now $\Phi_\pm\left(k^\pm_{s1/2}\right)$ can be evaluated, and reduced to one of the cases. Here a little care need be taken to account for how inverse trigonometric functions behave with arguments shifted by π, and one case is shown in detail, for how $\Phi_+(k^+_{s2})$ reduces to $\Phi_+(k^+_{s1})$.

First we comment on notation. The $\pm$ indices on k_s's are now redundant, since the functions $\Phi_\pm$ are of course each evaluated at its own stationary point, $\Phi_+(k_{s1}) = -\alpha k^+_{s1} + \omega(k^+_{s1})$ for example, but we keep carrying them for clarity. We will keep compact expressions throughout (cutting down the complexity of algebra is a priority!), and here for reference we show one explicit expression,

$$\Phi_\pm(k_{s1}) = \mp\,\alpha\sin^{-1}\left(\alpha\sqrt{\frac{1-p}{p(1-\alpha^2)}}\right) \pm \cos^{-1}\sqrt{\frac{p-\alpha^2}{1-\alpha^2}},$$

obtained by manipulating the expression $\cos^{-1}\left[\sqrt{p}\cos\left(\sin^{-1}\left(\frac{\alpha}{\sqrt{p}}\sqrt{\frac{1-p}{1-\alpha}}\right)\right)\right]$ simply using the trigonometric identity on the cos. Keeping compact expressions, functions $\Phi_\pm(k^\pm_{s1/2})$ reduce to each other in the following manner.

$$\begin{aligned}\phi_+\left(k^+_{s2}\right) &= -\alpha(\pi - k^+_{s1}) + \cos^{-1}\left[\sqrt{p}\cos\left(\pi - k^+_{s1}\right)\right] \\ &= -\alpha\pi + \pi - \left[-\alpha k^+_{s1} + \cos^{-1}\left(\sqrt{p}\cos\left(k^+_{s1}\right)\right)\right] = -\alpha\pi + \pi - \Phi_+\left(k^+_{s1}\right),\end{aligned}$$

where $\cos^{-1}\left[\sqrt{p}\cos\left(\pi - k^+_{s1}\right)\right] = \cos^{-1}\left[-\sqrt{p}\cos\left(k^+_{s1}\right)\right] = \pi - \cos^{-1}\left[\sqrt{p}\cos\left(k^+_{s1}\right)\right]$ has been used, along with some rearrangements. Other cases are processed similarly. At this

point we lighten the notation, introducing $\Phi^+_{s1} \equiv \Phi_+\left(k^+_{s1}\right)$, etc. One gets relations

$$\begin{aligned} &\Phi^+_{s1} = -\alpha k^+_{s1} + \omega\big(k^+_{s1}\big) = -\alpha k^+_{s1} + \cos^{-1}\big[\sqrt{p}\cos\big(k^+_{s1}\big)\big], \quad \text{and} \\ &\Phi^+_{s2} = -\alpha\pi + \pi - \Phi^+_{s1}, \quad \Phi^-_{s1} = -\Phi^+_{s1}, \quad \Phi^-_{s2} = -\alpha\pi - \pi + \Phi^+_{s1}. \end{aligned} \tag{G.3}$$

We finally need to summarize relations between functions $f(k_s)$ in the integrand at various k_s's, along with the property of the second derivative of Φ's, and then the integrals can be manipulated algebraically. It is established by direct calculation that

$$f_1\big(k^\pm_{s1}\big) = f_1\big(k^\pm_{s2}\big) = \frac{1-\alpha^2}{1-p}, \quad \text{and} \quad f_2\big(k^\pm_{s1}\big) = f_2\big(k^\pm_{s2}\big) = \pm\frac{\alpha}{p} \times \mathrm{sgn}(\alpha),$$

and that $\Phi''_\pm = \pm\omega''_k = \pm\left[\frac{\sqrt{p}\cos k}{\sqrt{1-p\cos^2 k}} - \frac{p\sqrt{p}\cos k\sin^2 k}{(1-p\cos^2 k)^{3/2}}\right]$, thus $|\omega''_s|$ is the same for all $k^\pm_s$. Finally, since we also have

$$k^\pm_{s2} = \pi \mp k^\pm_{s1} \quad \Rightarrow \quad \cos k_{s1} \xrightarrow{s1\to s2} -\cos k_{s1} = \cos k_{s2}, \quad \text{then}$$

$\mathrm{sgn}\left[\Phi''_\pm\big(k_{s1}\big)\right] = -\mathrm{sgn}\left[\Phi''_\pm\big(k_{s2}\big)\right]$. We now have all factors for the integrals. The stationary points fall in intervals $k_{s1} \in (0,\pi/2)$ and $k_{s2} \in (\pi/2,\pi)$ and one can break up the stationary phase method integration as $\int_0^{2\pi} = \int_0^{\pi/2} + \int_{\pi/2}^{2\pi}$, agreeing with the spirit and the letter of the method. Then, using the formula (G.2),

$$\begin{aligned} I_{t,\omega_k} \sim \frac{1}{\sqrt{t}} \Bigg\{ &\frac{p-1}{8\pi} \times \\ &\Bigg[\left(f_1\big(k^+_{s1}\big) e^{\boldsymbol{i}\, t\, \Phi^+_{s1}} \sqrt{\frac{2\pi}{\left|\Phi_+\big(k^+_{s1}\big)''\right|}} e^{\boldsymbol{i}\,\frac{\pi}{4}\,\mu^+_{s1}} + f_1\big(k^+_{s2}\big) e^{\boldsymbol{i}\, t\, \Phi^+_{s2}} \sqrt{\frac{2\pi}{\left|\Phi_+\big(k^+_{s2}\big)''\right|}} e^{\boldsymbol{i}\,\frac{\pi}{4}\,\mu^+_{s2}} \right) \\ &+ \left(f_1\big(k^+_{s1}\big) e^{\boldsymbol{i}\, t\, \Phi^-_{s1}} \sqrt{\frac{2\pi}{\left|\Phi_-\big(k^-_{s1}\big)''\right|}} e^{\boldsymbol{i}\,\frac{\pi}{4}\,\mu^-_{s1}} + f_1\big(k^-_{s2}\big) e^{\boldsymbol{i}\, t\, \Phi^-_{s2}} \sqrt{\frac{2\pi}{\left|\Phi_+\big(k^-_{s2}\big)''\right|}} e^{\boldsymbol{i}\,\frac{\pi}{4}\,\mu^-_{s2}} \right) \Bigg] \\ +\frac{\sqrt{p}}{4\pi} \times &\Bigg[\left(f_2\big(k^+_{s1}\big) e^{\boldsymbol{i}\, t\, \Phi^+_{s1}} \sqrt{\frac{2\pi}{\left|\Phi_+\big(k^+_{s1}\big)''\right|}} e^{\boldsymbol{i}\,\frac{\pi}{4}\,\mu^+_{s1}} + f_2\big(k^+_{s2}\big) e^{\boldsymbol{i}\, t\, \Phi^+_{s2}} \sqrt{\frac{2\pi}{\left|\Phi_+\big(k^+_{s2}\big)''\right|}} e^{\boldsymbol{i}\,\frac{\pi}{4}\,\mu^+_{s2}} \right) \\ &- \left(f_2\big(k^-_{s1}\big) e^{\boldsymbol{i}\, t\, \Phi^-_{s1}} \sqrt{\frac{2\pi}{\left|\Phi_-\big(k^-_{s1}\big)''\right|}} e^{\boldsymbol{i}\,\frac{\pi}{4}\,\mu^-_{s1}} + f_2\big(k^-_{s2}\big) e^{\boldsymbol{i}\, t\, \Phi^-_{s2}} \sqrt{\frac{2\pi}{\left|\Phi_-\big(k^-_{s2}\big)''\right|}} e^{\boldsymbol{i}\,\frac{\pi}{4}\,\mu^-_{s2}} \right) \Bigg] \end{aligned}$$

$$+\frac{1}{4\pi}\times\left[\left(e^{\boldsymbol{i}\,t\,\Phi^{+}_{s1}}\sqrt{\frac{2\pi}{\left|\Phi_{+}\left(k^{+}_{s1}\right)''\right|}}e^{\boldsymbol{i}\,\frac{\pi}{4}\,\mu^{+}_{s1}}+e^{\boldsymbol{i}\,t\,\Phi^{+}_{s2}}\sqrt{\frac{2\pi}{\left|\Phi_{+}\left(k^{+}_{s2}\right)''\right|}}e^{\boldsymbol{i}\,\frac{\pi}{4}\,\mu^{+}_{s2}}\right)\right.$$
$$\left.+\left(e^{\boldsymbol{i}\,t\,\Phi^{-}_{s1}}\sqrt{\frac{2\pi}{\left|\Phi_{-}\left(k^{-}_{s1}\right)''\right|}}e^{\boldsymbol{i}\,\frac{\pi}{4}\,\mu^{-}_{s1}}+e^{\boldsymbol{i}\,t\,\Phi^{-}_{s2}}\sqrt{\frac{2\pi}{\left|\Phi_{-}\left(k^{-}_{s2}\right)''\right|}}e^{\boldsymbol{i}\,\frac{\pi}{4}\,\mu^{-}_{s2}}\right)\right]\Bigg\}.$$

Using explicit expressions $f_1\left(k^{\pm}_{s1/2}\right)=\frac{1-\alpha^2}{1-p}$ and $f_2\left(k^{\pm}_{s1/2}\right)=\pm\frac{\alpha}{\sqrt{p}}$ and the fact that $|\Phi''|=|\omega''|$ for all k_s, and with

$$\mu^{+}_{s1}=1,\quad \mu^{+}_{s2}=-1,\quad \mu^{-}_{s1}=-1,\quad \text{and}\quad \mu^{-}_{s2}=1,$$

we get with some grouping of terms

$$I_{t,\omega_k}\sim\frac{1}{\sqrt{t}}\sqrt{\frac{2\pi}{|\omega''_s|}}\times\Bigg\{$$
$$\frac{p-1}{8\pi}\times\frac{1-\alpha^2}{1-p}\left[\left(e^{\boldsymbol{i}\,t\,\Phi^{+}_{s1}}\,e^{\boldsymbol{i}\,\frac{\pi}{4}}+e^{\boldsymbol{i}\,t\,\Phi^{+}_{s2}}\,e^{-\boldsymbol{i}\,\frac{\pi}{4}}\right)+\left(e^{\boldsymbol{i}\,t\,\Phi^{-}_{s1}}\,e^{-\boldsymbol{i}\,\frac{\pi}{4}}+e^{\boldsymbol{i}\,t\,\Phi^{-}_{s2}}\,e^{\boldsymbol{i}\,\frac{\pi}{4}}\right)\right]$$
$$+\frac{\sqrt{p}}{4\pi}\times\frac{\alpha}{\sqrt{p}}\left[\left(e^{\boldsymbol{i}\,t\,\Phi^{+}_{s1}}\,e^{\boldsymbol{i}\,\frac{\pi}{4}}+e^{\boldsymbol{i}\,t\,\Phi^{-}_{s2}}\,e^{-\boldsymbol{i}\,\frac{\pi}{4}}\right)-\left(-e^{\boldsymbol{i}\,t\,\Phi^{-}_{s1}}\,e^{-\boldsymbol{i}\,\frac{\pi}{4}}+(-1)e^{\boldsymbol{i}\,t\,\Phi^{-}_{s2}}\,e^{\boldsymbol{i}\,\frac{\pi}{4}}\right)\right]$$
$$+\frac{1}{4\pi}\left[\left(e^{\boldsymbol{i}\,t\,\Phi^{+}_{s1}}\,e^{\boldsymbol{i}\,\frac{\pi}{4}}+e^{\boldsymbol{i}\,t\,\Phi^{+}_{s2}}\,e^{-\boldsymbol{i}\,\frac{\pi}{4}}\right)+\left(e^{\boldsymbol{i}\,t\,\Phi^{-}_{s1}}\,e^{-\boldsymbol{i}\,\frac{\pi}{4}}+e^{\boldsymbol{i}\,t\,\Phi^{-}_{s2}}\,e^{\boldsymbol{i}\,\frac{\pi}{4}}\right)\right]\Bigg\}$$

Note that all square brackets are the same and

$$I_{t,\omega_k}\sim\frac{1}{\sqrt{t}}\sqrt{\frac{2\pi}{|\omega''_s|}}\,\frac{\alpha^2-1+2\alpha+2}{8\pi}\times$$
$$\left[e^{\boldsymbol{i}\,t\,\Phi^{+}_{s1}}\,e^{\boldsymbol{i}\,\frac{\pi}{4}}+e^{\boldsymbol{i}\,t\,\Phi^{+}_{s2}}\,e^{-\boldsymbol{i}\,\frac{\pi}{4}}+e^{\boldsymbol{i}\,t\,\Phi^{-}_{s1}}\,e^{-\boldsymbol{i}\,\frac{\pi}{4}}+e^{\boldsymbol{i}\,t\,\Phi^{-}_{s2}}\,e^{\boldsymbol{i}\,\frac{\pi}{4}}\right].$$

At this point it is time to use the relations (G.3),

$$I_{t,\omega_k}\sim\frac{1}{\sqrt{t}}\sqrt{\frac{2\pi}{|\omega''_s|}}\,\frac{(1+\alpha)^2}{8\pi}\times$$
$$\left[e^{\boldsymbol{i}\,t\,\Phi^{+}_{s1}}\,e^{\boldsymbol{i}\,\frac{\pi}{4}}+e^{-\boldsymbol{i}\,t\,\Phi^{+}_{s1}}\,e^{-\boldsymbol{i}t\alpha\pi}\,e^{\boldsymbol{i}t\pi}\,e^{-\boldsymbol{i}\,\frac{\pi}{4}}+e^{-\boldsymbol{i}\,t\,\Phi^{+}_{s1}}\,e^{-\boldsymbol{i}\,\frac{\pi}{4}}+e^{\boldsymbol{i}\,t\,\Phi^{+}_{s1}}\,e^{-\boldsymbol{i}t\alpha\pi}\,e^{-\boldsymbol{i}t\pi}e^{\boldsymbol{i}\,\frac{\pi}{4}}\right].$$

Since $\alpha = \frac{n}{t}$ we can use $e^{-\boldsymbol{i}t\alpha\pi} = (-1)^n$ and $e^{\pm\boldsymbol{i}t\pi} = (-1)^t$, and group terms

$$I_{t,\omega_k} \sim \frac{1}{\sqrt{t}} \times \frac{1}{2\sqrt{2\pi}} \frac{(1+\alpha)^2}{\sqrt{|\omega_s''|}} \cos\left(\Phi_{s1}^{+}\, t + \frac{\pi}{4}\right) \times \left[1 + (-1)^{t+n}\right].$$

Using the explicit expression $\omega''(k_s) = (1-\alpha^2)\sqrt{\frac{p-\alpha^2}{1-p}}$ shows fully the α and p dependence, and with $c_p(\alpha) = \frac{(1+\alpha)^2}{\sqrt{1-\alpha^2}} \left[\frac{1-p}{p-\alpha^2}\right]^{1/4}$ and $\phi_p(\alpha) = \Phi_+(k_s^+)$, we have for $\alpha > 0$,

$$I_{t,\alpha} \sim \frac{1}{\sqrt{t}} \times \frac{c_p(\alpha)}{2\sqrt{2\pi}} \cos\left[\phi_p(\alpha)\, t + \frac{\pi}{4}\right] \times \left[1 + (-1)^{t+n}\right].$$

Note that $\frac{c_p(\alpha)}{2\sqrt{2\pi}} \lesssim 1$ over α for most of the range of p, while $\phi_p(\alpha)$ varies between 0.1 and 1.45 over α, including extreme values of p (0.01 to 0.99), while it is between 0.5+ and 0.8− for $p \sim 0.5$. Thus, roughly, $I_t \lesssim \frac{1}{\sqrt{t}} \cos(t + \pi/4)$.

The above expression provides an analytical estimate, $a_t(n) \sim I_{1+2} + I_{t,\omega_k}(\alpha, t)$, with (exact) I_{1+2} given in Eq. (4.5). Since this is an asymptotic result its agreement with numerics is practically better than one hopes for, specially for small n, see Fig. G.1.

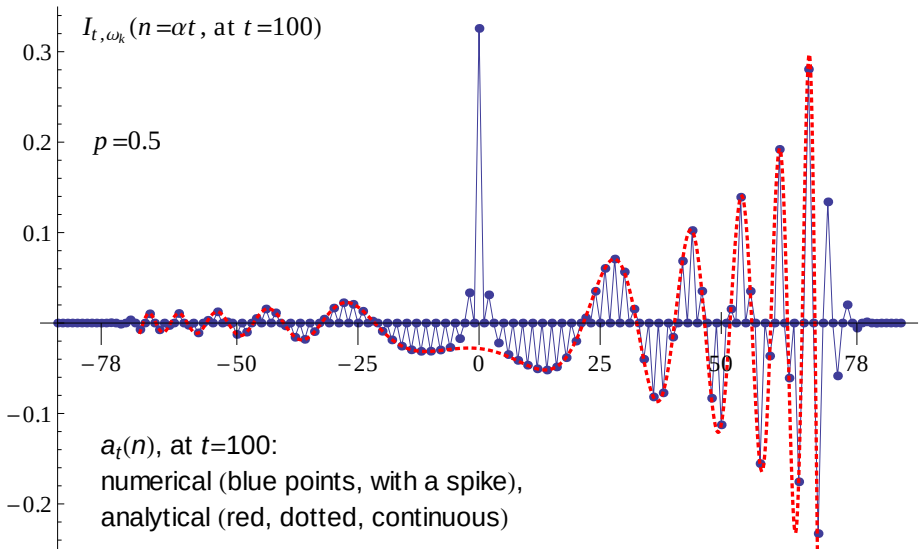

Figure G.1: The analytical (red dotted) and numerical (blue points) results. The spike in the numerical result is an analytically calculated time-independent part of the integral and is identical in the analytical solution, and thus not shown with that curve. Analytical solution is zero at all odd sites as well but is plotted here continuously for clarity.

G.1.2 Stationary phase for $\alpha = \pm\sqrt{p}$

The results of interest are determined in the regime $|\alpha| \leq \sqrt{p}$, but the boundary covers only one point of interest and we mostly need the inequality, calculated above. However, it is needed for consistency to see what is obtained for the boundary as well and thus this calculation is shown here. It is presented also for completeness.

Since $\Phi''_{k_s} = 0$ here, we now apply the theorem in the form

$$I(t) \sim \; 2 \times f(k_s) e^{\boldsymbol{i}\, t\, \Phi(k_s)} \left[\frac{n!}{t \left| \Phi^{(n)}(k_s) \right|} \right]^{1/n} \frac{\Gamma\left[\frac{1}{n}\right]}{n} \, e^{\boldsymbol{i}\, \frac{\pi}{2n}\, \mu}, \tag{G.4}$$

where $\Phi^{(n)}(k_s)$ is the value of the n–th derivative of $\Phi(k)$ at k_s and $\mu = \operatorname{sgn}\left[\Phi^{(n)}|_{k_s}\right]$, and n is the order of the first such non-zero derivative. In our case $n = 3$, and we already see $I(\alpha, t) \sim 1/\sqrt[3]{t}$. Stationary points for different cases can be classified as

$$\alpha = +\sqrt{p}: \qquad k_s = \pm\sqrt{\frac{1-p}{p}} \frac{\sqrt{p}}{\sqrt{1-(\sqrt{p})^2}} = \pm 1 \quad \Rightarrow \begin{cases} k_s = \frac{\pi}{2}, & \text{for } \Phi_+ \\ k_s = \frac{3\pi}{2}, & \text{for } \Phi_- \end{cases}$$

$$\alpha = -\sqrt{p}: \qquad k_s = \mp\sqrt{\frac{1-p}{p}} \frac{\sqrt{p}}{\sqrt{1-(\sqrt{p})^2}} = \mp 1 \quad \Rightarrow \begin{cases} k_s = \frac{3\pi}{2}, & \text{for } \Phi_+ \\ k_s = \frac{\pi}{2}, & \text{for } \Phi_-. \end{cases}$$

Using Eqs. (4.7) and (G.4) we now obtain the estimate of the asymptotic behavior of the integrals. Note that $f_1(k_s) = 1$ at both k_s, while $f_2\left(k_s = \frac{\pi}{2}, \frac{3\pi}{2}\right) = \pm 1$, for the respective values of k_s. We will also need some of:

$$\Phi^{(3)}_+\left(k_s = \frac{\pi}{2}, \frac{3\pi}{2}\right) = -\sqrt{p}(1-p) \quad \text{and} \quad \Phi^{(3)}_-\left(k_s = \frac{\pi}{2}, \frac{3\pi}{2}\right) = +\sqrt{p}(1-p).$$

The case $\alpha = +\sqrt{p}$ The stationary points (G.1) give $\Phi_+(\frac{\pi}{2})$ and $\Phi_-(\frac{3\pi}{2})$. Then,

$$\Phi_+\left(k_s = \frac{\pi}{2}\right) = +\frac{\pi}{2}(1-\sqrt{p}), \qquad \Phi^{(3)}_+\left(\frac{\pi}{2}\right) = -\sqrt{p}(1-p) \quad (\text{so } \mu = -1)$$

$$\Phi_-\left(k_s = \frac{3\pi}{2}\right) = -\frac{\pi}{2}(1+3\sqrt{p}), \qquad \Phi^{(3)}_-\left(\frac{3\pi}{2}\right) = -\sqrt{p}(1-p) \quad (\text{so } \mu = -1)$$

Now the asymptotic estimate of the integral evaluates to

$$
\begin{aligned}
I_{t,\omega_k} \sim \frac{1}{\sqrt[3]{t}}\,\frac{p-1}{8\pi}&\left\{ e^{\boldsymbol{i}\,t\,\Phi_+(\sqrt{p},\frac{\pi}{2})}\frac{6^{\frac{1}{3}}\,\Gamma[\frac{1}{3}]\,e^{-\boldsymbol{i}\,\frac{\pi}{6}}}{3\left[\sqrt{p}(1-p)\right]^{\frac{1}{3}}} + e^{\boldsymbol{i}\,t\,\Phi_-(\sqrt{p},\frac{3\pi}{2})}\frac{6^{\frac{1}{3}}\,\Gamma[\frac{1}{3}]\,e^{-\boldsymbol{i}\,\frac{\pi}{6}}}{3\left[\sqrt{p}(1-p)\right]^{\frac{1}{3}}} \right\}\times 2 \\
+\frac{1}{\sqrt[3]{t}}\,\frac{\sqrt{p}}{4\pi}&\left\{ e^{\boldsymbol{i}\,t\,\Phi_+(\sqrt{p},\frac{\pi}{2})}\frac{6^{\frac{1}{3}}\,\Gamma[\frac{1}{3}]\,e^{-\boldsymbol{i}\,\frac{\pi}{6}}}{3\left[\sqrt{p}(1-p)\right]^{\frac{1}{3}}} + e^{\boldsymbol{i}\,t\,\Phi_-(\sqrt{p},\frac{3\pi}{2})}\frac{6^{\frac{1}{3}}\,\Gamma[\frac{1}{3}]\,e^{-\boldsymbol{i}\,\frac{\pi}{6}}}{3\left[\sqrt{p}(1-p)\right]^{\frac{1}{3}}} \right\}\times 2 \\
+\frac{1}{\sqrt[3]{t}}\,\frac{1}{4\pi}&\left\{ e^{\boldsymbol{i}\,t\,\Phi_+(\sqrt{p},\frac{\pi}{2})}\frac{6^{\frac{1}{3}}\,\Gamma[\frac{1}{3}]\,e^{-\boldsymbol{i}\,\frac{\pi}{6}}}{3\left[\sqrt{p}(1-p)\right]^{\frac{1}{3}}} + e^{\boldsymbol{i}\,t\,\Phi_-(\sqrt{p},\frac{3\pi}{2})}\frac{6^{\frac{1}{3}}\,\Gamma[\frac{1}{3}]\,e^{-\boldsymbol{i}\,\frac{\pi}{6}}}{3\left[\sqrt{p}(1-p)\right]^{\frac{1}{3}}} \right\}\times 2,
\end{aligned}
$$

and by grouping terms

$$
I_{t,\omega_k} \;\sim\; \frac{1}{\sqrt[3]{t}}\times\frac{2\sqrt[3]{6}\,\Gamma[\frac{1}{3}]}{3\left[\sqrt{p}(1-p)\right]^{\frac{1}{3}}}\times e^{-\boldsymbol{i}\frac{\pi}{6}}\times\frac{(1+\sqrt{p})^2}{4\pi}\times\left\{e^{\boldsymbol{i}\,t\,\Phi_+(\frac{\pi}{2})}+e^{\boldsymbol{i}\,t\,\Phi_-(\frac{3\pi}{2})}\right\},
$$

where $(p-1)+2\sqrt{p}+2=(1+\sqrt{p})^2$. Also,

$$
e^{\boldsymbol{i}\,t\,\Phi_+(\frac{\pi}{2})}=e^{\boldsymbol{i}\,t\,\frac{\pi}{2}(1-\sqrt{p})}\quad\text{and}\quad e^{\boldsymbol{i}\,t\,\Phi_-(\frac{3\pi}{2})}=e^{-\boldsymbol{i}\,t\,\frac{\pi}{2}(1+3\sqrt{p})},
$$

and the expression in the braces can be written more compactly as

$$
e^{\boldsymbol{i}\,t\,\frac{\pi}{2}(1-\sqrt{p})}+e^{-\boldsymbol{i}\,t\,\frac{\pi}{2}(1+3\sqrt{p})}=e^{\boldsymbol{i}t\frac{\pi}{2}\sqrt{p}(1-p)}\left(e^{-\boldsymbol{i}t\pi\sqrt{p}p}+e^{+\boldsymbol{i}t\pi\sqrt{p}p}\right)=e^{\boldsymbol{i}\frac{\pi}{2}t\sqrt{p}(1-p)}\cos\left(p\sqrt{p}\pi t\right).
$$

Note that one cannot use $(e^{-\boldsymbol{i}\frac{3\pi}{2}})^{t\sqrt{p}}=(e^{\boldsymbol{i}\frac{\pi}{2}})^{t\sqrt{p}}$ since this changes the branch. Then we have

$$
I_{t,\omega_k} \;\sim\; \frac{1}{\sqrt[3]{t}}\times\frac{\sqrt[3]{6}\,\Gamma[1/3]\,(1+\sqrt{p})^2}{6\pi\left[\sqrt{p}(1-p)\right]^{1/3}}\times e^{-\boldsymbol{i}\frac{\pi}{6}}\times e^{\boldsymbol{i}\frac{\pi}{2}t\sqrt{p}(1-p)}\cos\left(p\sqrt{p}\pi t\right),
$$

and we can write our result as

$$
I_{t,\omega_k} \;\sim\; \frac{a_p}{\sqrt[3]{t}}\,e^{-\boldsymbol{i}\frac{\pi}{6}}\,e^{\boldsymbol{i}\frac{\pi}{2}t\sqrt{p}(1-p)}\cos\left(p\sqrt{p}\pi t\right)\quad\equiv\frac{a_p}{\sqrt[3]{t}}\,e^{-\boldsymbol{i}\frac{\pi}{6}}\,b_p(t)
$$

where $a_p=\frac{\sqrt[3]{6}\,\Gamma[1/3]\,(1+\sqrt{p})^2}{6\pi\left[\sqrt{p}(1-p)\right]^{1/3}}$, while $b_p(t)=e^{\boldsymbol{i}\frac{\pi}{2}t\sqrt{p}(1-p)}\cos\left(p\sqrt{p}\pi t\right)$.

For $p=1/2$, we have $a_p=1.27$ and $b_p(t)=e^{\frac{\boldsymbol{i}\,\pi\,t}{4\sqrt{2}}}\cos\left(1.11\,t+\frac{\pi}{4}\right)$.

The case $\alpha = -\sqrt{p}$ The stationary points are now reversed, $\Phi_+(\frac{3\pi}{2})$ and $\Phi_-(\frac{\pi}{2})$,

$$\Phi_+\left(k_s = \frac{3\pi}{2}\right) = +\frac{\pi}{2}(1+3\sqrt{p}), \qquad \Phi_+^{(3)}\left(\frac{3\pi}{2}\right) = \sqrt{p}(1-p) \quad (\mu = +1)$$
$$\Phi_-\left(k_s = \frac{\pi}{2}\right) = -\frac{\pi}{2}(1-\sqrt{p}), \qquad \Phi_-^{(3)}\left(\frac{\pi}{2}\right) = \sqrt{p}(1-p) \quad (\mu = +1)$$

The main difference from the $\alpha = +\sqrt{p}$ case is that now $f_1(k-\frac{3\pi}{2}) \sim -1$ while $f_2(k-\frac{\pi}{2}) \sim 1$, and there is an overall minus sign on the second group of two integrals; then the factors in front of integrals come together into $(1-\sqrt{p})^2$ and we have

$$I_{t,\omega_k} \sim \frac{a_p}{\sqrt[3]{t}}\, e^{+\boldsymbol{i}\frac{\pi}{6}}\, b_p(t), \qquad \text{where } a_p \text{ has } (1-\sqrt{p})^2 \text{ instead of the } (1+\sqrt{p})^2 \text{ above,}$$

while $b_p(t)$ is the same as above. For $p = 1/2$, these two expressions differ by about 34 times, what seems to agree with the computational result. $[(1+\sqrt{1/2})^2 = 2.91$ while $(1-\sqrt{1/2})^2 = 0.086.]$ This difference gets larger for larger p, and vice versa, what seems to make sense as well.

Appendix H: Coefficients of two-step-memoried walk's amplitude: Figures.

In this Appendix we gather figures related to the behaviour of the coefficients of the amplitude discussed and computed in the problem of Chapter 4. The figures show the coefficients by performing numerical integration of the relevant expressions (see text). Analytical asymptotic estimates are shown elsewhere.

The state in that problem has four components, and the coefficient of the first, $a_t(n)$ is given in the text, in Fig. 4.2, for an illustration. Here we show the remaining ones.

In the Fig. H.1 below the coefficient $b_t(n)$ is seen at a few time steps, with a structure similar to the one of $a_t(n)$. Note that the amplitude is visibly smaller, almost calling into question the existence of the peaks.

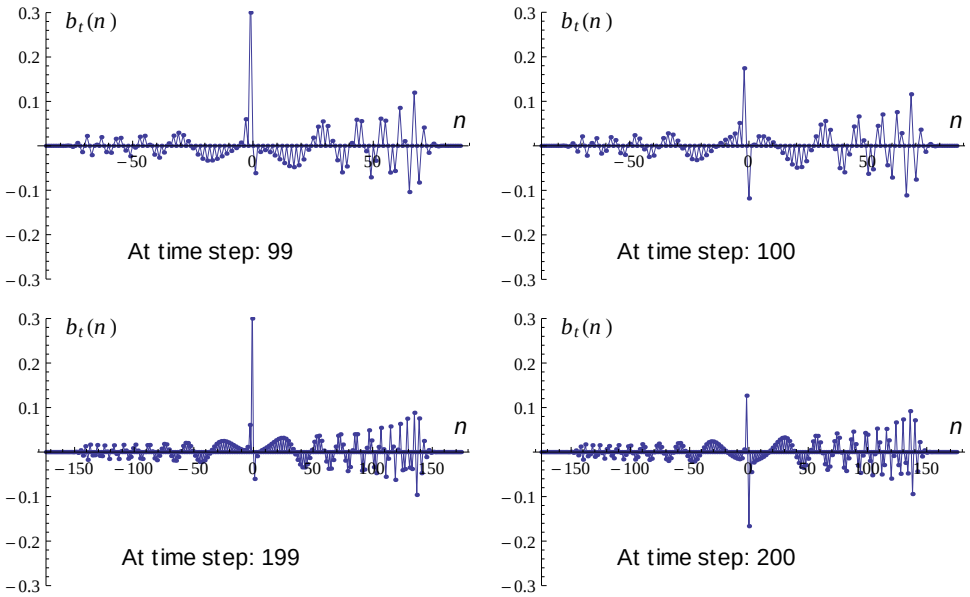

Figure H.1: The coefficient $b_t(n)$ as a function of position (site), at some time-steps.

Next, in Fig. H.2 the coefficient $c_t(n)$ is shown for two even and two odd times.

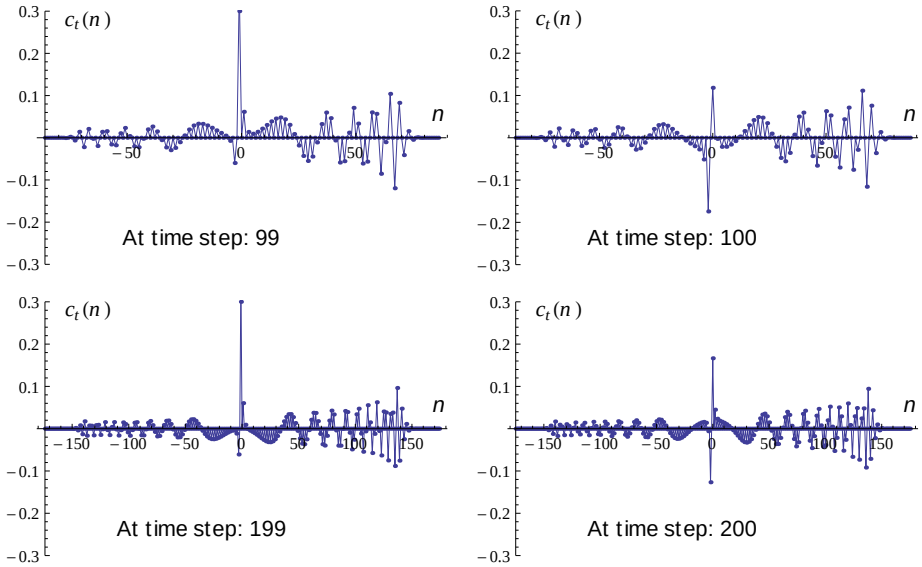

Figure H.2: The coefficient $c_t(n)$ as a function of position (site), at some time-steps.

Below (Fig. H.3) we see the same for the coefficient $d_t(n)$. Note that, starting from $a_t(n)$ (shown in text), the amplitude of the peaks is reduced for further coefficients.

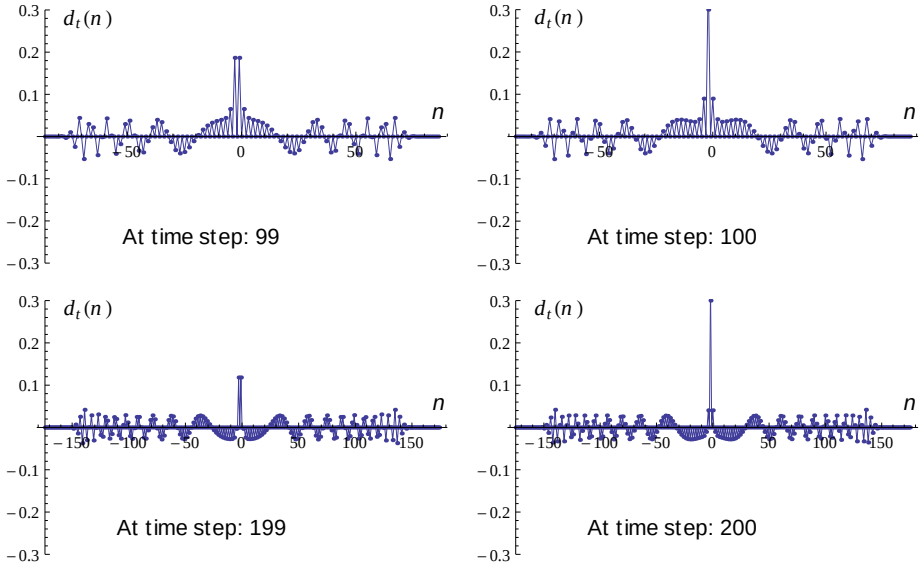

Figure H.3: The coefficient $d_t(n)$ as a function of position (site), at some time-steps.

Appendix I: Classical random walk on a semi-infinte line

For completeness here we provide the application of the method developed in [144, 145] (based on Karlin-McGregor spectral approach to random walks) to a classical walk on a binary tree.

If P is a reversible Markov chain over a sample space Ω, and π is a reversibility function (not necessarily a probability distribution), then P is a self-adjoint operator in $\ell^2(\pi)$, the space generated by the inner product

$$< f, g >_\pi = \sum_{x \in S} f(x) g(x) \pi(x)$$

induced by π. If P is tridiagonal operator (i.e. a nearest-neighbor random walk) on $\Omega = \{0, 1, 2, \dots\}$, then it must have a simple spectrum, and is diagonalizable via orthogonal polynomials as it was studied in the 50's and 60's by Karlin and McGregor. There the extended eigenfuctions $Q_j(\lambda)$ ($Q_0 \equiv 1$) are orthogonal polynomials with respect to a probability measure ψ and

$$p_t(i,j) = \pi_j \int_{-1}^{1} \lambda^t Q_i(\lambda) Q_j(\lambda) d\psi(\lambda) \quad \forall i, j \in \Omega,$$

where π_j ($\pi_0 = 1$) is the reversibility measure of P. Consider the following Markov chain

$$P = \begin{pmatrix} 0 & 1 & 0 & 0 & \dots \\ q & 0 & p & 0 & \dots \\ 0 & q & 0 & p & \ddots \\ \vdots & \vdots & \ddots & \ddots & \ddots \end{pmatrix} \qquad p > q.$$

Orthogonal polynomials are obtained via solving a simple linear recursion: $Q_0 = 1$, $Q_1 = \lambda$, and

$$Q_n(\lambda) = c_1(\lambda) \rho_1^n(\lambda) + c_2(\lambda) \rho_2^n(\lambda),$$

where $\rho_1(\lambda) = \frac{\lambda + \sqrt{\lambda^2 - 4pq}}{2p}$ and $\rho_2(\lambda) = \frac{\lambda - \sqrt{\lambda^2 - 4pq}}{2p}$ are the roots of the characteristic

equation for the recursion, and $c_1 = \frac{\rho_2 - \lambda}{\rho_2 - \rho_1}$ and $c_2 = \frac{\lambda - \rho_1}{\rho_2 - \rho_1}$. Now $\pi_0 = 1$ and $\pi_n = \frac{p^{n-1}}{q^n}$ $(n \geq 1)$. Also, we observe that

$$\begin{aligned} |\rho_2(\lambda)| &> \sqrt{q/p} \quad \text{on } [-1, -2\sqrt{pq}), \\ |\rho_2(\lambda)| &< \sqrt{q/p} \quad \text{on } (2\sqrt{pq}, 1], \\ |\rho_2(\lambda)| &= \sqrt{q/p} \quad \text{on } [-2\sqrt{pq}, 2\sqrt{pq}], \end{aligned}$$

and $\rho_1\rho_2 = \frac{q}{p}$. The above will help us to identify the point mass locations in the measure ψ since each point mass in ψ occurs when $\sum_k \pi_k Q_k^2(\lambda) < \infty$. Thus we need to find all $\lambda \in (2\sqrt{pq}, 1]$ such that $c_1(\lambda) = 0$ and all $\lambda \in [-1, -2\sqrt{pq})$ such that $c_2(\lambda) = 0$. But there are no such roots, as $c_1(-1) = 0$ and $c_2(1) = 0$, while $-1 \notin (2\sqrt{pq}, 1]$ and $1 \notin [-1, -2\sqrt{pq})$. Thus there are no point mass atoms in ψ, and the mass of ψ must be continuously distributed inside $[-2\sqrt{pq}, 2\sqrt{pq}]$. In order to find the density of ψ inside $[-2\sqrt{pq}, 2\sqrt{pq}]$ we need to find $(e_0, (P - sI)^{-1}e_0)$ for $\mathrm{Im}(s) \neq 0$, i.e. the upper left element in the resolvent of P.

Let $(a_0(s), a_1(s), \dots)^T = (P - sI)^{-1}e_0$, then

$$-sa_0 + a_1 = 1, \quad \text{and} \quad qa_{n-1} - sa_n + pa_{n+1} = 0$$

Thus $a_n(s) = \alpha_1\rho_1(s)^n + \alpha_2\rho_2(s)^n$, with $\alpha_1 = \frac{a_0(\rho_2 - s) - 1}{\rho_2(s) - \rho_1(s)}$ and $\alpha_2 = \frac{1 - a_0(\rho_1 - s)}{\rho_2(s) - \rho_1(s)}$. Since $(a_0, a_1, \dots) \in \ell^2(\mathbb{C}, \pi)$,

$$|a_n|\sqrt{\frac{p^n}{q^n}} \to 0 \qquad \text{as} \quad n \to +\infty$$

Hence when $|\rho_1(s)| \neq |\rho_2(s)|$, either $\alpha_1 = 0$ or $\alpha_2 = 0$, and therefore

$$a_0(s) = \frac{\mathbb{1}_{|\rho_1(s)| < \sqrt{\frac{q}{p}}}}{\rho_1(s) - s} + \frac{\mathbb{1}_{|\rho_2(s)| < \sqrt{\frac{q}{p}}}}{\rho_2(s) - s}.$$

Also $d\psi(z) = \varphi(z)dz$, where $\varphi(z)$ is an atom-less density function over $[-2\sqrt{pq}, 2\sqrt{pq}]$, and

$$a_0(s) = \int_{-2\sqrt{pq}}^{+2\sqrt{pq}} \frac{d\psi(z)}{z - s} = \int_{-2\sqrt{pq}}^{+2\sqrt{pq}} \frac{\varphi(z)dz}{z - s}.$$

Next we will use the following basic property of Cauchy transforms $Cf(s) = \frac{1}{2\pi i}\int_{\mathbb{R}} \frac{f(z)dz}{z - s}$

that can be derived using the Cauchy integral formula, or similarly, an approximation to the identity formula:

$$C_+ - C_- = I.$$

Observe that the curve in the integral need not be in $\mathbb{R}$ for $C_+ - C_- = I$ to hold. Here

$$\begin{aligned} C_+ f(z) &= \lim_{s \to z:\ \mathrm{Im}(s)>0} Cf(s), \quad \text{and} \\ C_- f(z) &= \lim_{s \to z:\ \mathrm{Im}(s)<0} Cf(s), \end{aligned}$$

for all $z \in \mathbb{R}$. The relation (I) implies

$$\varphi(x) = \frac{1}{2\pi i} \left(\lim_{\substack{s=x+i\varepsilon: \\ \varepsilon \to 0+}} a_0(s) - \lim_{\substack{s=x-i\varepsilon: \\ \varepsilon \to 0+}} a_0(s) \right),$$

for all $x \in (-2\sqrt{pq}, 2\sqrt{pq})$. Recalling (I), we express φ as $\varphi(x) = \frac{\rho_1(x)-\rho_2(x)}{2\pi i(\rho_1(x)-x)(\rho_2(x)-x)}$ for $x \in (-2\sqrt{pq}, 2\sqrt{pq})$, which in turn simplifies to

$$\varphi(x) = \begin{cases} \frac{\sqrt{4pq-x^2}}{2\pi q(1-x^2)} & \text{if } x \in (-2\sqrt{pq}, 2\sqrt{pq}), \\ 0 & \text{otherwise.} \end{cases}$$

Here $\varphi(x)$ always integrates to 1 over $(-2\sqrt{pq}, 2\sqrt{pq})$. Now

$$\begin{aligned} p_t(n,0) &= \int_{-2\sqrt{pq}}^{+2\sqrt{pq}} \lambda^t Q_n(\lambda) \varphi(\lambda) d\lambda \\ &= \int_{-2\sqrt{pq}}^{+2\sqrt{pq}} \lambda^t (c_1 \rho_1^n + c_2 \rho_2^n) \frac{(\rho_1 - \rho_2)\, d\lambda}{2\pi i (\rho_1 - \lambda)(\rho_2 - \lambda)}, \end{aligned}$$

and therefore, since $c_1 = \frac{\rho_2 - \lambda}{\rho_2 - \rho_1}$ and $c_2 = \frac{\lambda - \rho_1}{\rho_2 - \rho_1}$,

$$p_t(n,0) = \frac{1}{2\pi i} \int_{-2\sqrt{pq}}^{+2\sqrt{pq}} \lambda^t \left(\frac{\rho_2^n}{\rho_2 - \lambda} - \frac{\rho_1^n}{\rho_1 - \lambda} \right) d\lambda. \tag{I.1}$$

This can be treated as a complex integral, for example with steepest descent. But one

can observe directly in Eq.(I.1) that the tail of $p_t(n,0)$ decays as $(2\sqrt{pq})^t$ when $t \to +\infty$. Thus, using $p = 2/3$ and $q = 1/3$ for the classical symmetric walk on the semi-infinite binary tree, the decay rate will be $(2\sqrt{2}/3)^t$, giving us the exponential asymptotics. The probability integral (I.1) can be efficiently evaluated numerically, see Fig. I.1. This same plot is shown in Fig. 3.6 in the text as well.

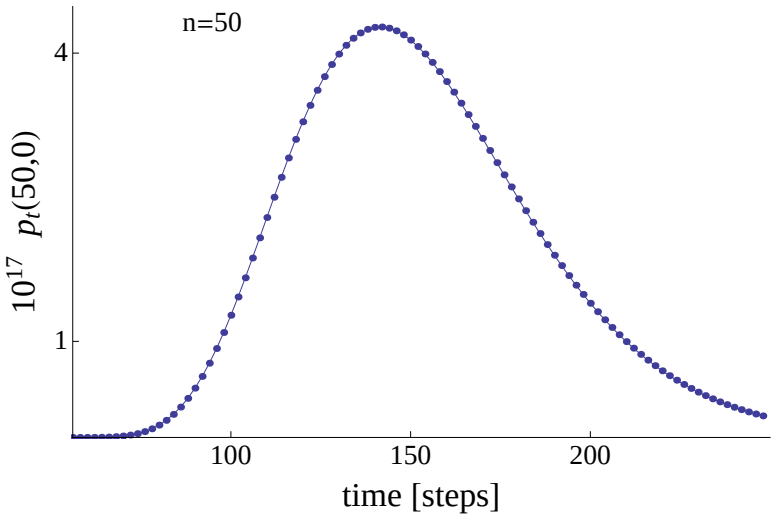

Figure I.1: Probability at the root for a classical random walk on a semi-infinte binary tree, for a starting level $n = 50$.